Carbon Dioxide Absorption and Durability of Carbonation Cured Cement and Concrete Compacts

by

Chad Oliver Logan

Department of Civil Engineering and Applied Mechanics
McGill University, Montréal, Québéc, Canada
January, 2006

A thesis submitted to McGill University in partial fulfilment of the requirements of the degree of Master of Civil Engineering

Library and
Archives Canada

Published Heritage
Branch

395 Wellington Street
Ottawa ON K1A 0N4
Canada

Bibliothèque et
Archives Canada

Direction du
Patrimoine de l'édition

395, rue Wellington
Ottawa ON K1A 0N4
Canada

Your file Votre référence
ISBN: 978-0-494-24988-8
Our file Notre référence
ISBN: 978-0-494-24988-8

NOTICE:
The author has granted a non-exclusive license allowing Library and Archives Canada to reproduce, publish, archive, preserve, conserve, communicate to the public by telecommunication or on the Internet, loan, distribute and sell theses worldwide, for commercial or non-commercial purposes, in microform, paper, electronic and/or any other formats.

The author retains copyright ownership and moral rights in this thesis. Neither the thesis nor substantial extracts from it may be printed or otherwise reproduced without the author's permission.

AVIS:
L'auteur a accordé une licence non exclusive permettant à la Bibliothèque et Archives Canada de reproduire, publier, archiver, sauvegarder, conserver, transmettre au public par télécommunication ou par l'Internet, prêter, distribuer et vendre des thèses partout dans le monde, à des fins commerciales ou autres, sur support microforme, papier, électronique et/ou autres formats.

L'auteur conserve la propriété du droit d'auteur et des droits moraux qui protège cette thèse. Ni la thèse ni des extraits substantiels de celle-ci ne doivent être imprimés ou autrement reproduits sans son autorisation.

In compliance with the Canadian Privacy Act some supporting forms may have been removed from this thesis.

While these forms may be included in the document page count, their removal does not represent any loss of content from the thesis.

Conformément à la loi canadienne sur la protection de la vie privée, quelques formulaires secondaires ont été enlevés de cette thèse.

Bien que ces formulaires aient inclus dans la pagination, il n'y aura aucun contenu manquant.

Canada

ABSTRACT

Intensification of the greenhouse effect from anthropogenic emissions of carbon dioxide and other greenhouse gases have, and will continue to increase the Earth's average global temperature. Intergovernmental demand to minimize human's influence on the global climate was entered into force in 2005, requiring participating industrialized countries to reduce collective greenhouse gas emissions by 5.2% compared to 1990 values. Along with clean energy and efficient system design, carbon dioxide sequestration becomes one of the critical measures in global greenhouse gas mitigation exercises.

Carbon dioxide sequestration through carbonation curing of concrete has the potential to reduce atmospheric carbon dioxide emissions. In the presence of water, carbon dioxide gas readily reacts with the calcium silicate compounds of cement to form calcium carbonate. In this manner, early-age concrete exposed to recovered carbon dioxide could be used as a sink for CO_2 storage. The focus of this study was to investigate the potential for carbon dioxide sequestration through carbonation curing of cement paste and concrete compacts, as well as their durability performance in structural applications.

To determine the feasibility of such a method, research was conducted on the carbon dioxide absorption potential and durability of carbonation cured concrete products. Carbonation curing was characterized by the mass of carbon dioxide absorbed, mass of water lost, peak sample temperature, dimensional stability, compressive strength, depth of carbonation and microstructure. Further testing was performed on the carbonation cured products to assess the long-term durability. Long-term durability was characterized by the mass of carbon dioxide absorbed, dimensional stability, freeze/thaw resistance and compressive strength in simulated service exposure. Carbon dioxide absorption in the order of 10% by mass was recorded during early-age carbonation curing. Weathering carbonation shrinkage of concrete samples was reduced by approximately 33% in carbonated samples as oppose to those hydrated. It was also found that carbonation curing reduced the mass loss during freeze/thaw durability testing by 90% over hydration curing.

RESUME

L'intensification ou par l'émissions anthropogénique de dioxyde de carbone et d'autres gaz à effet de serre a commencé et continuera à augmenter la temperature moyenne de la planète. En 2005, la demande intergouvernementale de réduire l'influence des humains sur le climat fût mise en place. Celle-ci exige que touts les pays industrialisés participant réduisent l'émission collective de gaz à effets de serre de 5.2% par rapport aux niveau de 1990. En plus de l'énergie propre et des système à conception efficace, la séquestration du dioxyde de carbone est une mesure critique dans l'exercice de la réduction des gaz à effet de serre.

La séquestration du dioxyde de carbone durant le mûrissement au carbone du béton a le potentiel de réduire les émissions de dioxyde de carbone dans l'atmosphère. En présence d'eau, le gaz du dioxyde de carbone réagit avec les composés de silicate de carbone pour former du carbonate de calcium. Ainsi, le béton frais exposé au dioxyde de carbone récupéré pourrait sévir de réservoir pour emmagasiner le $CO_{2.}$ Le but de cette étude était d'examiner la séquestration du dioxyde de carbone par le mûrissement au carbone des compactés de pâte de ciment et des compactés de béton ainsi que leur durabilité dans des applications de structure.

Pour déterminer la faisabilité d'une telle méthode, la recherche s'est concentrée sur le potentiel d'absoption du dioxyde de carbone et sur la durabilité du mûrissement au carbone. Le mûrissement au carbone a été caractérisé par la masse de dioxyde de carbone absorbée, la masse d'eau perdue, la température moyenne maximale des échantillons, la stabilité dimensionnelle , la résistance en compression, la profondeur de carbonation et la structure au niveau microscopique. D'autres tests on été éxecutés sur les produits du mûrissement au carbone pour évaluer la durabilité à long terme. La durabilité à long terme a été caractérisée par la masse de dioxide de carbone absorbée la stabilité, la résistance aux cycles de gel et de dégel et la résistance en compression une mise en service simulée. L'absorption de dioxyde de carbone de l'ordre de 10% de la masse a été enregistrée tôt durant la carbonation des échantillons. La perte de masse due à l'abrasion des échantillons de béton a été réduite d’environ 33% pour les échantillons sujets à la carbonation contre ceux simplement hydratés. De plus, il a été observé que la réduction de la masse des échantillons mûrir au carbone, durant les tests de gel/dégel est de 90% inférieur à la réduction subie par les des échantillons simplement hydratés.

ACKNOWLEDGMENTS

I would like to express my sincere appreciation to Dr. Yixin Shao for his guidance and support through the course of my graduate studies. A special thank you for your contributions in and out of the lab, as well as your invaluable knowledge and advice. Your assistance has been greatly appreciated.

Thanks are extended to the laboratory technicians J. Bartczak, D. Kiperchuk, M. Przykorski and R. Sheppard, and the administrative staff in the Department of Civil Engineering. I would also like to express my gratitude to my friends and colleagues X.D. Zhou and S. Monkman for their support and assistance throughout this thesis.

Finally, I would like to thank those closest to me, who helped make the completion of my graduate studies possible. To my father, mother and brothers, your constant encouragement and confidence in me cannot be thanked enough. Thank you to my friends for all the unforgettable memories you have given me over the past two years. And to Nikki, thank you for always being by my side and filling my life with joy.

TABLE OF CONTENTS

Page

LIST OF FIGURES

LIST OF TABLES

Page

CHAPTER 1 INTRODUCTION

1.1 GENERAL OVERVIEW

Since Arrhenius first concluded in 1896 that prolonged combustion of fossil fuels could stimulate a change in climate significant research has been conducted supporting his fundamental theory. Arrhenius associated carbon dioxide emissions with the radiation balance of the Earth and global climate. In the past century sophisticated models have been developed and past climates have been studied confirming the link (Field and Raupach, 2004). Increasing levels of greenhouse gases, particularly CO_2, from anthropogenic activities threaten to harm the Earth's atmosphere and living organisms.

1.1.1 The Global Carbon Cycle

Human activities have disturbed previous millennial periods of balance in the carbon cycle through anthropogenic CO_2 inputs. Carbon stored in the atmosphere, oceans and terrestrial biosphere is continually exchanged, with atmospheric CO_2 providing a channel between biological, physical and anthropogenic processes (Wigley and Schimel, 2000). A major component of the global carbon cycle is the relatively quick exchange of carbon through the ecosphere by photosynthesis and aerobic respiration. Carbon stored for decades as biomass in organic matter such as trees eventually returns to the atmosphere during decomposition. Trapped deposits of carbon underground are created when highly productive wetlands and other ecosystems accumulate dead organic matter and bacteria faster than it is decomposed. These deposits remain locked away for millions of years until they are extracted by human activities or long-term geological processes (Miller, 1998). Figure 1.1 illustrates the Earth's various carbon sources and sinks.

Sedimentary rocks, including limestone, are the largest carbon reservoir on earth. Cycling of carbon back into the atmosphere is extremely slow and occurs through dissolution of the sediments and geological processes exposing the sediments to chemical attacks from oxygen and acid rain. The second largest reservoir is the oceans. Carbon dioxide is stored in the oceans as dissolved CO_2 gas, some of which is used in photosynthesis, as well as storage in carbonate and bicarbonate ions (Miller, 1998).

Combustion of fossil fuels and cement production rapidly release previously stored carbon in the form of CO_2 into the atmosphere (Wigley and Schimel, 2000). Terrestrial ecosystem disturbances including deforestation, land use and subsequent soil oxidation are also a major cause of unbalance in the carbon cycle (Jaques *et al*, 1997). The resulting anthropogenic carbon is exchanged between the atmosphere, oceans and terrestrial biosphere. Cycling of carbon through the oceans and terrestrial biosphere is relatively slow leaving the cycle unbalanced with a surplus in the atmosphere (Wigley and Schimel, 2000). Anthropogenic perturbations will be long-lived with the CO_2 produced taking anywhere from one year to thousands of years to cycle back into the terrestrial biosphere and oceans.

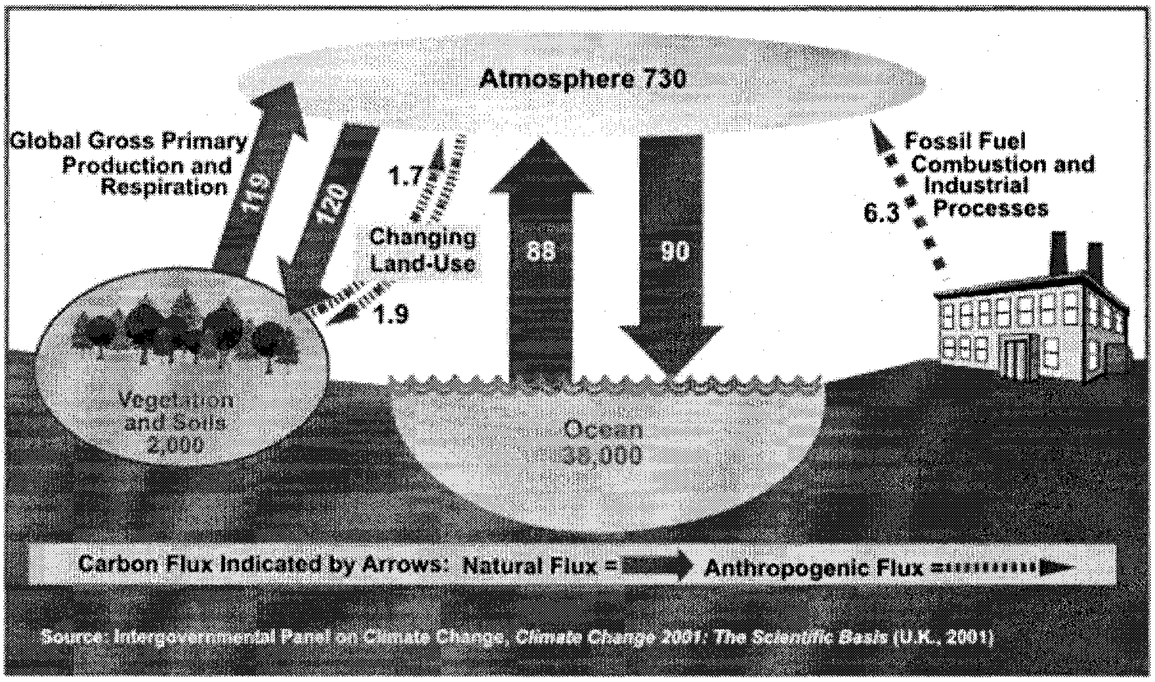

Source: Intergovernmental Panel on Climate Change, *Climate Change 2001: The Scientific Basis* (U.K., 2001)

Figure 1.1: The global carbon cycle (http://www.eia.doe.gov/oiaf/1605/ggccebro/chapter1.html)

1.1.2 The Greenhouse Gas Effect

Carbon dioxide, water vapour and trace amounts of methane, nitrous oxide, chlorofluorocarbons and other greenhouse gases have an important role in governing the Earth's climate. The average temperature of 15°C on Earth is maintained by these greenhouse gases which trap solar radiation from the sun. Without the atmosphere the temperature on Earth can be estimated around -19°C, comparable with that of the moon which receives similar solar radiation but has no atmosphere (Halmann and Steinberg, 1999). Light, infrared radiation and some ultraviolet radiation from the sun pass through the atmosphere to the Earth's surface where it is absorbed and degraded to longer-wave infrared radiation. Some of this heat is then trapped in the atmosphere, warming the air, while the remainder either passes into space or is radiated back to the Earth's surface (Miller, 1998).

Several greenhouse gases are responsible for maintaining the life sustaining environment on Earth. Heat is primarily trapped in the atmosphere by water vapor, with a concentration ranging between 1 and 5%. Emissions of water vapor from human activities have little influence on the greenhouse effect due to the abundance of this gas. Carbon dioxide gas also plays an important role in atmospheric heat retention, but in contrast to water vapor, anthropogenic CO_2 emissions have significant climatic affects. The concentration of atmospheric CO_2 is relatively small, 0.036%, such that large human induced outputs of this gas adversely influence the global climate (Miller, 1998). Greater quantities of CO_2 retain more infrared radiation and cause an increase in temperature. A secondary effect of this elevated temperature is that more water vapor is present in the atmosphere, trapping additional radiation and increasing temperatures further (Halmann and Steinberg, 1999). According to radiative forcing values the change in abundance of CO_2 is responsible for 60% of the total increased greenhouse effect. Other greenhouse gases, including methane (CH_4), nitrous oxide (N_2O), ozone (O_3), chlorofluorocarbons (CFCs) and fluorocarbons (CFs), primarily generated by human activities have an adverse effect similar to CO_2. The significance of these greenhouse gases on global climate change is not as significant as CO_2 and their contribution affecting the earth-atmosphere energy balance is indicated in Table 1.1 (Halmann and Steinberg, 1999).

Radiative forcing is a measure of the variation in balance between solar radiation coming to the Earth and outgoing infrared radiation. Positive radiative forcing indicates incoming solar radiation exceeds outgoing infrared radiation due to greenhouse gases trapping and reflecting infrared radiation back to Earth (http://www.evomarkets.com/ghg_glossary.html).

Table 1.1: Radiative forcing values for various greenhouses due to their change in abundance since pre-industrial times (Modified from IPCC, 2001)

Gas	Radiative Forcing, Wm^{-2}	Effect on Earth-Atmosphere energy balance, %
CO_2	1.46	60.2
CH_4	0.48	19.8
CFCs	0.277	11.4
N_2O	0.15	6.2
CF_4	0.003	0.1
Others	0.055	2.4
Total	2.425	100

Greenhouse gas levels have increased significantly since pre-industrial times as the result of human activities. Fossil fuel combustion, agriculture, deforestation and the use of CFCs are the main contributing factors to this increase. Table 1.2 shows the change in greenhouse gas levels since the industrial revolution, the rate of concentration change and the atmospheric lifetime of each gas. Large anthropogenic CO_2 inputs make it the most important human produced greenhouse gas despite the fact that methane, nitrous oxide and CFCs trap more heat per molecule. Carbon dioxide emissions have increased at a rate of 1.5 ppm/yr resulting in an atmospheric concentration approximately 85 ppm higher than pre-industrial levels. In considering the affect of each greenhouse gas on the global climate it is important to note the associated atmospheric lifetime. For example, perfluorocarbons such as CF_4 have a relatively low concentration of 80 ppt but persist in the atmosphere for more than 50 000 years. Increased emissions of this gas with little regard for its lifetime could have profound climatic implications. Elevated levels of greenhouse gases have already changed the global climate and threaten to continue with detrimental effects on the living environment (Miller, 1998).

Table 1.2: Greenhouse gases affected by human activities (IPCC, 2001)

	CO_2	CH_4	N_2O	CFC-11	*HFC-23*	CF_4
Pre-industrial concentration	~280 ppm	~700 ppb	~270 ppb	0	0	40 ppt
Concentration in 1998	365 ppm	1745 ppb	314 ppb	268 ppt	14 ppt	80 ppt
Rate of concentration change	1.5 ppm/yr	7.0 ppb/yr	0.8 ppb/yr	-1.4 ppt/yr	0.55 ppt/yr	1 ppt/yr
Atmospheric lifetime	5-200 yr	12 yr	114 yr	45 yr	260 yr	>50 000 yr

*ppm – parts per million, ppb – parts per billion, ppt – parts per trillion

Changes in the global climate have already been acknowledged by the scientific community. Mean surface temperatures have increased 0.3 to 0.6°C since measurements began in 1860. Although this change could completely or partly be the result of natural variation in global temperatures, the 1995 IPCC Second Assessment Report concluded that the changes are “unlikely to be entirely natural in origin” and that there has been “discernible human influence on global climate” (IPCC, 1995). Ocean levels have increased 9 to 18 cm from 1900 to 1990 with approximately 66% of the rise coming from global warming (Miller, 1998). Depending on climatic sensitivity values used to simulate and project the effect of continued human interference on global warming, temperatures are estimated to increase 1 to 3.5°C from 1990 values to 2100 with a best estimate of 2°C. As the result, average sea levels are expected to rise anywhere from 15 to 95 cm (best estimate of 50 cm) due to oceanic thermal expansion and glacial/ice-sheet melting (IPCC, 1995). Changes to the Earth’s climate greater than 1°C over a relatively short span of a few decades could cause profound disruptions to the Earth’s ecosystems including human life as it currently exists (Miller, 1998). Global warming is expected to influence storm patterns and their severity, displace millions of coastal residence, cause regional droughts and flooding, and disturb sectors such as agriculture, forestry and energy (Jaques *et al*, 1997). Without international policy to mitigate escalating levels of greenhouse gases by stabilizing or reducing current and future emissions, the adverse effects of increased global temperatures will continue to grow.

1.1.3 Sources of Carbon Dioxide

Although anthropogenic CO_2 emissions only represent approximately 2% of the total global carbon output, the remainder coming from natural sources, they are considered to be responsible for the accumulated surplus of atmospheric CO_2. Atmospheric CO_2 levels have increased significantly from about 280 ppm in pre-industrial times (approximately 1750) to around 365 ppm in 1998. This increase can mainly be attributed to human activities with global emissions increasing over the last 40 years from 6 to 22.5 gigatonnes (Jaques *et al*, 1997).

Emissions from fossil fuel combustion have been identified as a significant source of anthropogenic CO_2 (Jaques *et al*, 1997). Based on 1990 values, approximately 75% of global energy consumption came from burning fossil fuels. Table 1.3 indicates the energy produced by various sources and the quantity of carbon emitted as CO_2 (1990). Although oil produced an estimated 40% more energy than coal, both sources yielded very similar CO_2 emissions due to the carbon and hydrogen content of each. Industrial power and heat generation represent the largest energy consuming sector, accounting for 47% of global CO_2 emissions from energy production in 1990. The transportation and commercial/residential sectors were responsible for 22 and 31%, respectively, of the total 5.6 GT of CO_2 emissions produced by energy consumption (Halmann and Steinberg, 1999).

Cement production also contributes to anthropogenic CO_2 emissions through the decarbonization of limestone ($CaCO_3$) and energy-intensive manufacturing process. During the production of cement high temperatures are used to chemically change limestone and other calcium rich materials into calcium oxide (CaO) through a process called calcination. Not only does this chemical reaction (described by Equation 1.1) itself generate CO_2 but so does the combustion of fossil fuels in the kiln to produce heat.

The lime is combined with silica containing materials to produce clinker, which is then cooled, pulverized and mixed with gypsum to form Portland cement. Although raw material preparation, crushing and grinding of limestone, and cement making, clinker grinding, have high electricity demands, clinker production represents 70 to 80% of the total energy consumption for the process through fuel combustion. It is estimated that the cement industry accounts for almost 5% of global industrial energy consumption (2% of primary energy consumption) and approximately 5% of global anthropogenic CO_2 emissions (Worrell *et al*, 2001).

Table 1.3: Global energy consumption and CO_2 emissions for various energy sources (Halmann and Steinberg, 1999)

Energy Source	Energy Produced, EJ/yr[a]	Percent of Total Energy Produced	Amount of Carbon as CO_2 produced, GT/yr[b]	Percent of Total Carbon Produced
Coal	91	23.7	2.3	40.4
Oil	128	33.2	2.4	42.7
Gas	71	18.4	0.9	16.9
Nuclear	19	4.9	-	-
Hydro	21	5.5	-	-
Biomass	55	14.3	-	-
Total	385	100	5.6	100

[a] EJ represents 10^{18} joules

[b] GT represents 10^6 tonnes

$$CaCO_3 + \text{Heat} \rightarrow CaO + CO_2 \qquad (1.1)$$

1.1.4 International Policy

Numerous international conferences addressing the issue of climate change have been held since the 1979 First World Climate Conference in Geneva acknowledged an intergovernmental demand to minimize human's affect on the global climate. The 1992 Earth Summit in Rio de Janeiro saw the adaptation of Agenda 21, a global plan for sustainable development integrating environmental, economical and social concerns. At this conference, better known as the UN Conference on Environment and Development, 154 nations signed the UN Framework Convention on Climate Change (UNFCCC). The

Convention was the first binding international legal instrument providing a framework for addressing climate change issues. By 1995 UNFCCC parties became aware that the voluntary goals of the Convention would not be met. Under the authorization of the Framework Convention on Climate Change (FCCC) a Conference of Parties (COP) began constructing legally binding measures to reduce greenhouse gas emissions (Field and Raupach, 2004).

Following a two year analysis and assessment period of regulatory instruments to limit greenhouse gases, more than 160 nations met in Kyoto, Japan in 1997 to negotiate binding limitations on greenhouse gases (http://www.eia.doe.gov/oiaf/kyoto/kyotorpt .html). The established treaty, an amendment to the UNFCC, was ratified by 141 countries and entered into force on February 16, 2005. Officially named the Kyoto Protocol to the United Nations Framework Convention on Climate Change, the legally binding agreement requires industrialized countries to reduce collective greenhouse gas emissions by 5.2% compared to 1990 values. Participating nations must reduce emissions for six major greenhouse gases including carbon dioxide, methane, nitrous oxide, sulfur hexafluoride, HFCs and PFCs. This reduction is calculated as an average during the period of 2008 to 2012 and countries that maintain or increase levels must engage in emissions trading in order to conform to the protocol. Canada ratified on December 17, 2002 and while the United States of America (USA) singed the protocol it has neither ratified nor withdrawn, leaving the treaty non-binding. There was strong opposition in Canada not to ratify the treaty as an effort to remain economically competitive against the USA. Joining the Kyoto Protocol means Canadian companies have to pay for their emissions, increasing production costs, while firms in the USA will not be subject to this additional cost (http://en.wikipedia.org/wiki/Kyoto_Protocol).

1.2 GREENHOUSE GAS MITIGATION STRATEGIES

Natural processes currently absorb an estimated 50% of anthropogenic CO_2 into the terrestrial biosphere and oceans. It has been suggested by some scientists that as CO_2 emissions continue to increase the oceans and land will absorption more and more CO_2, and that life on Earth will adapt to survive. Contrary to this adaptive theory others suggest that if CO_2 emissions continue at the current level or accelerate, the oceans and terrestrial biosphere will be unable to slow escalating atmospheric CO_2 (Sanders, 2005). Intergovernmental action as outlined in Section 1.1.4 indicates that an approach of mitigation and prevention to global warming is being implemented with a proactive attitude. Methods of CO_2 mitigation include reduction of emissions and enhancement of physical and biological carbon sinks. These methods mainly focus on improved fossil fuel usage since two-thirds of the greenhouse gases acknowledged in the Kyoto Protocol are from energy production (IPCC, 2001).

The following greenhouse gas mitigation options to limit or reduce emissions were outlined in the 2001 IPCC Mitigation Report.

1. Improved efficiency and energy conservation.
2. Transfer to low-carbon and renewable biomass fuels.
3. Zero-emissions technology.
4. Improved energy management.
5. Reduce industrial by-products and gas emissions.
6. Carbon removal and storage.

Since the IPCC Second Assessment Report in 1995, significant technical progress has been made to mitigate greenhouse gas emissions. Examples include the introduction and advancement of wind turbines, hybrid car engines and fuel cell technology, elimination of industrial by-products including N_2O and perfluorocarbons, and the implementation and investigation of various carbon storage techniques (IPCC, 2005)

Several methods for the storage of carbon dioxide through sequestration exist. These methods include disposal in the ocean, depleted gas wells, active oil wells, aquifers, coal mines and natural minerals. Oceanic sequestration involves discharging carbon dioxide below the thermocline where there is a negligible dissolved concentration of this gas. The ocean has adequate capacity to absorb CO_2 from combustion of all the Earth's fossil fuel resources. Depleted natural gas wells are another option for sequestration, but only have the capacity to store CO_2 from natural gas combustion since one volume of natural gas burnt produces one volume of waste CO_2. Enhanced oil recovery is another method using CO_2 to remove the substantial portion of oil remaining in wells after primary production removes approximately one-third of the oil. Only a fraction of CO_2 from oil combustion can be stored in oil wells because of the high volume of compressed waste gas compared to liquid oil. Methods for sequestration in coal mines and deep beds are under investigation. The main objective is to inject CO_2 into these formations, displacing the natural gas present and allowing CO_2 to absorb into the coal. Salt domes are another possibility for sequestration, storing CO_2 in solution-mined salt domes. Methods of deep aquifer storage of CO_2 are currently being practiced in Norway and Indonesia where waste CO_2 from natural gas purification is being pumped below the North Sea and South China Sea respectively. The last sequestration method of storing CO_2 in igneous rocks such as those containing magnesium oxide bound to silica and alumina-forming aluminosilicates is under investigation (Halmann and Steinberg, 1999).

Experimental carbon dioxide sequestration projects using geological storage methods are currently in progress at various locations. In Weyburn, Saskatchewan carbon dioxide pumped from North Dakota is used for enhanced oil recovery, storing approximately 14 million tons of CO_2 over 15-20 years (Mourtis, 2003). Another project in New Mexico, the West Pearl Queen project, will inject 2200 tons of carbon dioxide in a depleted oil field over 42 days. Carbon dioxide sequestration projects using unmined coal seams are taking place in Virginia and New Mexico. It is anticipated that the Virginia project will store 26 000 tons of carbon dioxide over 1 year and the New Mexico project will take 280 000 tons over 6 years. Storage of carbon dioxide in saline formations is also being practiced with a project in Frio, Texas expecting to store 3000 tons of CO_2 over 3 months (NETL, 2004).

Carbon dioxide sequestration methods using natural minerals are currently under investigation. Magnesium silicate minerals such as olivine and serpentine can be reacted with CO_2 to form stable carbonates. Estimates indicate that vast quantities of these natural minerals exist and their abundance far exceeds known fossil fuel reserves

(Lackner *et al*, 1995). While it has been found that the carbonation reaction efficiency can reach about 60-80%, it is inherently expensive. Research is currently being directed towards improving the process and reducing costs (Penner *et al*, 2004).

1.3 CARBON DIOXIDE ABSORPTION BY CEMENT

Another method of carbon dioxide sequestration involves the exothermic reaction of CO_2 with calcium silicate. Calcium silicate has shown its ability to uptake carbon dioxide and the process can be incorporated into concrete product production to achieve economic benefit. This process is referred to as carbonation curing and involves the intentional absorption of CO_2 by fresh concrete. Generally the curing process occurs at a high CO_2 pressure and concentration, generating a rapid, highly exothermic reaction. Equations (1.2) and (1.3) summarize the main cement anhydrate reactions (Young *et al*, 1974). Intermediate reactions not included in Equations (1.2) and (1.3) are the dissolution of $CO_2(g)$ to $CO_2(aq)$; reaction of $CO_2(aq)$ with H_2O producing H^+ and HCO_3^- ions; reaction of H^+ ions with $3CaO{\bullet}SiO_2$ and $2CaO{\bullet}SiO_2$ releasing $Ca^{2+}(aq)$; and reaction of Ca^{2+} and HCO_3^- producing $CaCO_3$.

$$3CaO{\bullet}SiO_2 + 3CO_2 + X H_2O \rightarrow SiO_2{\bullet} X H_2O + 3CaCO_3 \qquad (1.2)$$

$$2CaO{\bullet}SiO_2 + 2CO_2 + X H_2O \rightarrow SiO_2{\bullet} X H_2O + 2CaCO_3 \qquad (1.3)$$

Partial hydration prior to carbonation curing may be favourable or unpreventable in some instances, allowing both cement hydrate and anhydrate carbonation reactions to occur. Hydration products formed through partial hydration follow Equations (1.4) and (1.5), as outlined later in this section. Both fresh and partly hydrated carbonation curing methods will be investigated in this thesis.

As well as creating a sink for CO_2 storage, carbonation curing has several manufacturing and product advantages. The rapid reaction between CO_2 and anhydrate products yields higher early age strengths than those with conventional methods of curing. Production rates can therefore be increased with less time required to achieve the green strength. Carbonation curing is also expected to provide significant benefits in terms of durability. Accelerated carbon dioxide curing research at McGill University is being conducted to investigate the feasibility of using recovered CO_2 to cure concrete products, while sequestering CO_2 in calcium silicate minerals at the same time. There exists a large potential to use this technology for prefabricated concrete products such as siding panels, bricks and blocks, cement board and fiberboard. Carbonation curing can be applied to several other products where the process can be modified to allow a period of exposure to carbon dioxide gas. Concrete product manufacturing facilities could be located adjacent to cement plants, power plants or other large CO_2 emitting industries. The flue gases from these industries could then be cost effectively injected or passed through a large chamber at low pressure where concrete products absorb the CO_2, producing cleaner emissions while also positively benefiting the manufacturing process.

Carbonation curing is completely different from weathering carbonation in which atmospheric carbon dioxide reacts with calcium containing products to form calcium carbonates. Weathering carbonation involves the reaction of hydration products in hardened concrete with atmospheric CO_2 over a relatively long period. The main weathering carbonation reactions involve calcium hydroxide ($Ca(OH)_2$) and calcium silicate hydrate (CSH), as shown in Equations (1.4) and (1.5) respectively. Several other minor hydration products also react to form calcium carbonate. Weathering carbonation is unfavourable because it causes shrinkage induced cracking and in reinforced concrete products it deteriorates the protective passive film on the surface of reinforcing steel, accelerating steel corrosion. Extensive research has been performed to understand the mechanisms and develop preventative measures.

$$Ca(OH)_2 + CO_2 \rightarrow CaCO_3 + H_2O \tag{1.4}$$

$$3CaO \bullet 2SiO_2 \bullet 3H_2O + 3CO_2 \rightarrow 3CaCO_3 + 2SiO_2 \bullet 3H_2O \tag{1.5}$$

1.4 RESEARCH OBJECTIVES

To promote commercialization of carbonation technology for carbon dioxide sequestration and product development, technical benefits of the approach have to be demonstrated. These benefits include fast strength gain and enhanced long-term durability. While previous research has focused on the effect of weathering carbonation on the durability of mature concrete, it is the purpose of this investigation to research durability issues associated with carbonation cured concrete. Furthermore, while the quantity of carbon dioxide absorbed during weathering carbonation was previously of little concern, this characteristic is of significant importance when investigating carbonation curing as a method of CO_2 sequestration. The primary focus of this project will be on the carbon dioxide absorption potential by concrete products as well as their dimensional stability during the carbonation curing process and subsequent weathering carbonation in service. Other durability issues that will be investigated include compressive strength and freeze/thaw resistance. Cement paste compacts will be studied to observe the contribution by the binder while concrete compacts will be used to simulate the behaviour of concrete masonry units and pavers. The objectives of this study are explicitly itemized as follows:

1) Summarize available information pertaining to the reaction mechanism of carbonation curing and weathering carbonation as well as associated durability issues.
2) Investigate pertinent characteristics of carbonation curing, including carbon dioxide absorption, water loss and peak temperature. As well, determine the effect of presetting by partial hydration and the duration of carbonation curing on the aforementioned carbonation behaviour.
3) Quantify and compare the overall dimensional length change of various carbonation curing treatments and obtain in-situ measurements of length change during carbonation curing.
4) Measure the compressive strength of carbonation cured samples following carbonation curing and a subsequent 7-day post-curing hydration period.

Compare the strengths between various carbonation curing treatments as well as with reference hydration samples of similar ages.

5) Assess qualitatively the depth of carbonation and pH patterning observed after carbonation curing using a phenolphthalein pH indicator solution.
6) Examine through x-ray diffraction and scanning electron microscopy the products formed during carbonation curing and compare with those from conventional hydration curing.
7) Evaluate the weathering carbonation behaviour of samples cured through various carbonation curing treatments and compare with that of hydration cured samples. The behaviour will be characterized by the quantity of carbon dioxide absorbed, dimensional stability and compressive strength.
8) Verify the quantity of carbon dioxide absorbed during curing and weathering carbonation using infrared carbon dioxide analysis. Compare the values obtained between the surface layer and core of each compact.
9) Assess the freeze/thaw resistance of carbonation cured samples compared with those cured by conventional hydration.

The work of accomplishing the aforementioned objectives is presented in the remainder of this thesis. To fulfill the first objective, a comprehensive summary of relevant references is documented in Chapter 2. The experimental program executed to accomplish the remainder of the objectives is detailed in Chapter 3. The equipment, procedures, experiments conducted and methods of analysis are described in this chapter. Chapter 4 presents a summary of the qualitative and quantitative results obtained from the experimental program. This chapter also contains a detailed discussion of the results and their implications. Finally, a summary of conclusions and recommendations for future work is given in Chapter 5. Other pertinent information is shown in the Appendices at the end of this thesis.

CHAPTER 2 LITERATURE REVIEW

This Chapter provides a comprehensive review on both carbonation curing and weathering carbonation. The former was developed for fast strength gain while the latter influences the long term behaviour of concrete exposed to atmospheric carbon dioxide.

2.1 CARBONATION CURING

2.1.1 Reaction Mechanism

Accelerated curing of fresh Portland cement using carbon dioxide is achieved through the rapid conversion of calcium silicate to calcium carbonate ($CaCO_3$). Research by Young *et al* using dicalcium silicate (β-C_2S) and tricalcium silicate (C_3S) mortar compacts found the carbonation reaction to be extremely rapid during the first 10 minutes. Initially the reaction occurred between calcium silicate and dissolved carbon dioxide forming calcium carbonate and calcium silicate hydrate (CSH). Subsequent reactions occurred primarily between carbon dioxide and CSH. For C_3S compacts the degree of reaction after 3 minutes was similar to that after 12 hours of normal hydration, with comparable stoichiometry except that calcium carbonate was formed instead of calcium hydroxide ($Ca(OH_2)$). Following the initial 3 minute period, subsequent carbonation primarily involved CSH. As the reaction progressed CSH produced through hydration was rapidly carbonated and depleted of lime (CaO) and water, forming silica gel. Equation 2.1 shows the initial reaction forming calcium carbonate and CSH, where x depends on the degree of carbonation (Young *et al*, 1974). Overall the reaction products were calcium carbonate and silica gel, as described by Equation 2.2. Research conducted using dry β-C_2S and C_3S powders treated with moist carbon dioxide found similar results to the compacts. While a small quantity of CSH was formed initially the reaction end products were calcium carbonate and silica gel (Goodbrake *et al*, 1979). (Cement chemists notation is used here and the abbreviations are as follows: C – CaO; S – SiO_2; H – H_2O; and $\overline{C}$ – CO_2.)

$$C_nS + (n-x)\overline{C} + yH \rightarrow C_xSH_y + (n-x)C\overline{C} \qquad (2.1)$$

$$C_nS + n\overline{C} + zH \rightarrow SH_z + nC\overline{C} \qquad (2.2)$$

The primary carbonation reaction shifted from calcium silicate to CSH because high heat developed initially evaporated the water remaining in the sample. Calcium silicate reacts with aqueous carbon dioxide and therefore water must be present to facilitate carbonation. Evolution of high heat also caused the core material of the sample to remain largely unreacted due to insufficient water. The water content of the sample and carbon dioxide gas had an important role in the reaction rate (Young *et al*, 1974).

Analysis by X-ray diffraction of the carbonated C_3S compacts after 81 minutes indicated that calcite was the only crystalline carbonate present, with no evidence of other carbonate compounds (Young *et al*, 1974). Carbonation of dry β-C_2S and C_3S powders found that aragonite was formed unless liquid water condensed on the sample, in which case calcite formed initially while aragonite formed as the sample dried (Goodbrake *et al*, 1979). Moreover, Bukowski and Berger (1979) found that calcite and vaterite were formed during the carbonation of C_2S mortars. Previous work completed by Cole and Kroone (1960) and Sauman (1971), as cited by Young *et al* (1974), detected both aragonite and vaterite in carbonated CSH gel.

Water is necessary for the dissolution of carbon dioxide to form carbonic acid, which subsequently dissolves calcium ions to form insoluble calcium carbonate. However, too much water restricts the carbonation reaction by blocking the pore system that allows carbon dioxide to permeate into the compact (Young *et al*, 1974). Research by Klemm and Berger (1972) using Portland cement mortar found an optimal water-cement ratio of 0.1. Above this ratio carbon dioxide was not able to penetrate as deep into the samples, decreasing the degree of carbonation and compressive strength. Simatupang *et al* (1995) discovered a higher optimal water-cement ratio of 0.3 using wood-cement composites. The difference in results was attributed to the higher porosity of wood fibres over sand aggregates.

2.1.2 Compressive Strength and Durability

When compared with conventional hydration, strength gain from carbonation was rapid and the quantity of C_3S reacted after three minutes (for a pure C_3S sample) was comparable to that after 12 hours of normal hydration (Young *et al*, 1974). Strength development in C_2S compacts was similar to that of C_3S when disregarding the initially slow reaction period. There appeared to be a correlation between the quantity of C_3S reacted and the compressive strength during the initial stages of carbonation. After 27 minutes of carbonation the strength continued to increase with little reduction in C_3S. This suggested that strength gain during later stages of carbonation is attributed to the reaction between CSH and carbon dioxide. Prolonged carbonation continued to change the CSH composition while producing little change in strength (Young *et al*, 1974). Other research using C_2S and Portland cement mortars found that after 5 minutes of carbonation strengths were comparable with those after 1 day of normal hydration (Bukowski and Berger, 1979).

Following carbonation the core material of the cement specimens remained largely unreacted, providing little added strength even after prolonged carbonation. Early age strength was primarily attributed to the outer carbonated edge. Subsequent moist curing of carbonated samples provided additional strength, paralleling that of normal hydration (Young *et al*, 1974).

Intentional carbonation treatments have also been reported to improve surface hardness and decrease permeability. This results from a reduction in porosity due to the formation of calcium carbonate in previously empty pore spaces. Consequently, carbonation treatments have been used as a means to improve frost and surface wear resistance, as well as resistance to subsequent atmospheric carbonation and alkali-aggregate reaction (Metha and Monteiro, 1993). The decrease in surface permeability also acts as a protective barrier, reducing the ingress of water that can destroy the concrete structure. Creep has been found to be reduced when carbonation occurs previous to loading, but increase when carbonation occurs while the concrete is under load (Orchard, 1979). It has also been reported that carbonation treatments reduce drying shrinkage during cycles of wetting and drying (Shideler, 1963).

2.2 WEATHERING CARBONATION

2.2.1 Reaction Mechanism

Atmospheric carbon dioxide with a concentration of approximately 0.03% reacts naturally with the hydration products of hardened cement paste to form calcium carbonate. Although the carbonation reaction primarily occurs between $Ca(OH)_2$ and CSH, theoretically all CaO except that in $CaSO_4$ participate in the reaction (Shideler, 1963). Detailed in Equations 2.3 and 2.4 below are the carbonation reactions for $Ca(OH)_2$ and CSH (St. John *et al*, 1998). The carbonates generally form as vaterite, calcite and aragonite. Aragonite tends to form in poorly hydrated samples and while vaterite initially forms it is typically converted into more stable calcite (Ramachandran *et al*, 1981).

$$Ca(OH)_2 + CO_2 \rightarrow CaCO_3 + H_2O \qquad (2.3)$$

$$CSH + CO_2 \rightarrow CaCO_3 + SiO_2 nH_2O + H_2O \qquad (2.4)$$

Water must be present in the concrete pores to allow the carbonation reaction to occur, however saturation of the pores will prevent carbonation. At relative humidities below 40 percent and above 80 percent the area of menisci at the air-water interface in the pores is inadequate for effective dissolution of CO_2. Relative humidities in the range of 50 to 70 percent provide the optimal surface area for carbon dioxide to dissolve into the pore water, thereby maximizing the carbonation reaction (Ramachandran and Beaudoin, 2001).

2.2.2 Dimensional Stability

It is well established that carbonation of cured Portland cement concrete results in overall shrinkage, referred to as carbonation shrinkage. The primary carbonation reaction is between calcium hydroxide and carbon dioxide, although several other hydration products react with carbon dioxide to form calcium carbonate. Calcium carbonate has an 11% greater molecular volume than the calcium hydroxide it replaces and despite this increase in volume the reaction results in overall shrinkage (St. John *et al*, 1998).

It was hypothesised by Powers that calcium hydroxide does not convert in situ to carbonate because the increase in volume would destroy the cement paste structure (Reardon *et al*, 1989; Powers, 1962). Instead the calcium hydroxide dissolves into the water phase before reacting with dissolved carbon dioxide (carbonic acid) to form calcium carbonate. The dissolution of calcium hydroxide under compressive stresses, generated by menisci effects in the CSH matrix, and deposition of the reaction products in stress free areas causes carbonation shrinkage (Neville, 1981). Carbonation of CSH on the other hand occurs through a topochemical reaction in which no shrinkage is induced because dissolution does not occur (Ramachandran *et al*, 1981). Other work suggests that carbonation of CSH occurs through decomposition by a pseudomorphic reaction, that is, no change in form and structure occurs (Reardon *et al*, 1989). Furthermore, it has been suggested that dehydration of CSH through carbonation will result in carbonation shrinkage (Neville, 1981).

In contrast to Powers theory postulating menisci forces are responsible for shrinkage, Ramachandran and Feldman propose that shrinkage is induced by van der Waals' surface forces. As $Ca(OH)_2$ is dissolved away between points of contact van der Waals' forces pull the crystallites together, filling in the hole. This theory also suggests that the carbonation of CSH contributes to shrinkage through silica polymerization (Ramachandran *et al*, 1981).

A third theory by Swenson and Sereda attributes shrinkage to both menisci and van der Waals' forces (Ramachandran *et al*, 1981). This hypothesis suggests carbonation progresses through the cyclic wetting and drying of carbonate products around lime. As calcium carbonate forms around lime carbonation is hindered and water developed during the reaction is dissipated to the atmosphere. The relatively imperious layer then dries, generating cracks and providing additional reaction sites. Shrinkage is induced by menisci and van de Waals' forces drawing particles closer together as lime is dissolved at contact points and deposited in free pore spaces. Similar to Ramachandran and Feldman's theory, silica polymerization is responsible for the carbonation shrinkage from CSH (Ramachandran *et al*, 1981).

Although a carbonation front is found to exist along the outer exposed edges, carbonation products may also be found throughout the material. Carbonation will penetrate along fissures between cement paste and aggregates as well as cracks with widths generally wider than 0.127 mm (Short and Kinniburg, 1968). The degree of carbonation beyond the carbonation front will depend mainly on the integrity of this outer layer.

2.2.3 Durability

The weathering carbonation of cured Portland cement concrete results in a reduction in porosity and permeability (Metha and Monteiro, 1993). The carbonation reaction of $Ca(OH)_2$ results in an increase in volume with the calcium carbonate being deposited in the empty pores and capillaries. Porosity is thereby reduced and there is an overall shift in the pore size distribution towards the lower values (Reardon *et al*, 1989). In contrast, the permeability of concrete may actually be increased and the strength decreased when pozzolanic materials are used, unless the material is sufficiently cured (Metha and Monteiro, 1993). The decrease in porosity and permeability produced by carbonation provides a protective outer layer against aggressive chemicals (Ramachandran and Beaudoin, 2001). However, in poorly cured concrete and concrete with a high porosity the decrease in permeability may not be sufficient to prevent oxygen and chloride infiltration, providing little protection from reinforcement corrosion (Metha and Monteiro, 1993).

Carbonation of reinforced concrete can be detrimental to the structural integrity of reinforcement if the pH of the concrete surrounding the steel is reduced. It is the high pH concrete around the steel that provides a protective passive film against corrosion. The pH of cured concrete subjected to carbonation varies from approximately 12 in the uncarbonated core material to 8 in the outer carbonated layer (Ramachandran and Beaudoin, 2001). Between these two zones exists a thin, ill-defined region of reduced $Ca(OH)_2$, the pH of which has not yet been determined (Metha and Monteiro, 1993).

Depths of carbonation may vary from 0.5 to 2 mm in well compacted, dense concrete after several years of atmospheric exposure. Depths of carbonation between 2 mm and 5 mm may be experienced in lesser quality concretes and depths exceeding 5 mm are possible in concrete with a porous outer layer. When the carbonation depth exceeds 5 mm the nature of the carbonation zone may change, with islands of uncarbonated cement paste present in the carbonation zone and isolated areas of carbonation beyond the carbonation zone (Metha and Monteiro, 1993). Areas of carbonation may also be found along aggregate-cement fissures or within cracks, but does not typically penetrate into cracks narrower than 0.127 mm. In weak, poorly compacted, lean concrete carbonation may penetrate up to 25.4 mm in two years. A depth of no greater than 2.54 mm is typical for lightweight concrete. Without further cracking carbonation generally stops, reducing the risk to reinforcement (Short and Kinniburg, 1968).

Pozzolanic additives tend to increase the rate and depth of carbonation when compared with pure Portland cement concretes. Calcium hydroxide is consumed by pozzolanic reactions and it therefore takes less CO_2 to carbonate the remaining calcium hydroxide (Neville, 1981). Madge and Al-moundi both reported that carbonation is increased for concretes containing fly ash, while Massazza and Oberti found carbonation depths were comparable for both Portland cements and pozzolanic cements given similar strength material was used (Metha and Monteiro, 1993). However, carbonation may be decreased by pozzolanic materials since the resulting concrete has a denser structure, reducing the permeability. The overall effect of these additives is highly dependent on the nature of curing (Neville, 1981).

Less dense, lightweight aggregate concretes are more susceptible to carbonation than denser concretes because the voids in the aggregate provide a pathway for CO_2 diffusion.

However, little evidence of corrosion of reinforcing steel arising from carbonation in good quality lightweight concrete has been reported (Neville, 1981).

The resistance of reinforcement to corrosion is highly dependent on the depth of carbonation. As outlined above the depth of carbonation varies significantly from a well compacted, dense concrete to a weak, poorly compacted, lean concrete. Should the integrity of the surface layer be maintained, carbonation will not continue to propagate through the entire sample and initial pH values of the core will be preserved. For cured concrete the pH of the core will remain at approximately 12 and corrosion of steel reinforcement will be prevented.

The weathering carbonation of concrete results in a decrease in efflorescence (Orchard, 1979). These aesthetically undesirable whitish deposits are formed by the precipitation of $CaCO_3$ on the outer surface of concrete. It is hypothesised that carbonation reduces the quantity of calcium available for precipitation, thus reducing efflorescence. In hardened concrete exposed to a carbonation treatment prior to service usage the calcium in the surface layer is stable in the form of $CaCO_3$ and is not available for efflorescence. The quantity of calcium hydroxide, which is also dissolved into the surface water layer during efflorescence, is limited. The low permeability of this outer carbonated region may also contribute in reducing efflorescence. Efflorescence may occur if cracks in the outer layer develop, allowing calcium from the core to precipitate on the surface (Dow and Glasser, 2002).

2.2.4 Pre-carbonation of Hydrated Concrete Products

Research has been conducted in the past looking at treating hardened cement bearing products with elevated concentrations of carbon dioxide prior to service. This treatment is used to reduce service shrinkage from weathering carbonation. Weathering carbonation is particularly unfavourable in concrete masonry units where wall cracking is attributed to linear shrinkage. It is important to make the distinction here between carbonation curing, as discussed in Section 2.1 and pre-carbonation. In the context of this section pre-carbonation refers to treating hardened concrete products with carbon dioxide such that the carbonation reaction is between hydration products and CO_2.

Shideler investigated the dimensional stability of steam cured masonry units subjected to pre-carbonation treatments. For blocks steam cured at atmospheric pressure the results indicated that service carbonation shrinkage was reduced as well as changes in volume during cyclic wetting and drying. It was also found that carbonation occurred to the greatest extent in blocks with moisture contents that were in equilibrium with 40 to 60% relative humidity. Pre-carbonation of autoclaved blocks indicated that long-term carbonation shrinkage was also reduced. However, with autoclaved blocks the volume changes during cycles of wetting and drying were increased (Shideler, 1963).

Similar research to Shideler's was performed by Toennies to develop a process of artificially carbonating concrete masonry units. Toennies study investigated the potential of using flue gases from combustion in steam boilers, used for steam curing, as a source of carbon dioxide. Pre-carbonation was tested with both pure carbon dioxide and flue gas and it was found that early-age drying shrinkage was reduced in both cases. With flue gas treatments the greatest reduction in drying shrinkage of 53% was observed when blocks were carbonated immediately after steam curing at 150°F (93°C). After a 10 month exposure period to atmospheric carbon dioxide, the amount of attributed shrinkage was less for carbonated than non-carbonated control samples. Both pure carbon dioxide and flue gas treatments had little effect on the compressive strength, absorption and unit weight of masonry units (Toennies, 1960).

CHAPTER 3 EXPERIMENTAL PROGRAM

Three sets of experiments were conducted to investigate durability issues associated with carbonation cured cement paste and concrete compacts.

- Series One tests were performed to analyze the dimensional stability during carbonation curing and weathering carbonation. Characteristics of carbonation curing such as carbon dioxide uptake, water loss and peak temperature were obtained during curing. Compressive strength and qualitative depth of carbonation testing were performed after carbonation as well as X-ray diffraction and scanning electron microscopy on selected samples. Characteristics of weathering carbonation that were determined include carbon dioxide uptake, compressive strength and qualitative depth of carbonation. The purpose of weathering carbonation testing was to study the effect of carbonation curing on the subsequent performance of cement paste and concrete compacts in service.
- Series Two experiments were primarily conducted to obtain in-situ strain measurements of cement paste and concrete compacts and quantify their shrinkage potential during carbonation curing. In-situ temperature readings were also obtained, along with the carbon dioxide uptake and water loss after carbonation.
- Series Three testing was completed to assess the freeze/thaw resistance of simulated concrete pavers. Characteristics of carbonation determined include carbon dioxide uptake, water loss, peak temperature and compressive strength. Freeze/thaw durability testing was also conducted on a few commercially produced pavers that were available.

3.1 CARBONATION CURING APPARATUS

The carbonation curing apparatus was used to subject fresh and preset cement paste and concrete samples to a high concentration and pressure of carbon dioxide gas. Major components of the set-up included a compressed carbon dioxide gas tank, pressure vessel, thermocouple, linear variable displacement transducer (LVDT), data acquisition unit and vacuum pump. Pure CO_2 gas of 99.8% purity was used in this project to simulate recovered carbon dioxide from sources. The carbonation curing apparatus is shown pictorially in Figure 3.1 and schematically in Figure 3.2. A brief discussion of the major components will be given in the following sub-sections.

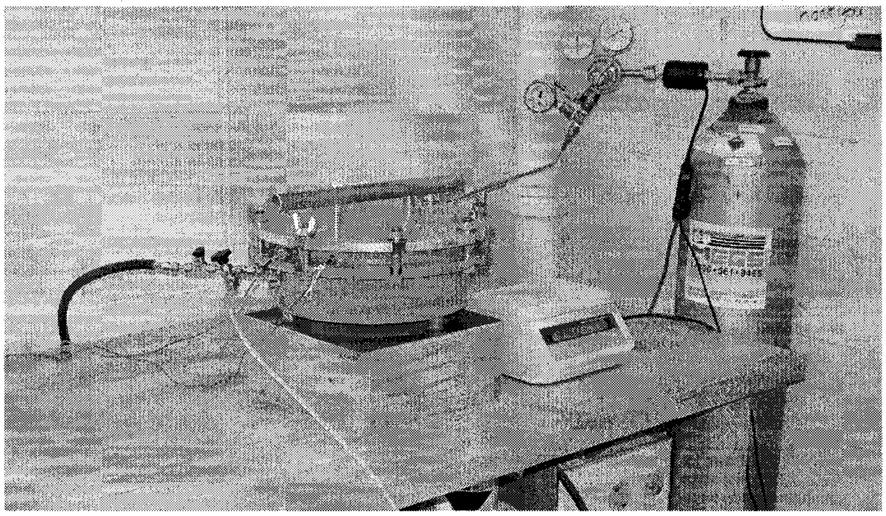

Figure 3.1: Carbonation curing apparatus

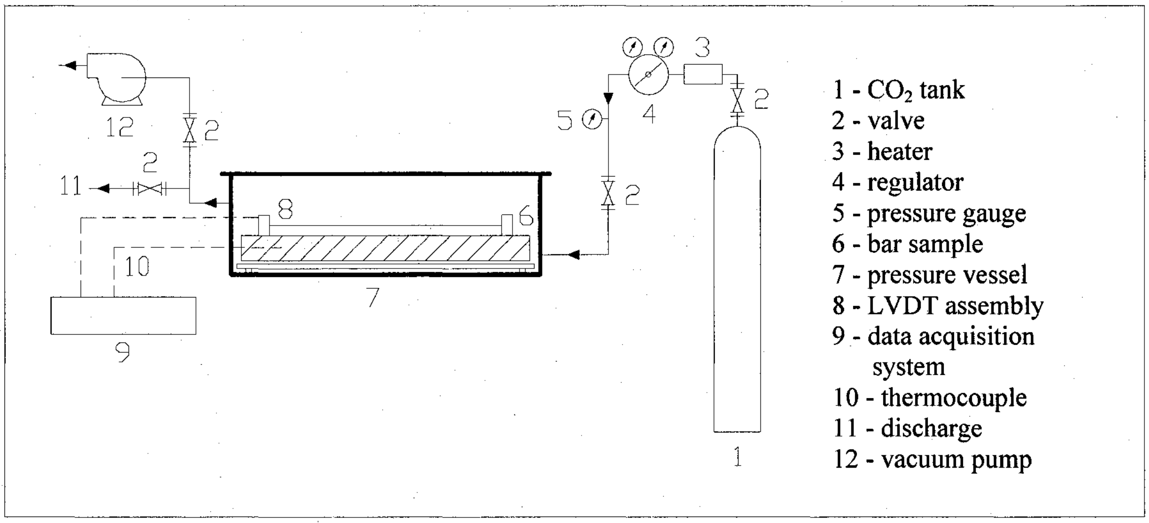

Figure 3.2: Schematic of carbonation curing apparatus

3.1.1 Compressed Carbon Dioxide Gas Tank and Fittings

Carbon dioxide gas was purchased from a local distributor (Megs Inc.) in a compressed liquid/gas state. The gas grade purity specifications were bone dry, 99.8% and the 1A cylinder size contained 27.22 kg of gas. The tank was fitted with a Model 425-125-320 Harris Calorific Inc. single stage regulator to moderate the gas pressure from the tank to the pressure vessel. Two pressure gauges were fitted to the regulator, one to monitor the tank pressure and the second to indicate the outlet pressure. The tank pressure gauge had a range of 0 to 28 000 kPa and precision of 1000 kPa, while the outlet gauge had a pressure range of 0 to 1400 kPa and precision of 50 kPa. Adjusting the regulator to the desired carbonation curing pressure allowed a constant pressure to be maintained during curing. Because the carbon dioxide gas was highly compressed in the tank it existed in a liquid/gas state at a temperature much cooler than room temperature. Therefore an electric heater was attached between the tank and regulator to warm the carbon dioxide as it exited the tank. The heater was manufactured by Matheson and thermostatically controlled to prevent overheating of the gas.

3.1.2 Pressure Vessel

Carbonation curing was conducted in a Model 1500 15 Bar Pressure Plate Extractor, manufactured by Soilmoisture Equipment Corp. The cylindrical vessel was 10 cm (4 in) deep with an inside diameter of 30 cm (12 in). Clamping bolts were used to secure the lid which was fitted with an O-ring seal. Several ports existed within the vessel walls to which the carbon dioxide supply and vacuum pump were attached. The ports also provided holes through which the thermocouple and LVDT wires were retrofitted. A third pressure gauge was attached between the regulator and pressure vessel to monitor the vacuum pressure and ensure the required pressure was supplied to the chamber. The gauge had a range of -100 to 1350 kPa and precision of 50 kPa.

3.1.3 Thermocouple

The carbonation curing chamber was equipped with a thermocouple to monitor the specimen temperature during carbonation. A Type T copper/Constantan thermocouple was used because of its superior corrosion resistance and accuracy over temperature gradients. When used in conjunction with either of the data acquisition systems detailed in Section 3.1.5 the precision was taken to 0.1°C.

3.1.4 LVDT

A Trans-Tek Model 200 LVDT was attached to Series Two specimens during carbonation curing to obtain in-situ strain measurements. The LVDT had a range of accuracy from -1.27 to +1.27 mm (-0.05 to +0.05 in) and precision of 0.00254 mm (0.0001 in). A connection was retrofitted through the pressure vessel wall to which the LVDT was connected inside the chamber once attached to a specimen. The LVDT was used in conjunction with the Measurement Group Inc data acquisition system, described in Section 3.1.5.

3.1.5 Data Acquisition Systems

A Scanning Thermocouple Thermometer was used to monitor the carbonation temperature of Series One and Three. The instrument was Model Number 692-8010 manufactured by Barnant Co. Temperatures were recorded every ten seconds and the peak temperature was easily displayed.

Series Two carbonation curing used Measurement Groups Inc System 5100 Scanner to monitor the thermocouple and LVDT. The data acquisition unit was integrated with StrainSmart Version 2.21. This application allowed data do be converted directly to engineering units, reduced and recorded at specified internals.

3.1.6 Vacuum Pump

The pressure vessel was attached to a vacuum pump to minimize the quantity of atmospheric air in the chamber prior to injecting carbon dioxide. The pump was manufactured by Central Scientific Company and was Catalogue Number 91308.

3.2 WEATHERING CARBONATION APPARATUS

Cement paste and concrete samples were exposed to accelerated weathering carbonation testing (AWCT) to simulate the conditions of prolonged exposure to atmospheric carbon dioxide during service. The AWCT chamber was designed to maintain an elevated concentration of carbon dioxide and constant humidity. Major components of the apparatus included a tank with a volume of 273 litres (60 gallons), compressed carbon dioxide gas cylinder, automatic humidity controller, dehumidification system, ultrasonic humidification system and carbon dioxide analyzer. The ACWT chamber configuration is shown pictorially in Figure 3.3 and schematically in Figure 3.4. A description of the major components is given in the following sub-sections.

3.2.1 AWCT chamber

A 273 litre (60 gallon) polyethylene tank was used as the exposure chamber for AWCT. The tank measured 889 mm in length by 584 mm in width and depth, and came fitted with a polyethylene lid. Plastic perforated shelves were placed in the chamber for the specimens to sit on and then the lid was sealed on the tank. A port was cut in the center of the lid and fitted with a Plexiglas door. A 102 mm (4 in), 0.052 m^3/s (110 cfm) fan was installed inside the chamber to provide circulation and maintain a consistent humidity and carbon dioxide concentration throughout the chamber. Where necessary, holes were made in the sides of the chamber and fittings were attached to connect with the external components.

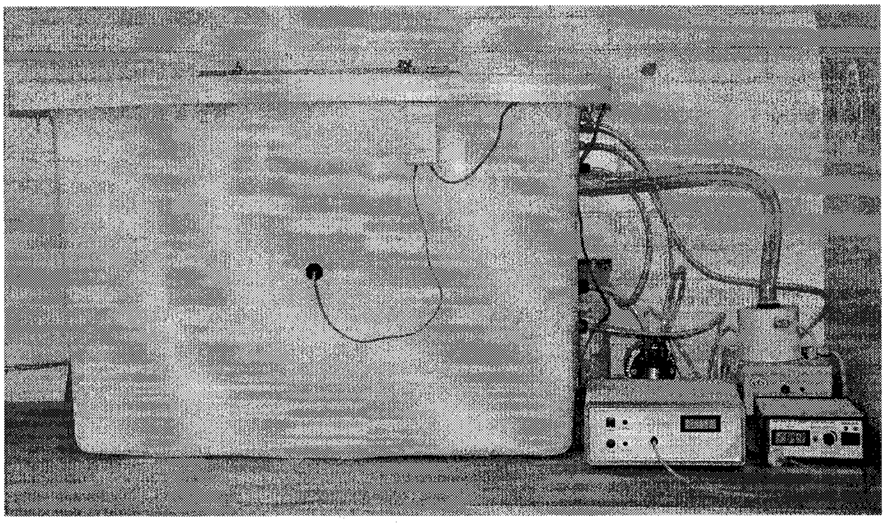

Figure 3.3: Weathering carbonation apparatus

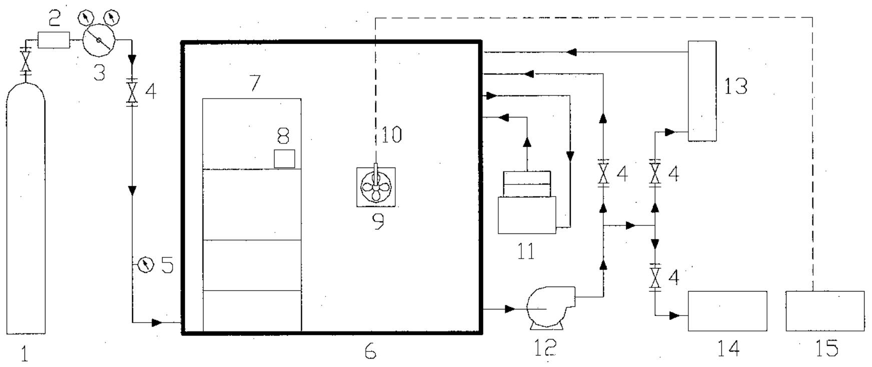

1 - CO_2 tank
2 - heater
3 - regulator
4 - pressure gauge
5 - valve
6 - AWCT chamber
7 - shelves
8 - temperature sensor
9 - fan
10 - humidity probe
11 - humidifier
12 - pump
13 - desiccator
14 - CO_2 analyzer
15 - humidity controller

Figure 3.4: Schematic of weathering carbonation apparatus

3.2.2 Compressed Carbon Dioxide Gas Cylinder and Fittings

Compressed carbon dioxide gas was used to replenish the carbon dioxide rich environment after each measuring period. The cylinder and fittings were the same as those previously discussed in Section 3.1.1.

3.2.3 Automatic Humidity Controller

Relative humidity was maintained at a constant level within the AWCT chamber through Electro-Tech Systems Inc. Model 514C Automatic Humidity Controller. The unit was capable of controlling and measuring humidity levels from 0 to 100% with a control accuracy of ±0.5% from the humidity set point. Humidity was detected through a sensing element mounted inside the chamber that provided a fast response over the entire range of 0 to 100% relative humidity (rh) with an accuracy of ±2% from 0 to 90% rh and ±3% over 90% (at 20°C). The sensor was located on the opposite wall of the chamber as the fan to ensure direct air flow, thereby minimizing moisture build up on the probe. External humidification and dehumidification systems were connected to the humidity controller and operated automatically as necessary to maintain the set relative humidity level.

3.2.4 Dehumidification System

Electro-Tech's Model 561 Dehumidification System was used in conjunction with the Automatic Humidity Controller to reduce the chamber humidity when necessary. The system was comprised of a 328 cm^3/s (1200 in^3/min) pump and calcium sulphate desiccator unit. An acrylic plastic column measuring 67 mm (2 5/8 in) in outside diameter by 289 mm (11 3/8 in) in height filled with 8 mesh indicating DRIERITE made up the desiccator unit. When switched on by the controller the pump sucked air from the chamber, forced it through the desiccator unit and then back into the chamber.

3.2.5 Ultrasonic Humidification System

In order to maintain a closed system Electro-Tech's Model 572 Ultrasonic Humidification System was retrofitted with a pump to recirculate air from the chamber. An external water tank filled with distilled water gravity fed the humidifier. When humidification was necessary the ultrasonic humidifier was switched on by the control unit and air was sucked from the chamber, through the humidifier and back into the chamber.

3.2.6 Carbon Dioxide Analyzer

The concentration of carbon dioxide in the AWCT chamber was monitored using a solid-state infrared analyzer; Quantek Instruments Model 906 Carbon dioxide Analyzer. The analyzer had a full detection range of 0 to 100% with a precision of 0.1%. Air flow through the analyzer was generated with the pump from the dehumidification system. The valve directing air flow to the desiccator unit was shut and a valve allowing flow to the analyzer was then opened. A third valve was opened directing a portion of the pumped air back into the chamber, thereby reducing flow through the analyzer to an appropriate level. Flow through the analyzer was very small and therefore it was not necessary for this system to operate in a closed loop.

3.3 PROPERTIES OF MATERIALS

3.3.1 Cementitious Binder

Experiments were conducted using CSA Type 10 Portland cement and the chemical composition is shown below in Table 3.1. The carbon dioxide content of the as received cement was 0.54% and the fineness was 373 m^2/kg.

Table 3.1: Chemical composition of Type 10 Portland cement

CaO	SiO_2	Al_2O_3	Fe_2O_3	MgO	SO_2	LOI	CO_2
63.1	19.8	4.9	2.0	2.0	3.8	2.8	0.54

3.3.2 Coarse Aggregate and Sand

Due to the bench scale nature of the experiments coarse aggregate for concrete samples was prepared by crushing 6 mm (¼ in) crushed limestone. The stone was reduced in size using a cone crusher and then sieved to collect the portion passing 4.75 mm but greater than 2.36 mm. Fine material used for the concrete samples was river sand with a fineness modulus of 2.3.

3.4 MIX DESIGN AND SAMPLE PREPARATION

The required proportions of cement, water, river sand and limestone were combined in accordance with the batch mix designs in Table 3.2. The constituents were immediately mixed for approximately 5 minutes using an industrial bakery mixer. A board dampened on the surface was then placed over the mixing bowl to prevent the evaporation of water during moulding. Samples were individually cast under a pressure of 8 MPa and then stored in a sealed container above a layer of water to minimize evaporation while the remaining samples were made.

Table 3.2: Batch mix designs

Series[2]	Batch[1]	Cement, g	Water, g	w/c Ratio[3]	River Sand, g	Limestone, g	Mix per sample, g
S1 – CP	B1-B4	5000	750	0.15	-	-	370
S1 – C	B5-B8	2019	525	0.22	2692	5383	385
S2 – CP	B9-B12	340	51	0.15	-	-	370
S2 – C	B13-16	75	20	0.22	100	200	385
S3 – P	B17-B18	1594	414	0.22	2125	4250	770

[1] quantities indicated are for each individual batch
[2] CP – cement paste, C – concrete, P – concrete pavers
[3] w/c ratio adjusted for 1% absorption by the river sand and limestone

Moulding was performed in custom made 12.7 mm (½ in) thick steel moulds that were screwed together for easy removal of a compacted sample. Bar samples were cast in a mould with inside dimensions of 25 mm (1 in) by 279 mm (11 in) and plate samples were cast in a 76 mm (3 in) by 127 mm (5 in) mould. The top plate of the moulds was a thick sliding fit steel plate. Once the appropriate mass of material was weighed out and spread evenly through the mould, the top plate was inserted and loaded. Samples were compacted using an MTS test machine to a peak load of 56 and 77 kN for bar and plate specimens respectively, yielding a compaction pressure of 8 MPa. After compaction the mould was disassembled and the sample removed and stored in a sealed container. Once all bar and plate samples had been cast they were subjected to one of four curing treatments.

The mass used to cast each sample was based on the amount of material required to achieve a 25 mm square bar, 279 mm long. This resulted in cement paste samples requiring 370 g of material per sample and concrete samples requiring 385 g. For each batch, the mix design given in Table 4.2, 4 bar and 12 plate samples were moulded. Half of each batch was carbonation cured while the other half was purely hydrated and used as reference samples. Bar samples were used for strain measurements and plate samples were used for destructive testing. Destructive testing included compressive strength testing, qualitative depth of carbonation analysis, carbon dioxide content analysis and microstructure characterization. Further information on the use of each sample and the analysis methods employed are provided in Sections 3.5 to 3.7.

The above procedure was followed for Series One cement paste and concrete samples. Batches paralleling those of Series One were made for Series Two except only one bar sample was prepared per batch. Series Three samples were prepared in a similar fashion to Series One except only 10 concrete plate samples were prepared per batch and the sample thickness was doubled to simulate concrete pavers.

3.5 SERIES ONE TESTS: CARBON DIOXIDE ABSORPTION AND CARBONATION DURABILITY

3.5.1 Carbonation Curing and Hydration

Carbonation curing was conducted on half of the specimens of each batch while the remaining half was hydrated for use as reference samples. Four different carbonation curing treatments, shown in Table 3.3, were invested to determine the effect of prolonged carbonation and partial hydration on the specimen behaviour during curing. Where presetting was required the samples were simply left in the sealed container for 17 hours. Batches B1 to B4 were cement paste samples and B5 to B8 were concrete samples.

Table 3.3: Series One carbonation curing treatments

Batch	Preset, hr	Carbonation Curing, hr
B1, B5	0	2
B2, B6	17	2
B3, B7	0	18
B4, B8	17	18

Prior to carbonation curing pre-drilled stainless steel discs approximately 5 mm in diameter were mounted on the bar samples using epoxy. Two discs were attached 203 mm (8 in) apart centre to centre down the middle of the bar for strain measurement. The holes in the centre of the discs were used by a demountable mechanical strain gauge (DEMEC) to obtain a length measurement accurate to 0.00254 mm (0.0001 in). After allowing the epoxy to dry for 1 hour the length of each bar sample and mass of every sample was recorded. A small hole about 2 or 3 mm deep by 4 mm wide was made in the side of one plate sample for the temperature probe. The mass of each sample was then measured using a 12 kg scale with a precision of 0.1 g. Half of the samples (2 bars and 6 plates) were placed in the carbonation curing chamber and the remaining samples were placed back in the sealed container for reference hydration curing.

Once the samples were in the chamber and the temperature probe was inserted into the previously made hole, the pressure vessel lid was bolted shut. The chamber was then vacuumed to 69 kPa (10 psi) and the lid bolts were again tightened. Carbon dioxide was then injected to 517 kPa (75 psi), ensuring the heater was on at least 5 minutes prior to the injection. The regulator was adjusted such that the pressure was maintained at 517 kPa for the entire duration of carbonation. After the required time had passed the carbon dioxide was released from the chamber and the vacuum was reapplied to 69 kPa. The bolts were then loosened, the vacuum released and the lid removed, taking care not to loose any evaporated water.

Immediately after removing the lid the length of each bar sample and the mass of every sample was measured. Water driven out of the samples during carbonation was collected from the chamber and weighed. Length measurements were then obtained from the hydration bar samples and the mass of every hydration sample was determined. Two carbonation cured and two hydrated samples were kept aside for compressive strength testing. The remainder of the samples were placed in a sealed container above a layer of water for a 7-day post-setting period.

In the case of concrete samples carbonated immediately after moulding it was not feasible to measure the carbonation curing strain. The samples were far too fragile prior to carbonation and attempting to measure the length would have broken the samples. The stainless steel discs for length measurement were attached after carbonation curing and purely used to determine weathering carbonation strains.

3.5.2 Dimension Stability

Using the DEMEC strain gauge length measurements were obtained from samples before and after carbonation. Three measurements were taken and the average was calculated. The carbonation curing strain was determined using Equation 3.1 below. A reading was taken from an Invar reference bar prior to each measuring period to correct strain gauge readings for minor changes in ambient temperature. Figure 3.5 shows the strain gauge taking a length measurement from a sample.

$$Carbonation\ Strain\ (\mu\varepsilon) = \frac{L_{2\,corrected} - L_1}{G} \times 10^6 \qquad (3.1)$$

Where:

$L_{2\,corrected} = L_2 - (R_2 - R_1)$

$G = 203.2 - (R_1 - L_1)$

L_1 = length before carbonation, mm

L_2 = length after carbonation, mm

$L_{2\,corrected}$ = L_2 corrected for temperature effects, mm

R_1 = reference reading before carbonation, mm

R_2 = reference reading after carbonation, mm

G = gauge length, mm

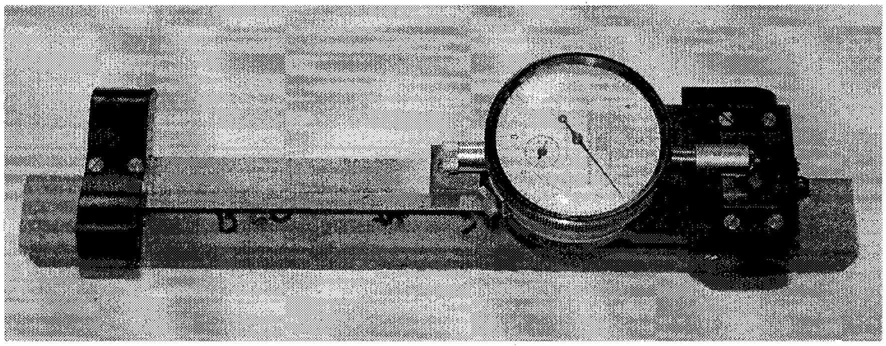

Figure 3.5: DEMEC strain gauge taking a length measurement

3.5.3 Characteristics of Carbonation Curing

Three characteristics of carbonation curing were calculated based on the data obtained; namely mass gain, water loss and peak temperature. Mass gain was a measure of the quantity of carbon dioxide absorbed per unit mass of cement and was calculated based on Equation 3.2. The average value was calculated from all the samples carbonated. Water loss during carbonation was added back into the final mass in order to determine the absolute quantity of carbon dioxide absorbed.

$$Mass\ Gain\ (\%) = \frac{M_{2\,corrected} - M_1}{M_c} \tag{3.2}$$

Where:

$M_{2\,corrected} = M_2 + W$

M_1 = combined mass of samples before carbonation, g

M_2 = combined mass of samples after carbonation, g

$M_{2\,corrected}$ = M_2 corrected for water loss, g

M_c = combined mass of cement in each sample, g

Evaporation of water from the samples during carbonation curing occurred due to the physical carbonation reaction itself and the high heat developed. Water loss was calculated to determine the percentage of total water that was lost during carbonation curing. The calculation was based on the mass of water collected on the chamber walls divided by the total water in all samples carbonated. Water loss is analogous to drying shrinkage and this figure was thought to provide some insight into the carbonation strain results obtained.

The carbonation reaction was exothermic and generated considerable heat due to the controlled curing environment. The thermocouple and Scanning Thermocouple Thermometer monitored the temperature during carbonation and the peak temperature was recorded after curing. Peak temperature data was collected to assist in evaluating the response of cement paste and concrete samples to various carbonation treatments.

3.5.4 Compressive Strength Testing

Immediately following carbonation curing two carbonated and two hydrated samples were subjected to compressive strength testing. Cement paste samples were loaded at a rate of 1 mm/min to failure using an MTS testing machine. Similarly, the compressive strength of concrete samples was tested but with a loading rate of 0.5 mm/min. The loading rates were different for the two types of samples because a higher capacity MTS testing machine was necessary for cement paste samples. Compressive strength testing of a concrete sample is shown in Figure 3.6 and the loading orientation can be observed.

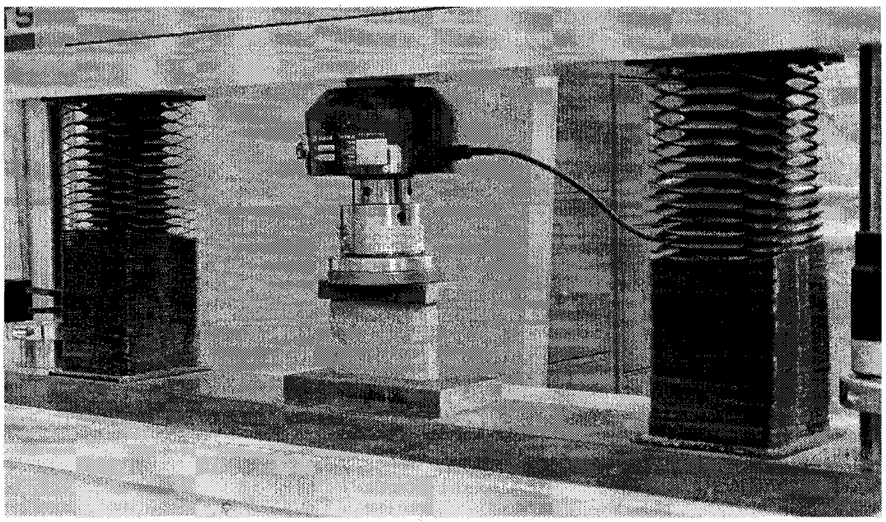

Figure 3.6: Typical compressive strength testing set-up for Series One samples

3.5.5 Qualitative Depth of Carbonation

Immediately following compressive strength testing the fresh fracture surface of a piece of each sample was sprayed with a phenolphthalein solution. After 24 hours the colour pattern was observed and a photograph was taken. Phenolphthalein solution is an acid/base indicator that turns purple at a pH above 9 (Lo and Lee, 2001). Therefore, the sample should turn purple where calcium hydroxide is present due to the high pH and colourless where calcium carbonate has been formed due to the low pH (below 9). The physical depth was not measured and the test was simply used as a qualitative measure to compare the difference in patterning between curing treatments.

3.5.6 Carbon Dioxide Content Analysis

Powder samples were collected from each fractured specimen after compressive strength testing and used for carbon dioxide content analysis. For cement paste samples powder was collected from the surface and core of each using a rotary drill. Due to the small quantity of cement paste in concrete specimens it was not feasible to collect powder from the surface and core. Instead the entire sample used for compressive testing was crushed up to liberate the cement paste from the aggregate, taking caution not to exert too much force as to crush the aggregate itself. The crushed sample was then sieved using a 45 μm sieve to collect a powder for carbon dioxide analysis. Due to the inclusion of some limestone in the concrete powder sample, a reference sample that had negligible amounts of absorbed carbon dioxide was analyzed and subtracted from each value. It was assumed within each batch that the same amount of limestone was included in each powder sample. This was found to be reasonably accurate and sufficient for means of comparing the directly measured mass gain values.

Carbon dioxide content analysis was performed using an automated ELTRA CS-800 analyser with an induction furnace and infrared detector. The instrument was calibrated using cement reference materials and synthetic carbonate standards. Only a small portion of the powder sample collected was used for carbon dioxide content analysis and the remainder was retained for future analyses. Calculation of the carbon dioxide content is shown below in Equation 3.3. The difference in the mass gain and carbon dioxide content calculation can be attributed to the denominator. For mass gain the denominator was the combined mass of cement put in each sample. Conversely, the carbon dioxide content denominator was the mass of sample tested, which included reacted water.

$$CO_2\ Content\ (\%) = \frac{CO_2\ evaporated}{mass\ of\ powder\ sample\ tested} \tag{3.3}$$

3.5.7 X-ray Diffraction

X-ray diffraction (XRD) was conducted using a Phillips PW1710 Powder Diffractometer with Cu Kα radiation. Patterns were scanned at a 2θ from 5 to 60° and a 0.02° step with 0.5 seconds per step. XRD was performed on powder samples that were collected simultaneously with carbon dioxide content samples, as outlined in Section 3.5.6.

3.5.8 Scanning Electron Microscopy

Scanning electron microscopy (SEM) was performed using a JEOL JSM-840A fitted with an EDAX Phoenix EDS microanalysis system. Photomicrographs and EDS scans were obtained for each sample tested and the crystal structure and chemical composition were compared. Small specimens with a cross section going from the surface to the core were collected from compressive strength testing samples. The specimens were stored in alcohol to prevent further carbonation and hydration from occurring before SEM was performed. Prior to SEM samples were removed from the alcohol, allowed to dry, mounted and then sputter coated with gold to prevent charging.

3.5.9 Accelerated Weathering Carbonation Testing

Following a 7-day post setting period, measured from the end of moulding, samples were subjected to accelerated weathering carbonation testing (AWCT). First, the mass of each carbonation cured and hydrated sample was determined and the length of bar samples was measured using the DEMEC strain gauge. Two carbonated and two hydrated plate samples were retained for compressive strength testing and carbon dioxide analysis while the remainder of the samples were then placed in the AWCT chamber. Carbon dioxide was injected into the chamber to a concentration of 50% and the relative humidity was set to 65%. Compressive strength testing and carbon dioxide analysis were conducted according to Sections 3.5.4 and 3.5.6.

Initially length and mass measurements were taken every day. After a few days the frequency was reduced and samples were measured every couple day. As the measurements approached a steady state the frequency was reduced further to once a week. Every time measurements were taken the chamber carbon dioxide concentration, relative humidity and temperature were recorded. A reading was taken from the Invar reference bar and then the length and mass of each bar sample was individually measured. The mass of each plate sample was then measured. Following all measurements the chamber was sealed shut, carbon dioxide was injected to a concentration of 50% and the Automatic Humidity Control was either set to humidify or dehumidify (depending on the current humidity).

The AWCT strain at time i was calculated according to the following equation:

$$Weathering\ Strain_i\ (\mu\varepsilon) = \frac{L_{i\ corrected} - L_0}{G} \times 10^6 \qquad \text{Equation 3.4}$$

Where:

$L_{i\ corrected} = L_i - (R_i - R_0)$

$G = 203.2 - (R_0 - L_0)$

L_0 = length before start of weathering carbonation, mm

L_i = length at time i after start of weathering carbonation, mm

$L_{i\ corrected}$ = L_i corrected for temperature effects, mm

R_0 = reference reading before start of weathering carbonation, mm

R_i = reference reading at time i after start of weathering carbonation, mm

G = gauge length, mm

Mass gain as previously defined in Section 3.5.3 could not be determined during AWCT due to the unquantified change in mass due to water loss. Therefore mass change, as defined for weathering carbonation, was simply the absolute change in mass in grams from the beginning of AWCT to time *i*. This measure of mass change is useful as a qualitative comparison between the behaviour of carbonation and hydration cured samples.

After a 61 day exposure period AWCT was terminated and the final measurements were recorded. Compressive strength testing and carbon dioxide analysis was performed on two carbonation cured and two hydrated plate samples according to Sections 3.5.4 and 3.5.6.

3.6 SERIES TWO TESTS: IN-SITU STRAIN DURING CARBONATION CURING

Samples of Series Two were used to obtain in-situ strain and temperature reading during carbonation curing. Each batch consisted of one bar sample and the carbonation treatments paralleled those of Series One, shown in Table 3.4. Batches B9 to B12 were cement paste samples and B13 to B16 were concrete samples. Presetting was employed in the same manner as Series One samples.

Table 3.4: Series Two carbonation curing treatments

Batch	Preset, hr	Carbonation Curing, hr
B9, B13	0	2
B10, B14	17	2
B11, B15	0	18
B12, B16	17	18

Prior to carbonation curing a small hole was made in the side of the bar sample for the thermocouple and the mass was recorded to determine the actual quantity of cement in the sample. The LVDT coil assembly was fixed in a Plexiglas mount and the core shaft was extended with a brass rod mounted in a second piece of Plexiglas. The two mounts were attached to the sample using epoxy such that the inside faces of the mounts were 203 mm (8 in) apart. The mass of the sample and LVDT assembly was then recorded as the mass before carbonation and the sample was placed in the carbonation chamber. All mass measurements were made with the same scale used for Series One, described in Section 3.5.1. The LVDT assembly mounted on a sample is shown in Figure 3.7.

Once the sample was in the carbonation chamber the LVDT was connected, the thermocouple was inserted in the previously made hole and the lid was bolted shut. The vacuum was then applied to 69 kPa (10 psi) and the lid bolts were re-tightened. Ensuring the heater had been on for at least 5 minutes, carbon dioxide was then injected to 517 kPa (75 psi) and the regulator adjusted to maintain the pressure. After the required carbonation period has elapsed the carbon dioxide was released, the vacuum was applied to 69 kPa and the bolts were loosened. The vacuum was then released and the lid removed, taking care not to loose any evaporated water. During set-up and the initial carbonation period data was recorded every second on the System 5100 Scanner. After the temperature and strain reading began to level out reading were recorded every 30 seconds. The recording interval was again increased to every second prior to releasing the carbon dioxide.

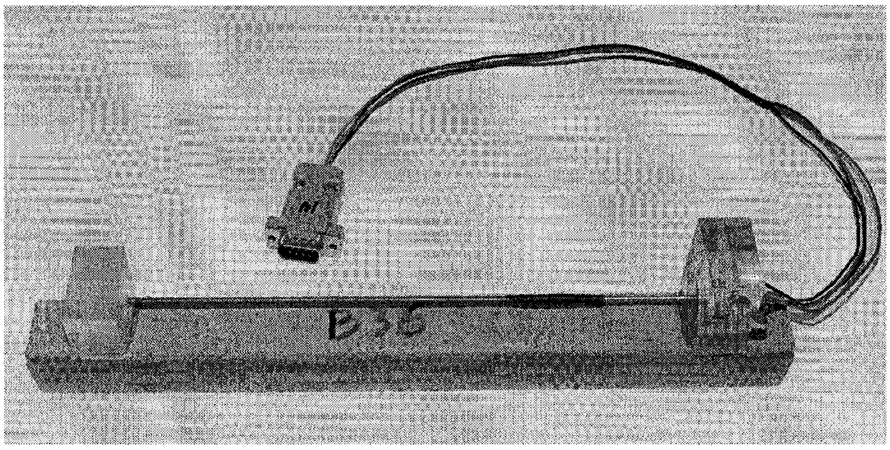

Figure 3.7: LVDT assembly mounted on a sample

Immediately after removing the lid the LVDT was disconnected and the sample mass was measured. The sample was then reconnected to the data acquisition system and left to cool for 1 hour. Water driven out of the sample during curing was then collected from the chamber walls and weighed. During cooling the recording rate was decreased to every 30 seconds once the strain readings began to level out. The distance between the inside faces of the Plexiglas mounts was measured after cooling using a vernier calliper with a precision of 0.0254 mm (0.001 in) and the gauge length was back calculated.

Carbonation strain was calculated at each data point recorded (i) according to Equation 3.5. The initial length was taken as the value before the vacuum was applied to the chamber. The immediately after carbonation length was taken as the value after the lid of the chamber was removed. These values were used so factors that influenced Series One strains were also included in Series Two.

$$Carbonation\ Strain_i\ (\mu\varepsilon) = \frac{L_i - L_1}{G} \times 1000000 \quad (3.5)$$

Where:

L_1 = initial length, mm

L_i = length at time i after the beginning of carbonation, mm

G = gauge length, mm

Mass gain and water loss were calculated in a similar fashion to that outlined in Section 3.5.3. The peak temperature was extracted from the temperature data recorded during carbonation.

3.7 SERIES THREE TESTS: FREEZE/THAW DURABILITY

3.7.1 Carbonation Curing and Hydration

Freeze/thaw durability testing was conducted with Series Three concrete samples. Due to the limited size of the carbonation chamber two identical batches of 10 samples each were prepared. Carbonation curing was performed on 5 samples from each batch and the remaining 5 were kept in a sealed container above a layer of water for use as reference hydration samples. The sample thickness was doubled from that of Series One to more closely simulate concrete pavers. The presetting and carbonation curing duration were also increased to 22 hours each for ease of sample preparation, as shown in Table 3.5.

Table 3.5: Series Three carbonation curing treatments

Batch	Preset, hr	Carbonation Curing, hr
B17, B18	22	22

Series Three samples were preset, carbonation cured and hydrated in a similar manner as Series One, outlined in Section 3.5.1.

3.7.2 Characteristics of Carbonation Curing

The mass gain, water loss and peak temperature were calculated according to Section 3.5.3.

3.7.3 Compressive Strength Testing

Following carbonation compressive strength testing was performed on two carbonated and two hydrated samples from B17 and one carbonated and one hydrated sample from B18. Compressive strength testing was conducted with an MTS testing machine at a loading rate of 0.5 mm/min. In contrast to Series One strength testing the unaxial load was applied to the broad side of the samples, as shown in Figure 3.8. Samples were tested in this fashion to obtain the compressive strength of primary concern in concrete pavers. The remaining samples were then stored in a sealed container above a layer of water for 28 days. After 28 days the compressive strength of the samples was again tested utilizing the same quantity of samples as before.

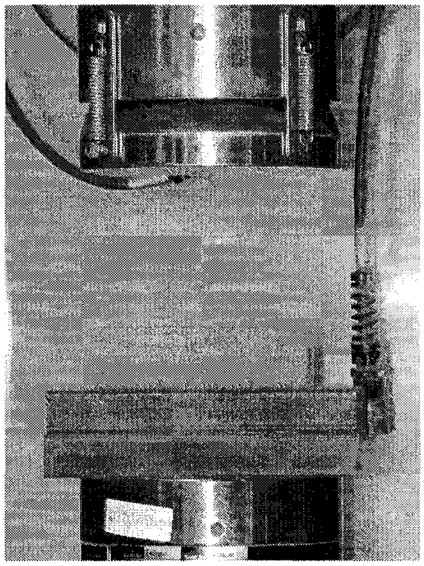

Figure 3.8: Typical compressive strength testing set-up for Series Three samples

3.7.4 Freeze/Thaw Durability Testing

Deicing salt freeze/thaw durability testing was performed according to Canadian Standards Association (CSA) A231.2-95 for Precast Concrete Pavers. Following a minimum 28-day post-setting period 3 carbonation cured and 3 hydrated samples from B18 were tested for freeze/thaw durability. The samples were brushed clean of any loose material and oven conditioned for 48 hours at 60°C. Plastic containers with a volume less than three times the sample volume were fitted with 5 mm plastic spacers on the bottom. Each sample was placed in a separate container, ensuring at least 5 mm clearance on each side, and 3% sodium chloride was poured in the container to a level 5 mm above the samples surface.

After a 24 hour saturation period the samples were subjected to cyclic freezing and thawing for 16 and 8 hours respectively. During the freezing cycles samples were stored in a freezer at -15°C. Thawing was conducted at room temperature, but never greater than 30°C and at least 5°C for the last hour.

Following 10, 25 and 50 (if necessary) complete cycles of freezing and thawing the mass loss of each sample was determined. Samples were rinsed with deionized water and the loose particles were collected using a 75 μm sieve and oven dried. The dry mass of residual material was recorded and the cumulative weight after 25 and 50 cycles was determined for each sample. If freeze/thaw testing was to continue the samples were placed back in the plastic containers, a new sodium chloride solution was poured in and freeze/thaw cycling continued. Freeze/thaw durability testing continued for 50 cycles if the cumulative mass loss after 25 cycles exceeded 200 g/m^2, but was less 500 g/m^2.

3.7.5 Supplementary Freeze/Thaw Durability Testing

Commercially produced concrete pavers previously carbonation cured at McGill University as part of a separate investigation were made available for durability testing. Table 3.6 details the samples and curing treatments they were subjected to. Deicing salt freeze/thaw durability testing was performed on the commercial pavers according to CSA

A231.2-95 for Precast Concrete Pavers. A similar procedure to that outlined above in Section 3.7.4 was used.

Table 3.6: Series Three supplemental samples carbonation curing treatments

Batch	Preset, hr	Carbonation Curing, hr
P1	2	4
P2	24	5
P3	hydration	

CHAPTER 4 RESULTS AND DISCUSSION

This chapter summarizes the results of three series of experiments conducted to determine the CO_2 absorption and durability of cement paste and concrete samples cured using carbon dioxide. Series One experiments were used for measuring carbonation curing and service weathering carbonation strain, compressive strength testing, carbon dioxide content analysis, qualitative depth of carbonation comparison, x-ray diffraction and scanning electron microscopy. As discussed in Section 3.6, Series Two testing paralleled samples of Series One with the primary purpose of obtaining in-situ strain measurements during carbonation curing. Batches B1 to B4 of Series One were cement paste samples, with similar carbonation curing treatments in batches B9 to B12 of Series Two. Concrete samples were investigated in batches B5 to B8 of Series One and parallel samples were tested in B13 to B16 of Series Two. In all tests the mass gain, water loss and peak temperature were measured. While summaries of the results are presented throughout the text, a detailed collection of the data is attached in Appendix A for Series One testing and Appendix B for Series Two testing. A third series, batches B17 and B18, was used to assess the freeze/thaw durability of carbonation cured concrete. Summarized results for these tests are presented in Section 4.3, with the complete data attached in Appendix C.

4.1 CARBONATION CURING

Four carbonation curing treatments were investigated on both cement paste and concrete samples. These treatments included 2 hour carbonation curing, 17 hour preset followed by 2 hour carbonation curing, 18 hour carbonation curing, and 17 hour preset followed by 18 hour carbonation curing. Carbonation curing durations of 2 and 18 hours were tested in order to assess the effect of exposure time on carbon dioxide uptake, dimensional stability and compressive strength. Similarly, samples were carbonated immediately and after 17-hour presetting to determine the effect of hydration products on carbonation.

4.1.1 Carbon Dioxide Absorption

4.1.1.1 Cement Paste

Results for carbon dioxide absorption by cement paste samples are shown in Table 4.1. The duration of carbonation curing was investigated for 2 and 18 hours to determine the effect of carbonation time on absorption. It was found that carbonation for a period of 18 hours resulted in 1.85% higher carbon dioxide absorptions than that for 2 hours, with samples carbonated immediately (batches B1 and B3). Preset samples (batches B2 and B4) had a mass gain 2.37% higher with 18 hour exposure as oppose to 2 hours. Young observed that the carbonation of calcium silicates was extremely rapid during the initial period. It explains why an eight times increase in carbonation duration resulted in only a 17 to 39% larger mass gain. This could potentially be the result of water starvation or the build up of reaction products in the surface layer blocking further CO_2 ingress (Young *et al*, 1974).

Table 4.1: Characteristics of carbonation curing for Series One cement paste samples

Batch	Carbonation Treatment	Mass Gain, %	Adjusted Average CO_2 Content, %	Water Loss, %	Peak Temperature, °C
B1	2 hr	10.83	9.00	20.76	89.4
B2	17 hr Preset + 2 hr	10.85	8.71	11.87	77.0
B3	18 hr	12.68	10.37	22.41	97.3
B4	17 hr Preset + 18 hr	13.22	12.23	13.73	86.2

Other characteristics of carbonation curing for cement paste samples are also shown in Table 4.1. Although the peak temperature seemed to be higher for 18 hour than 2 hour carbonation of both fresh and preset samples, their difference was mainly attributed to the experimental variations. As will be shown in Section 4.1.2, the peak temperature was approximately reached within the first 30 minutes of carbonation, decreasing beyond this period as reactions occurred at a much slower rate. Since the highly exothermic carbonation curing reaction predominately occurred during the initial stage of curing, it was expected that the peak temperature for batches B1 and B3, as well as B2 and B4 should not be dependant on the total carbonation duration. In comparing water loss, only

1.65 and 1.86% more evaporated water was produced for fresh and preset samples respectively when carbonation was increased from 2 hours to 18 hours. This occurred because the initial rapid reaction generating high temperatures, where the majority of water loss occurred, was short lived. During later periods of carbonation the reaction was slowed down, therefore producing less heat and driving off less water.

Carbon dioxide content results for samples collected from batches B1 to B4 and analyzed by infrared technology are shown in Table 4.2. It is important here to distinguish the difference between carbon dioxide content and mass gain. As detailed in Section 3.5.6 the CO_2 content was measured using an infrared-based CO_2 analyzer where as mass gain was determined by calculating the overall increase in mass during carbonation curing. CO_2 content data is presented in Table 4.2 for samples that underwent carbonation curing as well as their parallel hydration samples. The CO_2 content values are based on the average of two similar samples. Results for hydrated samples were fairly consistent with the average core carbon dioxide level measured at 0.52%, which is comparable with the as received cement CO_2 content of 0.54%. Surface levels were slightly higher, ranging between 0.73 and 0.86%, indicating that a small amount of CO_2 was absorbed during hydration of these samples. Therefore, a base carbon dioxide level of 0.52% was used to determine the adjusted CO_2 content of carbonated samples.

Table 4.2: Carbon dioxide absorption as measured by an infrared-based CO_2 analyzer for Series One cement paste samples

Batch	Carbonation Treatment	CO_2 Content, %					
		Carbonation Samples			Hydrated Samples		
		Surface	Core	Average	Surface	Core	Average
B1	2 hr	10.21	8.83	9.52	-	-	-
B2	17 hr Preset + 2 hr	9.52	8.95	9.23	0.82	0.52	0.70
B3	18 hr	11.70	10.08	10.89	0.86	0.51	0.68
B4	17 hr Preset + 18 hr	13.46	12.04	12.75	0.73	0.52	0.62

In order to correct for carbon dioxide present in the samples prior to carbonation, which was included in the raw CO_2 content data, an adjusted value was calculated. The base level CO_2 content of 0.52% was subtracted from the average CO_2 content to determine the overall batch carbon dioxide absorption during carbonation. As shown in Table 4.1, the adjusted average CO_2 content results generally support the duration of carbonation trend observed in the mass gain measurement, but in each instance the CO_2 content was found to be 1 to 3% lower. This could partly be due to the preferential sampling process, where a small quantity of powder sample cored from the surface or core was analyzed. Another reason results differ between methods of measuring CO_2 uptake was the absorption calculation. As shown in Equations 3.2 and 3.3 the mass gain calculation used the initial mass of cement before carbonation, where as the CO_2 content calculation incorporated the total powder sample mass prior to analysis. Therefore, in the CO_2 content analysis the bound water was included in the denominator and the carbon dioxide absorption value was found to be less than that in the mass gain calculation.

Comparing carbon dioxide content results between the surface and core of each carbonation sample in Table 4.2 indicates that significant carbonation occurred in the core region. After 2 hour carbonation the surface CO_2 content was only 1.38 and 1.62% higher than the core for immediate and preset treatments respectively. As would be expected there was even less variation between the surface and core after 18 hour carbonation, with differences of 0.57% for fresh samples and 0.36% for those preset. Closer surface and core carbon dioxide contents after 18 hours than 2 hours could be the result of more carbon dioxide being able to permeate deeper into the sample (of 19 mm thickness) with time, where there existed a larger portion of uncarbonated material. Similar surface and core carbon dioxide contents such as those described here suggest that the pore structure in the cement paste, with a w/c ratio of 0.15 and compaction load of 8 MPa, was interconnected and not completely saturated. Therefore, sufficient pore space existed for carbon dioxide to permeate through the matrix and dissolve in pore water, facilitating the carbonation reaction throughout the entire thickness of 19 mm.

Mass gain values for batches B1 to B4 in Table 4.1 indicate that presetting the samples for 17 hours, thus allowing hydration products to develop, had an insignificant effect on the CO_2 absorption. For 2 hour carbonation there was almost no difference in mass gain and with 18 hr carbonation there was a mere 0.54% increase when samples were preset. Previous work by Ye and Zhou found that variations in mass gain values of 1 or 2 % may be expected between replicated tests due to experimental variation (Ye, 2003 and Zhou, 2006). Therefore a difference of 0.54% is considered insignificant and mass gain appears to be similar between samples immediately carbonated and those preset first. This observation is supported by carbon dioxide content results, which found a 0.29% difference in CO_2 absorption between fresh and preset samples exposed to CO_2 for 2 hours and a 1.86% difference when carbonated for 18 hours.

Although carbon dioxide absorptions were similar between samples carbonated immediately and those preset, water loss was significantly higher for freshly tested specimens as shown in Table 4.1. Presetting the cement paste samples allowed the formation of some hydration products such as calcium hydroxide and calcium silicate hydrate. Part of the water was bound in hydration products during the hydration reaction and therefore less free water was able to escape during subsequent carbonation. Presetting also appeared to have the effect of reducing the peak temperature. As described above in the discussion about the effect of carbonation curing duration, the peak temperature was expected to be similar between 2 hour and 18 hour carbonation and the average of the two was taken to determine the effect of presetting. For samples carbonated immediately the mean peak temperature was 93.4°C and for preset samples it was found to be 81.6°C. A lower peak temperature in the preset samples was likely due to the developed hydration products dampening the rapid initial carbonation reaction.

Results for Series Two cement paste samples used to monitor in-situ strain during carbonation curing are shown in Table 4.3. Mass gain values of these samples tend to agree with those found for comparable carbonation treatments of Series One, supporting the effect of carbonation duration and presetting trends detailed above. Despite this, water loss and peak temperature values appeared to vary between comparable batches. Discrepancies in these values may be accounted for by the quantity of samples in the carbonation chamber. Batches B1 to B4 each contained eight samples in the carbonation chamber, two bars for strain measurement and six plates for compressive strength testing, while B9 to B12 had only one bar sample for strain measurement. It is interesting to note that even though Series One carbonation curing treatments contained two bars of 25 mm thickness and 6 plates of 19 mm thickness, the carbon dioxide was absorption was the same as that of Series Two with only one bar sample (25 mm thick).

In comparing similar batches, that is B1 to B9, B2 to B10, B3 to B11 and B4 to B12, the differences in carbonation curing characteristics between Series One and Two are clear. When eight samples were simultaneously carbonated the peak temperature was approximately double that of tests where only one sample was in the chamber. This was likely the combination of a smaller volume of CO_2 present in the chamber with eight samples as well as the cumulative heating effect from multiple concurrent exothermic reaction sources. CO_2 gas surrounding the samples absorbed heat generated during the reaction in order to reach a thermal equilibrium between the warm samples and cooler gas. With more samples in the chamber there was less CO_2 gas present to actively remove heat and also a greater quantity of heat being generated from the numerous samples. Water loss was also significantly higher during carbonation of multiple samples. This likely occurred because of the greater heat evolution evaporating more unbound water. It is important to note that although there was considerable difference in water loss between identical carbonation treatments, the mass gains were similar. For example, samples preset and subsequently carbonated for 18 hours had 13.73% water loss when multiple samples were carbonated simultaneously (Table 4.1) and 3.19% for one sample. Interestingly though the mass gains were comparable at 13.22 (Table 4.1) and 13.29% for multiple and single sample carbonation respectively. The influence of batch size on peak temperature during carbonation curing was apparent.

Table 4.3: Characteristics of carbonation curing for Series Two cement paste samples

Batch	Carbonation Treatment	Mass Gain, %	Water Loss, %	Peak Temperature, °C
B9	2 hr	10.65	13.99	51.6
B10	17 hr Preset + 2 hr	9.58	5.71	46.6
B11	18 hr	13.78	14.41	47.9
B12	17 hr Preset + 18 hr	13.29	3.19	41.4

4.1.1.2 Concrete

Carbonation curing results for Series One concrete samples are shown in Table 4.4. A similar duration of carbonation trend to that observed with cement paste was found for concrete samples. Increasing the duration of carbonation curing from 2 to 18 hours improved the mass gain, but to a greater extend than that observed for cement paste samples. The mass gain was 4.87% higher with 18 hour carbon dioxide exposure than that after 2 hours for fresh samples and 2.09% higher for preset samples. Carbon dioxide primarily reacted with cement during the initial stages of curing and subsequent absorption during prolonged carbonation occurred at a much slower rate.

Table 4.4: Characteristics of carbonation curing for Series One concrete samples

Batch	Carbonation Treatment	Mass Gain, %	Adjusted Average CO_2 Content, %	Water Loss, %	Peak Temperature, °C
B5	2 hr	10.15	8.01	16.49	59.9
B6	17 hr Preset + 2 hr	8.37	7.74	6.67	43.1
B7	18 hr	15.02	12.87	17.99	56.9
B8	17 hr Preset + 18 hr	10.46	10.86	5.93	41.7

Similar to cement paste samples, the peak temperatures were comparable for concrete samples that underwent 2 and 18 hour carbonation curing. The peak temperature did not increase during 18 hour carbonation because following the initial rapid carbonation reaction carbon dioxide reacted much slower with the cement and less heat was produced. Samples carbonated immediately and those preset had average peak temperatures of 58.4 and 42.4°C respectively, calculated as the average of the values shown in Table 4.4. These values represent approximately 63 and 52% of the peak temperatures achieved in cement paste samples, for immediate and preset carbonation treatments respectively. A significantly lower peak temperature occurred in the concrete samples due to a smaller quantity of cement, and therefore less simultaneous exothermic carbonation reactions. Similar to cement paste samples, water loss was only slightly higher for 18 hour carbonation than 2 hours. Significant water loss occurred during the initial rapid, highly exothermic reaction with minimal water loss during subsequent carbonation. For samples carbonated immediately the water loss was only 1.50% higher with 18 hour carbonation than 2 hours, as shown in Table 4.4. Contrary to fresh samples, preset samples experienced a slight decrease in water loss of 0.74%. This may have occurred because water lost initially was absorbed through the surrounding air back into the sample as it cooled. In both cases there was not a significant difference in water loss between 2 and 18 hour carbonation, as was seen in the cement paste carbonation curing results shown in Table 4.1.

Carbon dioxide analysis was performed on powder samples collected from the entire volume of each concrete sample. As described in Section 3.5.6 it was not possible to collect core and surface powder separately for concrete samples due to the relatively small quantity of paste present. Although efforts were made to avoid limestone aggregates in powder sampling for carbon dioxide content analysis, the collection process resulted in some limestone powder being included. In order to evaluate the CO_2 content absorbed by concrete during carbonation and eliminate the limestone effect, an adjusted CO_2 content was calculated similar to that for cement paste samples. The carbon dioxide content of hydration samples, using the same limestone aggregates, was subtracted from the CO_2 content for carbonated samples. It was assumed that the powder collection was relatively consistent between samples and the quantity of included limestone powder would be similar. Carbon dioxide content values as measured by infrared analysis are shown in Table 4.5. Adjusted carbon dioxide content values are shown in Table 4.4 and support the trend observed through mass gain measurements. Carbonation curing for a period of 18 hours had the effect of increasing the CO_2 absorption over that of 2 hour carbonation. Similar to mass gain results, the increase in carbon dioxide content from 2 hour carbonation to 18 hours was 4.86% for fresh samples and 3.12% for preset samples.

Table 4.5: Carbon dioxide absorption as measured by an infrared-based CO_2 analyzer for Series One concrete samples

Batch	Carbonation Treatment	CO_2 Content, %	
		Carbonation Samples	Hydrated Samples
B5	2 hr	15.22	7.22
B6	17 hr Preset + 2 hr	16.10	8.36
B7	18 hr	20.39	7.52
B8	17 hr Preset + 18 hr	20.11	9.25

Reviewing the mass gain results shown in Table 4.4 indicates that presetting had an adverse effect on carbon dioxide absorption. Samples carbonated for 2 hours had a mass gain 1.78% lower when they were preset rather than carbonated immediately. Similarly, fresh samples carbonated for 18 hours absorbed 4.56% more carbon dioxide, in terms of mass gain, than preset samples. Presetting the samples allowed partial hydration to occur and therefore some of the water became bound in hydration products. As a result there was less free water in the pore structure to facilitate carbonation. Although presetting had a negligible effect on cement samples, concrete samples were adversely affected by presetting, likely because of the small quantity of water in each sample. Therefore, the surface area of free water in the pores was much smaller, hindering the dissolution of CO_2 and the subsequent carbonation reaction. This behaviour would be similar to the effects of relative humidity on carbonation in which the pore water menisci area becomes too small for optimal carbonation below a humidity level of 50 percent (Ramachandran and Beaudoin, 2001). Carbon dioxide content results presented in Table 4.4 support the observation that presetting reduces the quantity of carbon dioxide absorbed during carbonation curing. Samples preset had a marginally lower CO_2 content over fresh samples when carbonated for 2 hours and with 18 hour carbonation there was a 2.01% decrease in CO_2 content when samples were preset.

Results displayed in Table 4.4 reveal that peak temperatures were lower during the carbonation of preset samples as oppose to fresh samples. Since the peak temperatures for 2 hour and 18 hour carbonation were similar, as previously described, the average value for fresh samples was determined to be 58.4°C. Preset samples had an average peak temperature of 42.4°C, representing a value 16.0°C lower than samples carbonated immediately. This trend is similar to that observed for cement paste samples and was likely due to insufficient free water in the pore structure to support the degree of rapid initial reaction that occurred in fresh samples. Water loss followed a comparable trend to that of peak temperature in that presetting the samples had the effect of reducing the quantity of evaporated water. For 2 hour carbonation curing the water loss was 9.82% less with preset samples than fresh samples and with 18 hour carbonation the difference was 12.06%. This large difference was due to water being bound in the hydration products of preset samples and therefore not as easily being able to evaporated. Less water loss in the preset samples also occurred because the initial rapid reaction and heat evolution was not as severe as in samples carbonated immediately.

Series two testing of concrete samples found carbon dioxide absorption results, in terms of mass gain, comparable with those of Series One. Table 4.6 shows the characteristics of carbonation curing for Series Two. These results support both the increase in mass gain during prolonged carbonation and decrease in mass gain due to presetting trends observed in Series One testing. However, with Series Two carbonation curing the peak temperature and water loss values were significantly lower. Samples carbonated immediately for 2 and 18 hours respectively had peak temperatures 19.7 and 15.5°C lower than Series One. Preset samples also had lower peak temperatures in Series Two testing but to a much lesser extent than that for fresh samples. In addition, water loss was affected by the difference in sample size between the test two series. Immediately carbonated and preset samples had approximately twice and ten times as much water loss, respectively, in Series One samples than Series Two. Lower peak temperatures and water loss also occurred for cement paste samples and were the result of the batch sample size during carbonation curing, as described in Section 4.1.1.1. Despite differences in peak temperature and water loss values between similar carbonation treatments of Series One and Series Two concrete samples, the carbon dioxide absorption values were relatively consistent. This observation was also noted for cement paste samples.

Table 4.6: Characteristics of carbonation curing for Series Two concrete samples

Batch	Carbonation Treatment	Mass Gain, %	Water Loss, %	Peak Temperature, °C
B13	2 hr	9.70	7.88	40.2
B14	17 hr Preset + 2 hr	7.38	0.65	41.0
B15	18 hr	12.98	6.31	41.4
B16	17 hr Preset + 18 hr	11.75	0.60	37.6

Although only average carbon dioxide contents could be obtained for concrete samples, it is suggestive from comparing cement paste carbon dioxide content results with concrete results that a high degree of carbonation occurred in the core of concrete samples. Both cement paste and concrete samples had relatively similar average carbon dioxide contents and mass gains. Cement paste samples had highly carbonated cores with marginally less carbon dioxide absorption than the surface. These results therefore suggest that the core material of concrete samples was also highly carbonated. It is interesting to note that although cement paste samples had approximately 2.5 times more cement than concrete samples, that both had relatively similar percentages of carbon dioxide absorption. Therefore, in these two mix designs the cement content had little effect on absorption and the quantity of carbon dioxide absorbed per unit mass of cement was of the same order of magnitude.

4.1.2 Dimensional Stability

4.1.2.1 Cement Paste

The dimensional stability of Series One samples was determined using pre-drilled stainless steel discs and a demountable mechanical strain gauge (DEMEC), as detailed in Section 3.5.2. Table 4.7 displays the strain results for carbonation curing of cement paste samples and the strains were based on the average of two specimens. Strain measurements were taken immediately after carbonation and following a 1 hour cooling period. Cooling the samples prior to taking the second strain measurement allowed each batch to equilibrate with room temperature, such that the sample temperature was similar before and after carbonation between each batch. In all instances carbonation curing resulted in overall shrinkage of the samples. Strain measurements after cooling ranged between -750 and -858 με, and when the deviation for each batch was taken into consideration there appeared to be little difference in the results. Deviation from the mean for each batch ranged from ±7 to ±59, indicating the results were fairly consistent. The order of magnitude for shrinkage of cement paste samples appears to be approximately 800 με.

Table 4.7: Carbonation curing strain measurements for Series One cement paste samples

Batch	Carbonation Treatment	Immediate		After Cooling	
		Strain, με	Deviation	Strain, με	Deviation
B1	2 hr	-565	±7	-783	±25
B2	17 hr Preset + 2 hr	-500	±33	-750	±46
B3	18 hr	-796	±34	-785	±31
B4	17 hr Preset + 18 hr	-771	±59	-858	±58

Immediately following 2 hour carbonation curing the strain was measured in the order of -500 με, as shown in Table 4.7. During cooling the order of magnitude decreased about -300 με, resulting in a strain of approximately -800 με. Samples carbonated for 18 hours on the other hand had strain in the order of -800 με immediately after carbonation, with little subsequent change in strain during cooling. It appears that little permanent strain occurred beyond the initial 2 hour period for 18 hour carbonation since the strains after cooling for both durations were similar. Comparable strain measurements before and after cooling for 18 hour carbonation indicate that the later 16 hours allowed the samples to cool. Therefore when the samples were removed from the chamber they were closer to equilibrium with room temperature than samples carbonated for 2 hours and a lesser degree of length change occurred. Samples carbonated for 2 hours were still relatively warm when removed from the carbonation curing chamber and the strain during cooling was much larger, approximately 3 times greater than samples carbonated for 18 hours.

Series Two dimensional stability testing was performed using a linear variable displacement transducer (LVDT) and the results for cement paste samples are shown in Table 4.8. The accuracy of measurements using the LVDT was greater than that using the DEMEC strain gauge and it was therefore possible to make distinctions between small differences in strain measurements. Strain measurements after cooling between 2 and 18 hour carbonation appear to differ for both immediately carbonated and preset samples. 18 hour carbonation of fresh samples resulted in 155 με less shrinkage than that for 2 hour carbonation and with preset samples the difference was 144 με. Examining the in-situ strain readings graphically in Figures 4.1 and 4.3 for 2 and 18 hour carbonation of fresh samples reveals the carbonation strain behaviour was similar for both durations. Figure 4.3 shows that the shrinkage for 18 hour carbonation was less than that for 2 hours because after approximately 2 hours of carbonation the strain began to increase, that is, the sample began to expand. Terminating the 2 hour carbonation test prior to or part way through this expansion stage resulted in a larger shrinkage measurement. It can be seen when closely inspecting the 2 hour in-situ carbonation strain results in Figure 4.1 that the sample was just starting to expand before the carbonation curing ended. Preset samples followed a similar carbonation strain trend between 2 and 18 hour treatments as fresh samples, shown in Figures 4.2 and 4.4.

Table 4.8: Strain measurements for Series Two cement paste samples

		Carbonation Strain, με			
Batch	Carbonation Treatment	Immediate	After Cooling	Maximum Shrinkage	Maximum Expansion
B9	2 hr	-444	-459	-486	182
B10	17 hr Preset + 2 hr	-369	-367	-392	380
B11	18 hr	-289	-315	-434	106
B12	17 hr Preset + 18 hr	-225	-223	-306	310

In comparing the strain results between immediately carbonated and preset samples of Table 4.8 it appears that less shrinkage occur for preset samples. Strain measurements after cooling indicate that the shrinkage for 2 hour carbonation was 444 με when the sample was carbonated immediately and 367 με when preset, representing a 77 με decrease in shrinkage. For 18 hour carbonation presetting caused a 92 με decrease in shrinkage, with strain measurements of -315 and -223 με for fresh and preset samples respectively. The reduction in shrinkage due to presetting for both durations was similar and likely occurred because hydration products had partially formed, developing some internal structure and strength to resist shrinkage. As well, preset samples had less free water that evaporated during the high heat evolution of carbonation, causing less shrinkage analogous to that of drying.

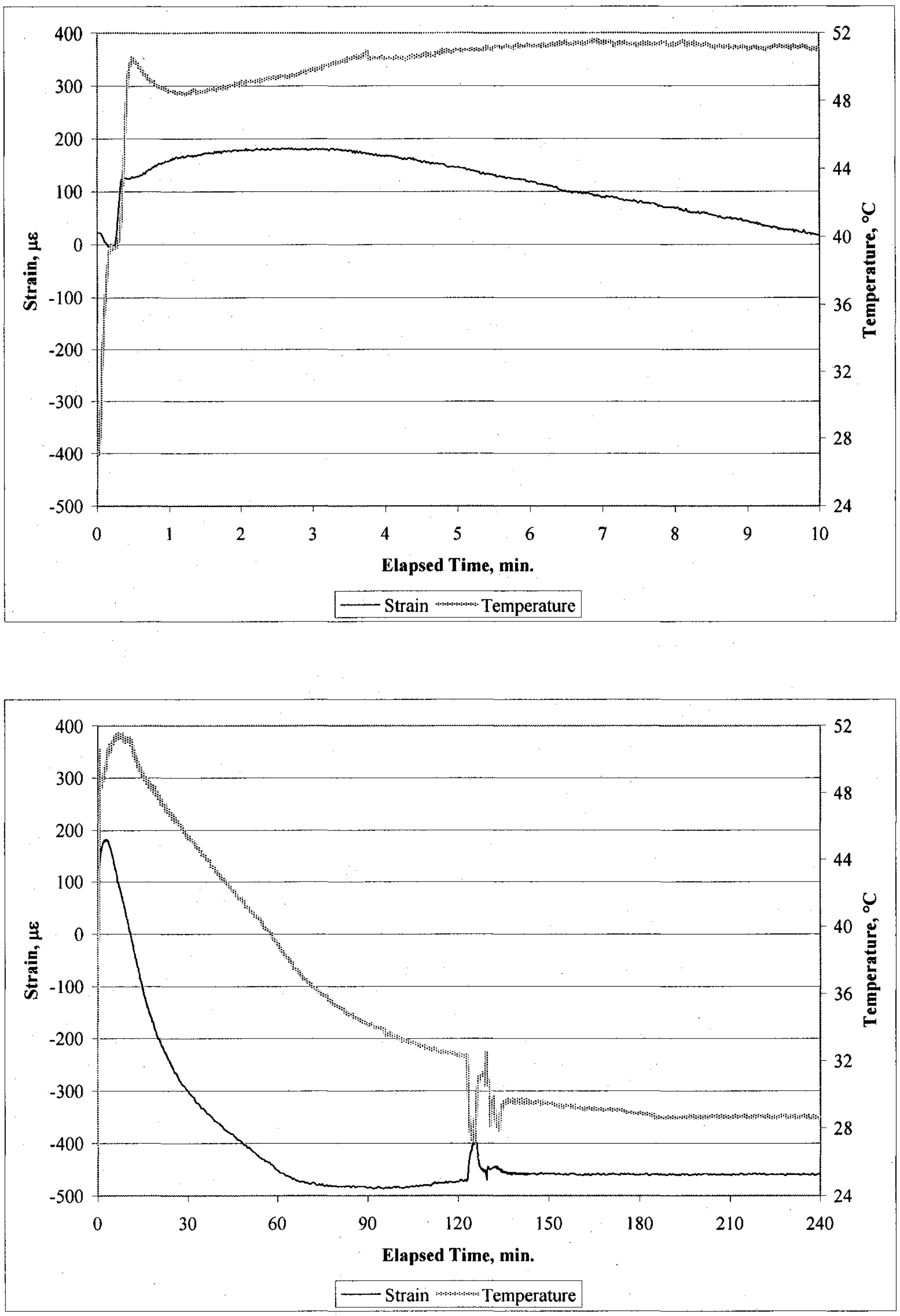

Figure 4.1: In-situ carbonation curing strain measurement for batch B9 (a) first 10 minutes, (b) full duration (2 hours)

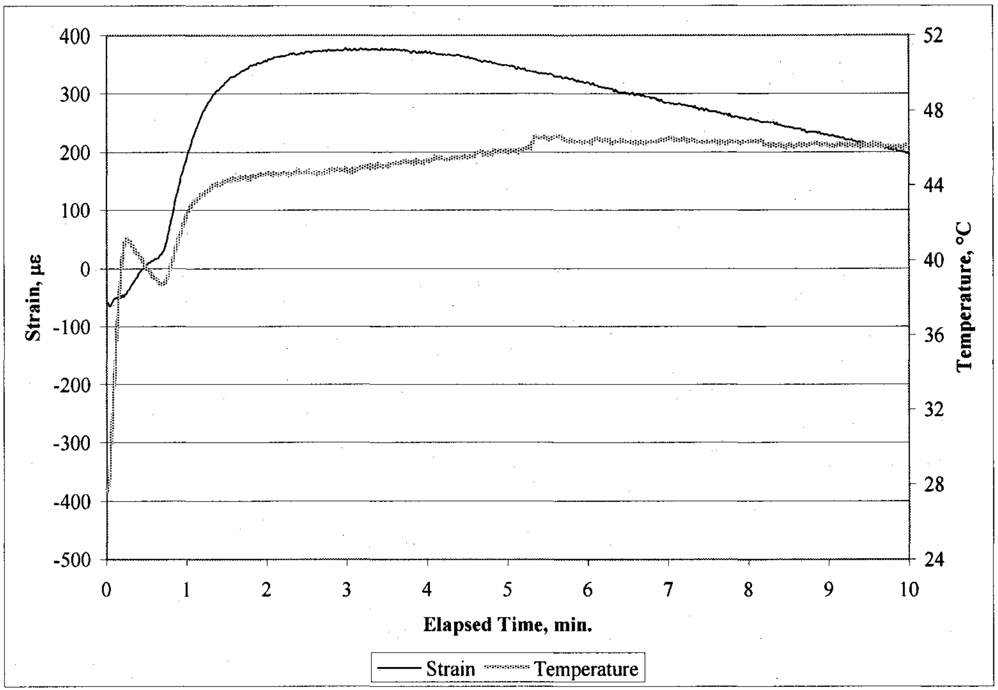

(a)

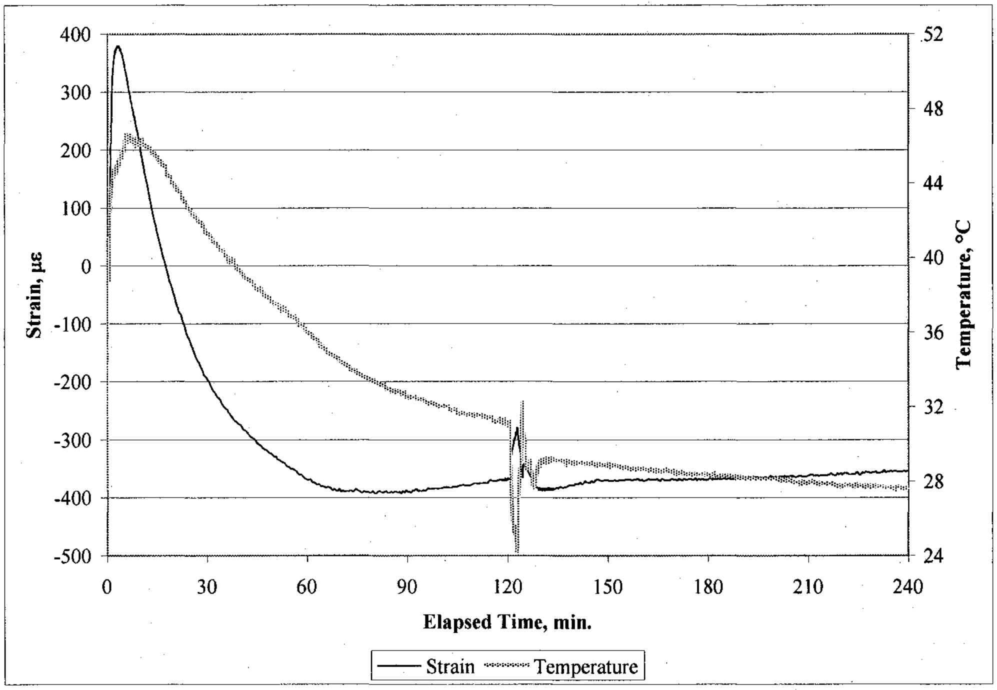

(b)

Figure 4.2: In-situ carbonation curing strain measurement for batch B10 (a) first 10 minutes, (b) full duration (2 hours)

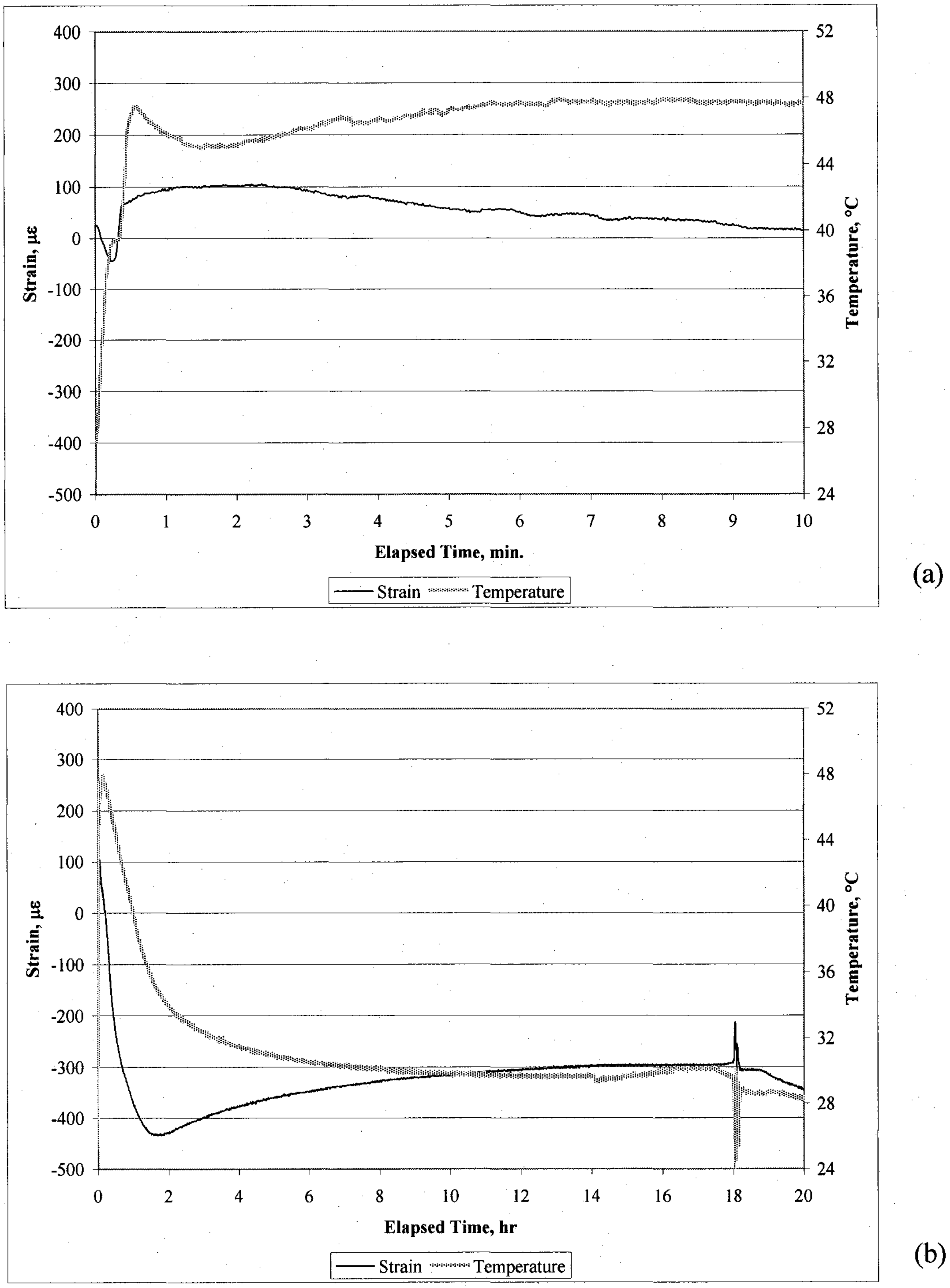

Figure 4.3: In-situ carbonation curing strain measurement for batch B11 (a) first 10 minutes, (b) full duration (18 hours)

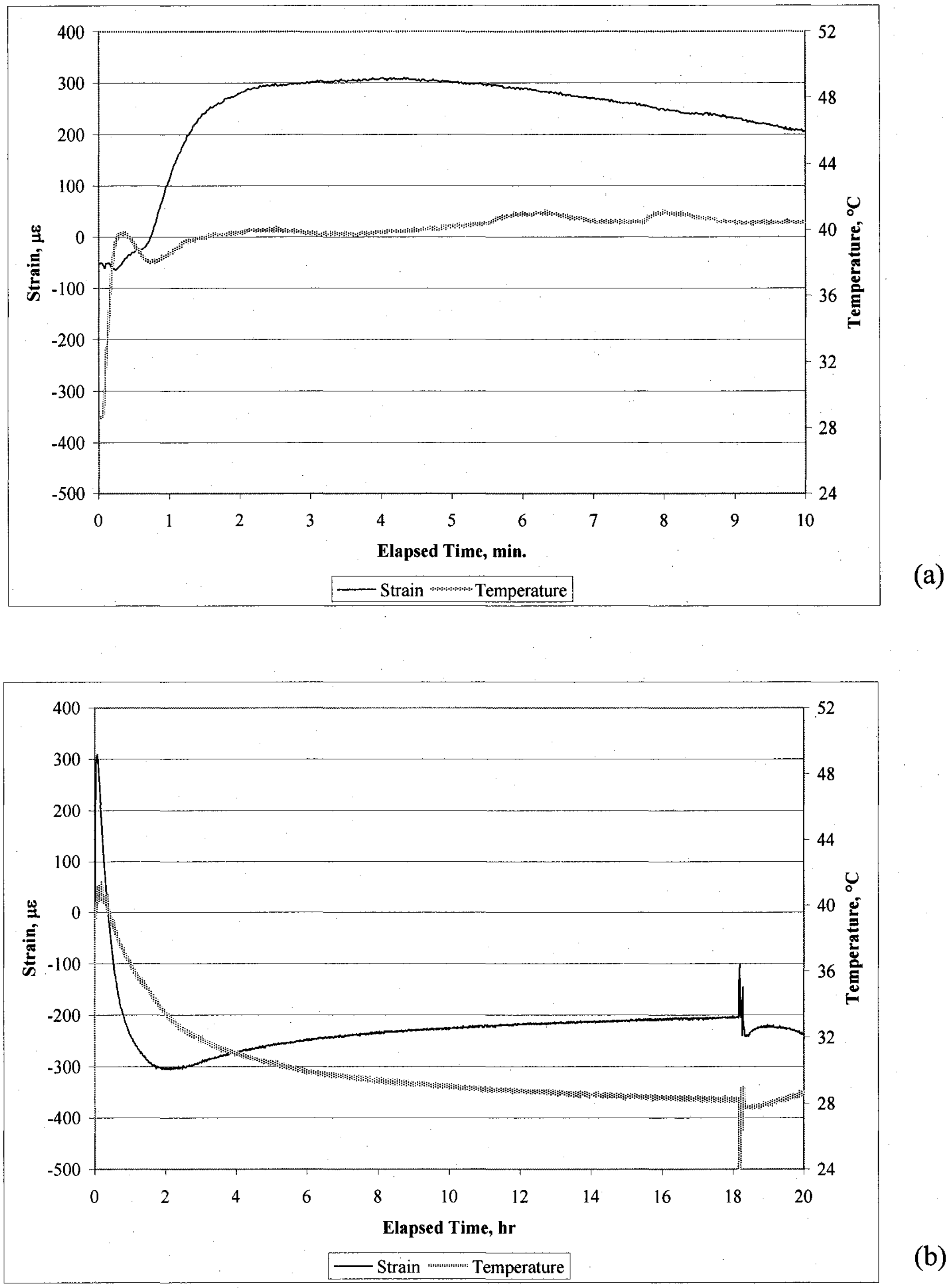

Figure 4.4: In-situ carbonation curing strain measurement for batch B12 (a) first 10 minutes, (b) full duration (18 hours)

In-situ carbonation curing strain results plotted in Figures 4.1 to 4.4 showed that the strain response for preset samples differed slightly from immediately carbonated samples. In both cases the samples experienced an initial period of expansion lasting approximately 2 to 4 minutes, shown in Figure 4.1a to 4.4a. In preset samples the expansive strain during this initial period was in the order of 200 $\mu\varepsilon$ greater than that for fresh samples, shown numerically in Table 4.8. Following this the samples shrank for about 2 hours, shown in Figures 4.1b to 4.4b, with fresh samples reaching a shrinkage strain approximately 100 $\mu\varepsilon$ more than preset samples. The end of the shrinkage stage marked the termination of 2 hour carbonation and resulted in the preset sample having an overall shrinkage value in the order of 100 $\mu\varepsilon$ less than the sample carbonated immediately. Continued carbonation curing for the 18 hours found that after approximately 2 hours the samples began to expand again. Expansion decreased with time and the samples reached dimensional equilibrium around 15 hours, with both the fresh and preset samples expanding approximately 100 $\mu\varepsilon$ from 2 to 18 hours. As a result, the overall shrinkage after 18 hour carbonation was about 100 $\mu\varepsilon$ less than that of 2 hours.

In addition to strain measurements, Figures 4.1 through 4.4 show the in-situ temperature readings. Temperature curves generally follow the same trend for each carbonation treatment, except the peak was higher for immediately carbonated samples than preset samples as discussed in Section 4.1.1.1. Reviewing the first 10 minute plots (Figures 4.1a through 4.4a) it can be seen that the temperature increased rapidly when carbon dioxide gas was first injected into the chamber due to the rapid initial reaction on the sample surface. Following this initial increase the temperature momentarily began to decrease as heat dissipated from the sample surface, but quickly increased again as the reaction continued. The temperature then reached a second maximum before beginning to decrease again. It is important to note that this all occurred quite rapidly within the first few minutes of carbonation and is only visible on the expanded plots. The temperature then continued to decrease with time as the carbonation reaction occurred at a much slower rate and heat dissipated from the system. It is interesting in comparing the strain and temperature plots for each test that the two curves have some significant similarities. When the temperature initially increased rapidly, the strain experienced a large expansive increase as well. The strain also began to decrease (shrinkage) at a relatively similar point as the temperature, both decreasing simultaneously until the strain reached a minimum. At this point the curves differed and the temperature continued to decrease, more and more slowly with time until equilibrium was reached, while the strain began to increase (expansion) once again before finally reaching a steady state.

Strain results for Series Two samples differ from Series One and are approximately 50% smaller. As described in Section 4.1.1 the sample size for Series Two testing was one-eight that of Series One, affecting the peak temperature and water loss during carbonation curing. With a smaller sample size, Series Two testing had a lower peak temperature, causing less water loss through evaporation, and thus less shrinkage. It is suggestive from this data that sample size, affecting the peak temperature and water loss, had a large influence on the strain achieved during carbonation. Both series underwent similar carbonation treatments and had comparable carbon dioxide absorptions, yet shrinkage was noticeably higher for Series One.

It is noteworthy here to point out that little variation existed between the immediate and after cooling strain measurements for both 2 and 18 hour carbonation curing in Series Two. This differs from Series One testing, where significant variation in strain was observed during cooling after 2 hour carbonation, because the peak temperatures for Series Two were significantly lower. Therefore, less time was required for the developed heat to dissipate and the samples were near room temperature prior to the cooling stage. Another feature of the in-situ strain plots is that the curves did not necessarily begin at zero strain. In order to obtain results comparable to those measured using the gage studs, zero strain was taken prior to putting the samples in the chamber and therefore some initial strain was created during vacuuming the chamber. Another feature is the fluctuations in the strain and temperature curves at approximately 2 hours in Figures 4.1 and 4.3, and 18 hours in Figures 4.2 and 4.4 which were caused during the termination of carbonation curing. Releasing the carbon dioxide gas from the chamber, and applying the vacuum caused these changes and they were included in the overall strain results since similar factors affected Series One measurements.

In general there was greater water loss during Series One carbonation than Series Two and shrinkage results between similar carbonation treatments related accordingly. For instance, batch B4 of Series One had a mass gain of 13.22% and its parallel batch B12 in Series Two had a comparable mass gain of 13.29%. Nevertheless, water loss was approximately 77% lower with Series Two than Series One and the carbonation strain had a similar reduction of 74%. A comparison of the reduction in water loss and shrinkage as the result of the smaller sample size is shown in Table 4.9. For preset samples the reduction in water loss and shrinkage appears to be similar, as was the case in the example illustrated above. With samples carbonated immediately a larger reduction in strain than water loss was observed. These results indicate that water loss had a strong influence on the degree of shrinkage observed during carbonation.

Table 4.9: Comparison of carbonation curing water loss and after-cooling strain between Series One and Series Two cement paste samples

Carbonation Treatment	Mass Gain, %		Water Loss, %		Shrinkage, με	
	Series One	Series Two	Series One	Series Two	Series One	Series Two
2 hr	10.83	10.65	20.76	13.99	783	459
17 hr Preset + 2 hr	10.85	9.58	11.87	5.71	750	367
18 hr	12.68	13.78	22.41	14.41	785	315
17 hr Preset + 18 hr	13.22	13.29	13.73	3.19	858	223

4.1.2.2 Concrete

Dimensional stability results for Series One testing of concrete samples are shown in Table 4.10. As discussed in Section 3.5.1 it was not feasible to collect strain measurements using the DEMEC strain gauge for concrete samples carbonated immediately because of the extremely fragile nature of the samples. In contrast to cement paste samples, concrete samples experienced expansion during carbonation curing as oppose to shrinkage. Expansion for 2 hour carbonation after cooling was 131 με, approximately twice that of 18 hour carbonation which had a strain of 56 με.

Minimal deviation from the mean was found between the two strain samples in each batch, with deviations of 19 με for 2 hour carbonation and 6 με for 18 hours.

Table 4.10: Strain measurements for Series One concrete samples

Batch	Carbonation Treatment	Immediate		After Cooling	
		Strain, με	Deviation	Strain, με	Deviation
B6	17 hr Preset + 2 hr	206	±19	131	±19
B8	17 hr Preset + 18 hr	138	±13	56	±6

Strain measurements immediately following carbonation curing were approximately 80 με higher than after cooling results. The fact that both 2 and 18 hour carbonation strain measurements changed by similar amounts when removed from the chamber indicates that there was negligible difference in sample temperature after carbonation for 2 and 18 hours. Conversely, Series One cement paste samples carbonated for 2 hours exhibited significantly higher changes in strain after cooling than 18 hour carbonation because evolved heat from the carbonation reaction had not fully dissipated and was possibly still being generated. This behaviour did not occur in concrete samples because there was approximately half the quantity of cement per sample and the peak temperature was significantly lower. Heat generated during carbonation had sufficiently dissipated and was not being produced at a high enough rate to elevate the sample temperature after 2 hours of exposure.

In-situ dimensional stability results for Series Two testing of concrete samples are displayed in Table 4.11. In all instances carbonation curing led to overall sample expansion with comparable magnitudes for both 2 hour and 18 hour carbonation curing. Immediate and after cooling strains were similar for each carbonation treatment because sufficient heat had dissipated from the samples prior to removal from the chamber. The strains after cooling for samples carbonated immediately were 15 and 26 με for 2 and 18 hour carbonation curing respectively. Preset samples also had similar strains between carbonation durations with 158 με for 2 hour carbonation and 141 με for 18 hours. Moreover, in-situ carbonation strain measurements plotted in Figure 4.5 to 4.8 indicate that both 2 hour and 18 hour carbonation followed similar strain paths during the first 2 hours. As previously discussed for cement paste samples, this behaviour was expected because the first 2 hours of carbonation curing are analogous between durations. Since most of the carbonation reaction, evolved heat and water evaporation occurred during the initial two hours, subsequent changes in strain were significantly less.

Table 4.11: Strain measurements for Series Two concrete samples

Batch	Carbonation Treatment	Carbonation Strain, με Immediate	After Cooling	Maximum Shrinkage	Maximum Expansion
B13	2 hr	15	15	-51	118
B14	17 hr Preset + 2 hr	158	158	-26	234
B15	18 hr	28	26	-87	96
B16	17 hr Preset + 18 hr	172	141	-56	240

Comparing strain results in Table 4.11 indicates that greater strain was exhibited in preset samples than those carbonated immediately. Preset samples had overall strains in the order of 150 με while fresh samples had approximately 20 με. Although the maximum shrinkage strain for each sample was similar, the effect of presetting on carbonation strain can be seen by the larger maximum expansive strains for preset samples. Maximum expansive strains for preset samples were approximately 100 με greater than those for fresh samples, accounting for the difference in overall expansion between carbonation treatments. This behaviour can also be observed graphically in Figure 4.5 through 4.8. The strain curves for fresh and preset samples followed the same general trend with the distinguishing feature between the two being the degree of expansion during the initial few minutes. In Figures 4.5 and 4.7 the strain curves for immediately carbonated samples tended to peak around 100 με while those in Figures 4.6 and 4.8 for preset samples continued increasing until approximately 200 με. Subsequent to the peak both treatments followed a similar strain path, resulting in an overall difference between fresh and preset samples.

Temperature readings recorded during Series Two carbonation curing testing are plotted along with the strain curves in Figures 4.5 to 4.8. For immediately carbonated samples the temperature increased rapidly within the first 30 seconds to about 37°C, then decreased a few degrees before increasing again to a second larger peak temperature of approximately 41°C around 2 minutes. The temperature then decreased slowly until equilibrium was reached at approximately room temperature. This behaviour differed for preset samples and it was found that the temperature peaked during the initial rapid increase within the first 30 seconds. Following this peak the temperature decreased more significantly than fresh samples and only rose again slightly before decreasing to equilibrium with room temperature. As discussed in Section 4.1.2.1, there appeared to be some correlation between temperature and strain. During the initial rapid increase in temperature the samples experienced slight shrinkage and when the temperature decreased temporarily, then increased again the samples went through expansion. Finally, while the temperature cooled to equilibrium the samples underwent shrinkage. This behaviour was similar for all carbonation treatments and variation in the overall strain between treatments was developed through differences in the magnitudes of shrinkage and expansion.

The after cooling strains observed for Series Two preset samples were slightly higher than those for Series One. As was discussed in Section 4.1.2.1 for cement paste, this occurred because the peak temperatures and water loss were lower during Series Two carbonation tests with one sample per batch than their parallel batch in Series One with 8 samples. A comparison of mass gain, water loss and strain for Series One and Series Two is presented in Table 4.12. In concrete samples the increased strain from Series One to Series Two was observed as greater expansion and was analogous to that of cement paste samples where the increased strain appeared as a decrease in shrinkage. That is, in both cases lower peak temperatures and water loss during Series Two testing resulted in greater overall strains.

Table 4.12: Comparison of carbonation curing water loss and after-cooling strain between Series One and Series Two concrete samples

Carbonation Treatment	Mass Gain, %		Water Loss, %		Expansion, με	
	Series One	Series Two	Series One	Series Two	Series One	Series Two
2 hr	10.15	9.70	16.49	7.88	-	15
17 hr Preset + 2 hr	8.37	7.38	6.67	0.65	131	158
18 hr	15.02	12.98	17.99	6.31	-	26
17 hr Preset + 18 hr	10.46	11.75	5.93	0.60	56	141

It is interesting to note that both cement paste and concrete samples had maximum strain values in Tables 4.8 and 4.11 with similar order of magnitudes, for related carbonation treatments, while the overall strains were significantly different. This can also be observed by comparing similar carbonation treatments between cement paste and concrete in Figures 4.1 to 4.8. It appears that during the initial carbonation reaction where expansion occurred, both cement past and concrete samples had comparable behaviours. Subsequent to this expansion, both types of samples underwent shrinkage and it was here where a significant difference was observed. While cement paste samples continued to shrink past their initial length at zero strain, shrinkage of concrete samples was considerably less and they remained in an expanded state. Less shrinkage may have occurred in concrete samples because the aggregate created a structure that resisted shrinkage. (In concrete samples the composition of fine and course aggregate was 76% by weight.) While in an expanded state the carbonation products, mainly calcium carbonate crystals, may have been formed between the aggregates, resulting in overall expansion after shrinkage ceased.

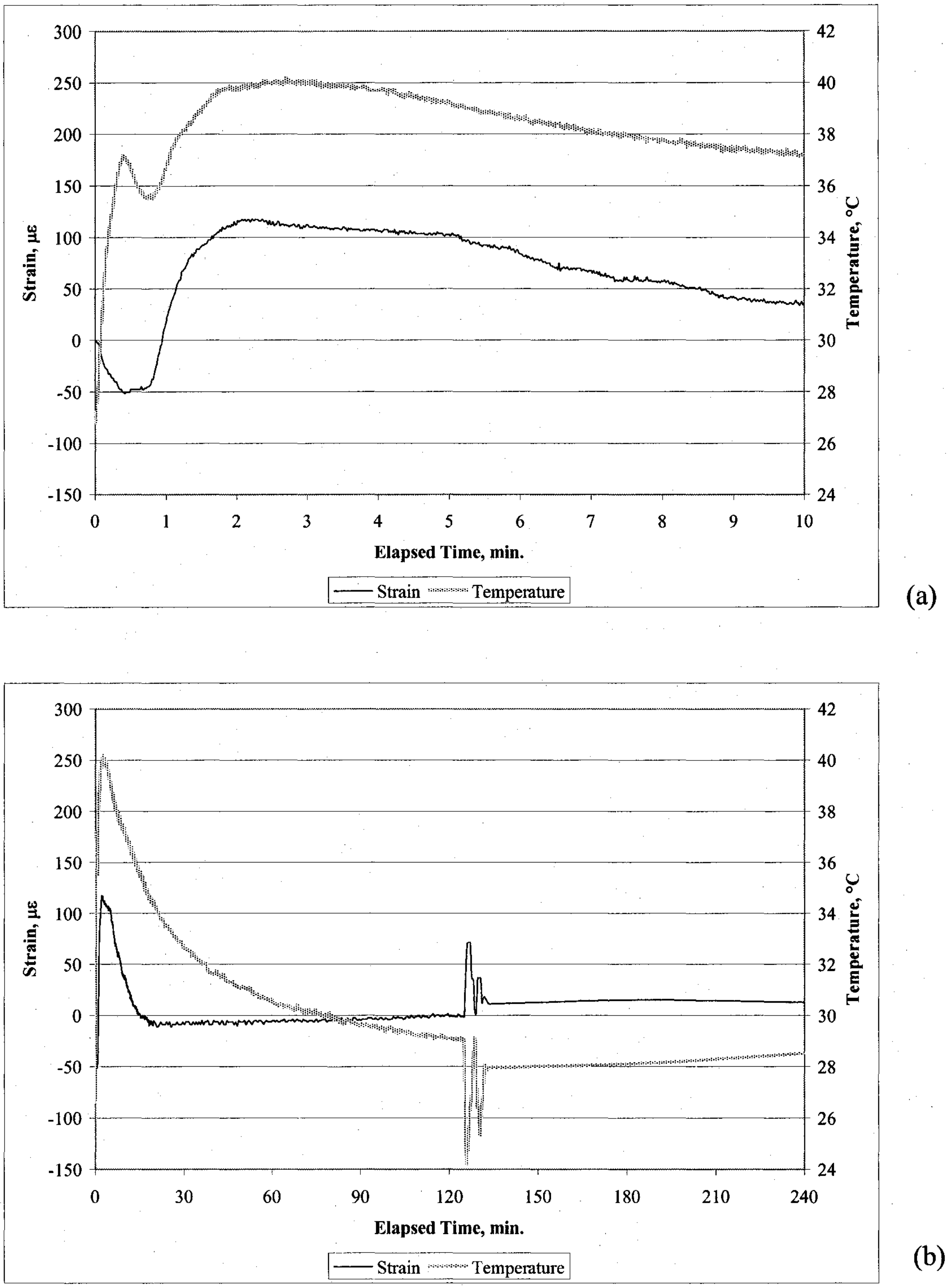

Figure 4.5: In-situ carbonation curing strain measurement for batch B13 (a) first 10 minutes, (b) full duration (2 hours)

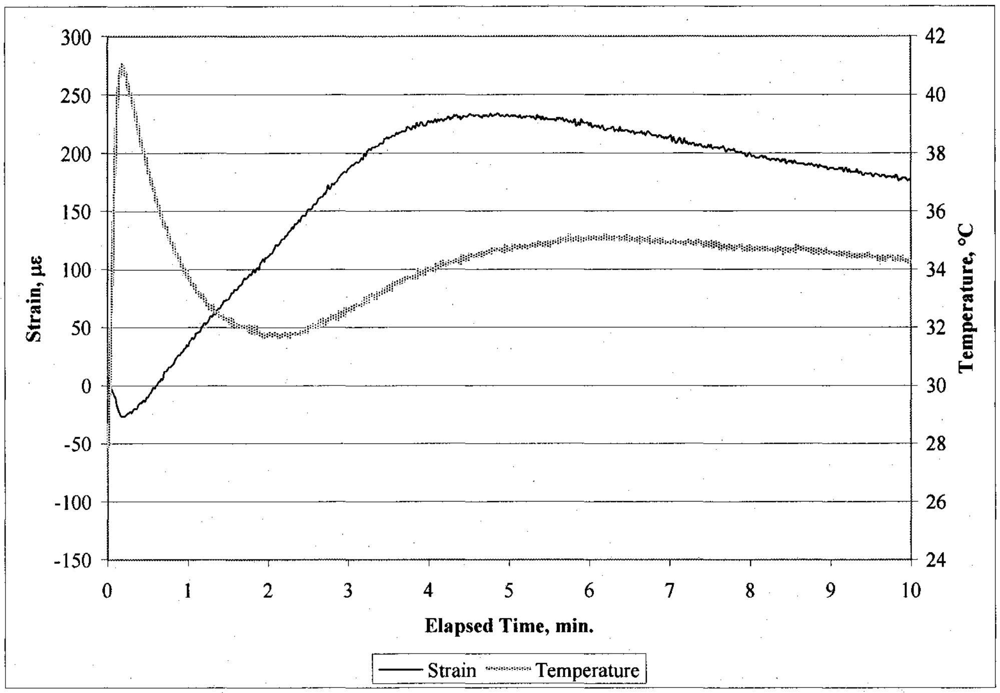

(a)

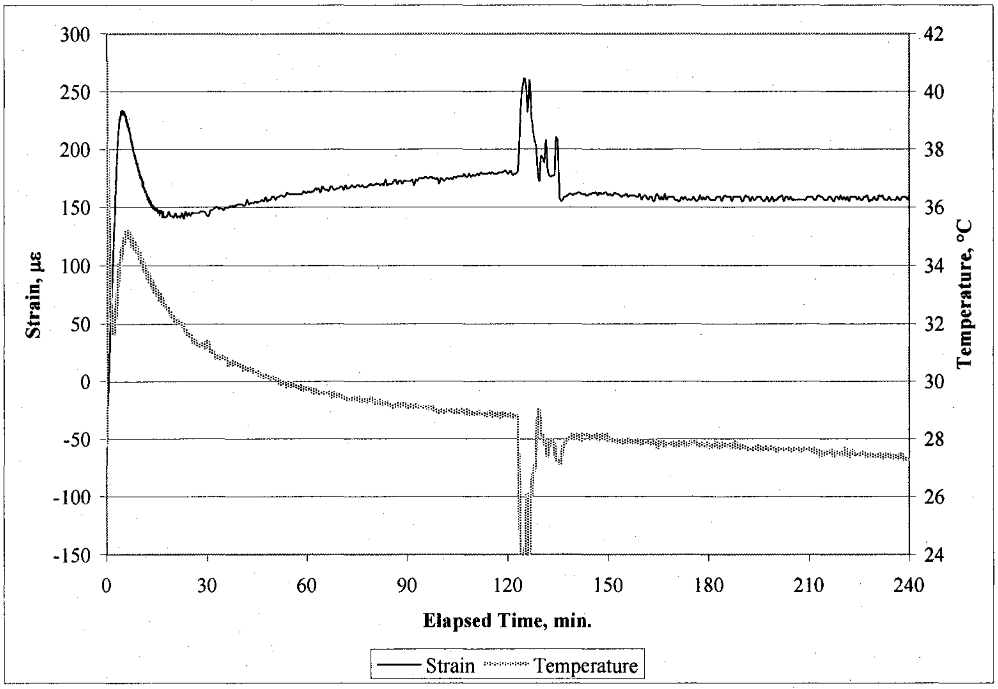

(b)

Figure 4.6: In-situ carbonation curing strain measurement for batch B14 (a) first 10 minutes, (b) full duration (2 hours)

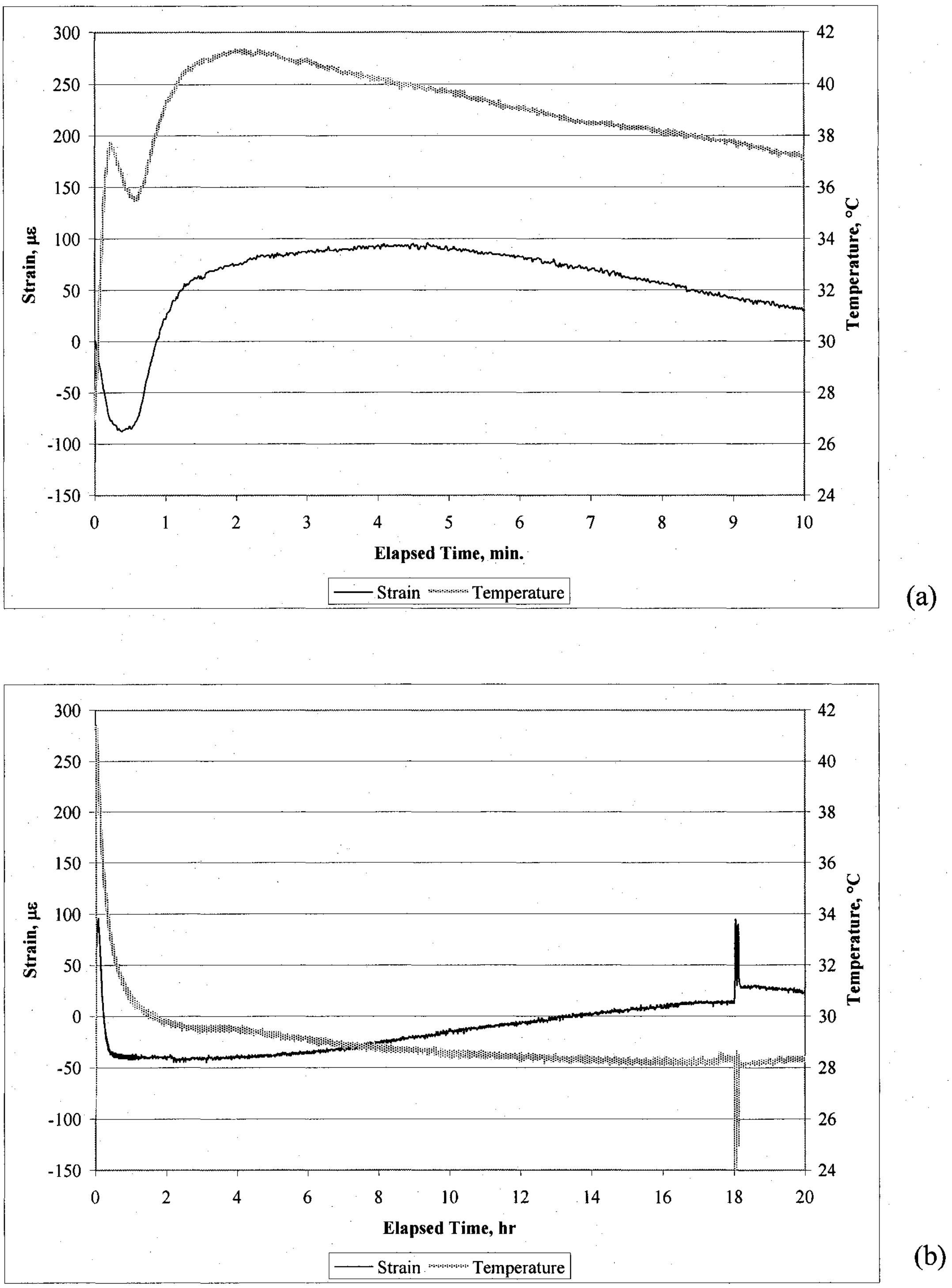

Figure 4.7: In-situ carbonation curing strain measurement for batch B15 (a) first 10 minutes, (b) full duration (18 hours)

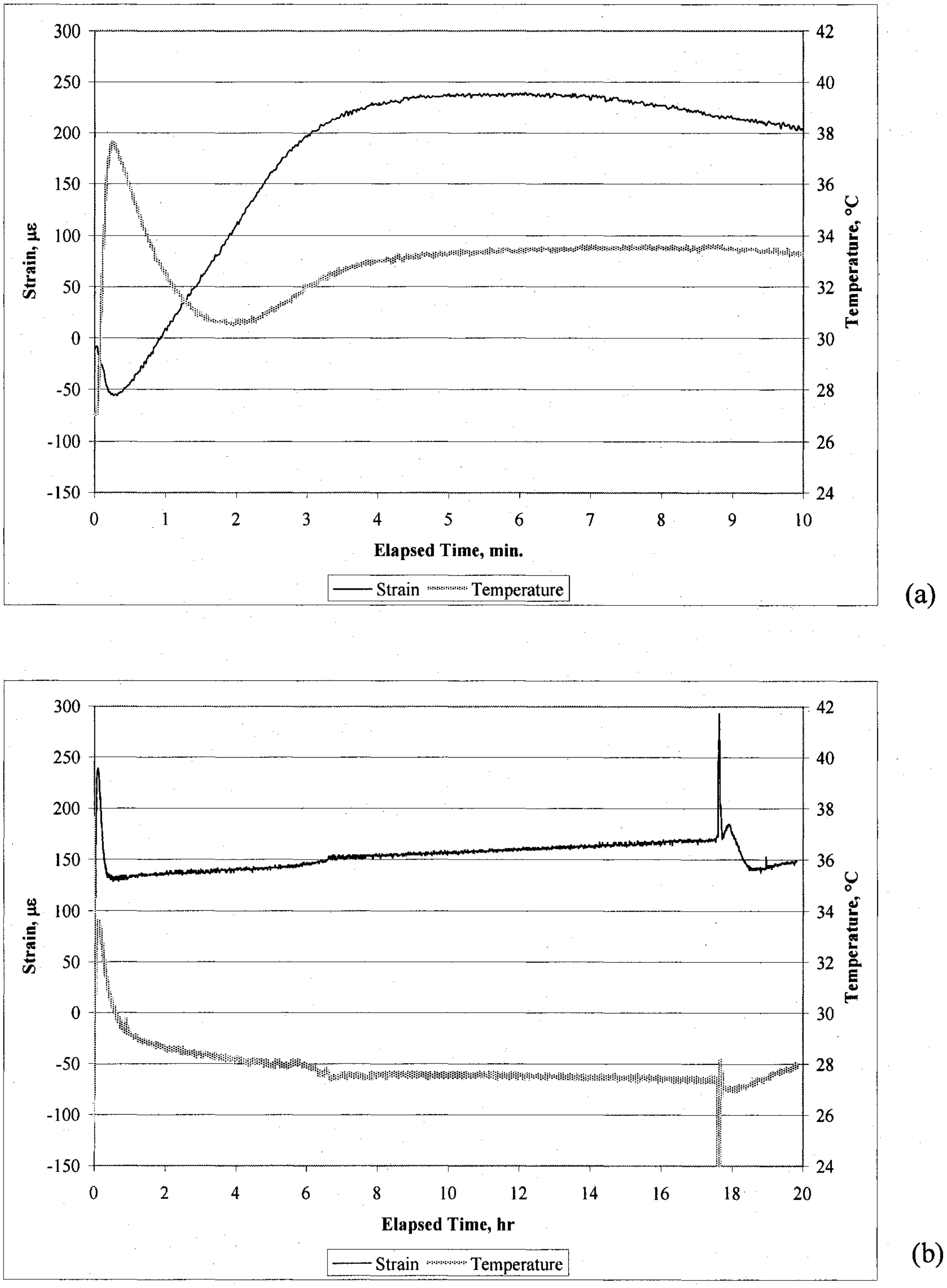

Figure 4.8: In-situ carbonation curing strain measurement for batch B16 (a) first 10 minutes, (b) full duration (18 hours)

4.1.3 Compressive Strength Testing

4.1.3.1 Cement Paste

Results for compressive strength testing of Series One cement paste samples are shown in Table 4.13. Compressive strengths reported are the average of two specimens and the deviation of each sample from the mean is also noted. The effect of increasing the carbonation curing duration from 2 to 18 hours differed from immediately carbonated samples to those preset. For samples carbonated immediately, the increase in strength with longer carbonation was negligible with average strengths of 45.2 and 48.9 MPa for 2 and 18 hours respectively. Conversely, preset samples saw an increase of 14.4 MPa for 18 hour carbonation over 2 hours. The average strengths were 67.1 and 81.5 MPa for 2 and 18 hour carbonation curing respectively. As previously discussed in Section 4.1.1.1 for carbon dioxide absorption, the majority of the carbonation reaction occurred during the initial period of curing. Therefore, extending the carbonation duration by eight times had a negligible effect on the immediately carbonated samples strength and only increased preset samples strength by 21%.

Table 4.13: Compressive strength results for cement paste samples

Batch	Carbonation Treatment	Sample Age, hours	Compressive Strength, MPa			
			Carbonation	Deviation	Hydration	Deviation
B1	2 hr	2	45.2	±0.9	-	-
B2	17 hr Preset + 2 hr	19	67.1	±6.8	39.7	-
B3	18 hr	18	48.9	±3.9	32.0	±1.2
B4	17 hr Preset + 18 hr	35	81.5	±0.5	37.7	±2.3

Comparing the compressive strengths in Table 4.13 between immediately carbonated and preset samples indicates that significant strength gain was achieved through presetting the samples. After 2 hour carbonation samples that were preset had an average compressive strength of 67.1 MPa while fresh samples had a strength of 45.2 MPa, a difference of 21.9 MPa. Samples carbonated for 18 hours experienced an even larger increase in strength of 32.6 MPa when preset, with immediately carbonated samples having an average strength of 48.9 MPa compared to preset samples at 81.5 MPa.

In assessing the compressive strength gain through carbonation curing it is important to compare with the strengths of conventionally hydrated samples for a similar duration. The strength after hydration for 2 hours was not measured, yet it can be seen in Table 4.13 that after 2 hours of carbonation curing the strength exceeded even that after 35 hours of hydration. With 18 hour carbonation there was a difference in strength of 16.9 MPa between samples subjected to carbonation curing and those that underwent hydration. The increased strength from carbonation was even larger for preset samples with a difference of 27.4 MPa for 2 hour carbonation and 43.8 for 18 hours. Not only did presetting followed by 18 hour carbonation produce the highest compressive strength, but it also yielded the greatest strength gain ratio over hydration for a similar period.

Following carbonation and hydration samples were stored in a sealed container with a relative humidity greater than 90% to promote further hydration. Compressive strength testing was conducted after 7 days (from the initial moulding date) and the results are displayed in Table 4.14. The results indicate that the compressive strengths were similar between 2 and 18 hour carbonation after this hydration period. Samples carbonated immediately had comparable strengths of 64.0 and 62.5 MPa for 2 and 18 hour carbonation respectively. Preset samples also had similar 2 and 18 hour carbonation strengths with values of 84.1 and 86.5 MPa respectively. Although strengths were similar for both carbonation durations, it is evident that samples preset had the greatest strengths after 7 days. This may have occurred because water loss during carbonation curing for fresh samples was greater than preset samples. Therefore, less water was available in immediately carbonated samples for subsequent hydration.

Table 4.14: Compressive strength results for cement paste samples after 7 days hydration

Batch	Carbonation Treatment	Sample Age, days	Compressive Strength, MPa			
			Carbonation	Deviation	Hydration	Deviation
B1	2 hr	7	64.0	±2.5	42.7	±0.2
B2	17 hr Preset + 2 hr	7	84.1	±5.0	42.3	±4.5
B3	18 hr	7	62.5	±3.5	47.3	±7.5
B4	17 hr Preset + 18 hr	7	86.5	±2.8	45.3	±3.0

The compressive strengths of hydrated samples after 7 days were relatively similar between batches, as shown in Table 4.14. Strengths for hydrated samples ranged between 42.3 and 47.3 MPa, with an overall average of 44.4 MPa. In comparing these results with the strengths of carbonation samples after 7 days of hydration it was observed that significantly higher strengths still existed in carbonated samples. The largest difference in strength between carbonated and hydrated samples was for those preset and carbonated for 18 hours, with carbonated samples having a strength 41.2 MPa higher.

4.1.3.2 Concrete

Compressive strength testing results for Series One concrete samples are displayed in Table 4.15. For immediately carbonated samples the difference in compressive strength between 2 and 18 hour carbonation curing was negligible with strengths of 12.7 and 12.9 MPa respectively. Preset samples on the other hand had an average strength 4.8 MPa higher for 18 hour carbonation than 2 hour. The individual strengths were 12.8 MPa for 2 hour carbonation and 17.6 MPa for 18 hours. Similar to cement paste samples, strength gain was not proportional to the carbonation duration because the majority of the carbonation reaction occurred during the initial period.

Table 4.15: Compressive strength results for concrete samples

Batch	Carbonation Treatment	Sample Age, hours	Compressive Strength, MPa			
			Carbonation	Deviation	Hydration	Deviation
B5	2 hr	2	12.7	±0.6	2.6	±0.1
B6	17 hr Preset + 2 hr	19	12.8	±0.9	6.6	±1.6
B7	18 hr	18	12.9	±0.8	5.6	±0.3
B8	17 hr Preset + 18 hr	35	17.6	±1.4	11.4	±1.5

In contrast to cement paste samples, presetting had negligible effect on the compressive strength of samples carbonated for 2 hours. The carbonation strengths for immediately carbonated and preset samples were 12.7 and 12.8 MPa respectively. Samples carbonated for 18 hours on the other hand behaved similar to cement paste and had a strength 4.8 MPa higher when preset. The strengths were 12.9 MPa for immediately carbonated samples and 17.6 MPa for those preset.

Comparing the carbonation curing strengths with hydration strengths after similar periods indicated that significant strength was achieved though carbonation curing. For 2 hour carbonation of fresh samples the strength was 10.1 MPa higher than the parallel hydration strength. The increase in strength from carbonation was less when the samples were carbonated for 18 hours, with a difference of 7.3 MPa. Preset samples carbonated for 2 and 18 hours had the same improvement in strength from carbonation as oppose to hydration of 6.2 MPa. Compressive strengths were increased the largest amount for 2 hour carbonation, when comparing hydrated and carbonated samples. The greatest overall strength was achieved through presetting and 18 hour carbonation, similar to cement paste samples.

Shown in Table 4.16 are the 7 day compressive strength results for carbonated and hydrated samples. It appears that the strengths of immediately carbonated samples for both 2 and 18 hours are relatively similar. The strengths for these samples were 12.1 and 14.3 MPa for 2 and 18 hours respectively. Likewise, the strengths of preset samples carbonated for 2 and 18 hours were comparable with strengths of 16.1 and 17.0 MPa. As discussed in Section 4.1.3.1 for cement paste samples, the highest strengths were achieved through presetting.

Table 4.16: Compressive strength results for concrete samples after 7 days hydration

Batch	Carbonation Treatment	Sample Age, days	Compressive Strength, MPa			
			Carbonation	Deviation	Hydration	Deviation
B5	2 hr	7	12.1	±0.4	7.3	±0.7
B6	17 hr Preset + 2 hr	7	16.1	±1.7	10.6	±1.5
B7	18 hr	7	14.3	±2.3	7.4	±1.0
B8	17 hr Preset + 18 hr	7	17.0	±0.1	10.9	±0.7

It can be seen in Table 4.16 that after 7 days of subsequent hydration the strengths of samples cured using carbon dioxide were still greater than those of samples purely hydrated. The concrete compressive strengths of hydrated samples ranged between 7.3 and 10.9 MPa, with an average of 9.1 MPa. Compressive strengths for carbonated samples ranged between 12.1 and 17.0 MPa. As was the case for cement paste samples, the greatest increase in strength from carbonation over hydration was for presetting followed by 18 hour carbonation with a difference of 6.1 MPa.

4.1.4 Qualitative Depth of Carbonation

4.1.4.1 Cement Paste

Illustrated in Figure 4.9 are typical qualitative depth of carbonation pictures obtained from each carbonation treatment. It can be seen that the patterns observed from spraying the samples with phenolphthalein were similar for both 2 hour and 18 hour carbonation. When carbonated immediately the outer most layers of the specimens remained colourless, indicating a pH below 8.3. Proceeding inwards from the outer layer to the core there then existed a band of purple, followed by another colourless band and then finally a core of purple. Bands of purple indicated a pH higher than 8.3, the pH above which phenolphthalein changes from colourless to purple. Phenolphthalein patterning on preset samples was also similar between 2 and 18 hour carbonation curing treatments. While the outer most layers of the samples remained colourless in the same way as immediately carbonated samples did, inwards from this outer layer the cement paste was purely purple. A typical hydration sample is also pictured in Figure 4.9 and it can be seen that the entire depth of sample turned purple.

Despite this method previously being used to investigate the depth of carbonation, colourless layers indicating a reduction in pH due to the formation of carbonation products, it was not found to be entirely representative during this study. While the outer layers were colourless and carbon dioxide content results matched accordingly, high carbon dioxide contents were found in the core where the purple colour would suggest negligible carbonation had occurred. In fact, carbon dioxide content results in Table 4.2 indicated that the maximum difference in absorbed CO_2 between the surface and core was only 1.62%. Furthermore, it can be seen in Table 4.2 that the core carbon dioxide contents after 18 hours carbonation were actually similar to or higher than the surface content after 2 hours carbonation. Nevertheless, a colourless outer layer and purple innermost core were observed for all carbonation treatments.

B1 - 2 hour carbonation curing

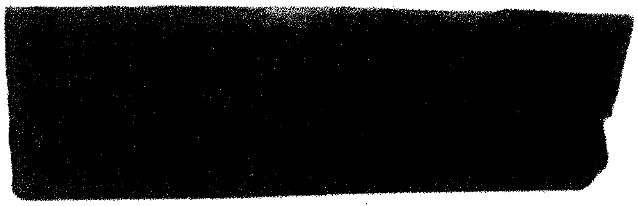

B2 - 17 hour preset and 2 hour carbonation curing

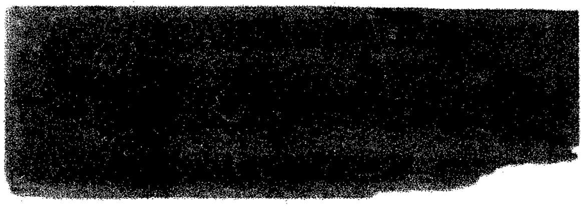

B3 - 18 hour carbonation curing

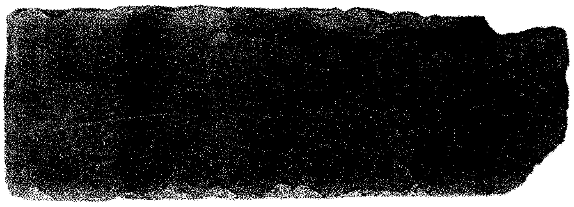

B4 - 17 hour preset and 18 hour carbonation curing

Typical hydration cured sample

Figure 4.9: Qualitative depth of carbonation after carbonation curing for cement paste samples

4.1.4.2 Concrete

Typical qualitative depth of carbonation pictures are shown in Figure 4.10. As previously found for cement paste samples the phenolphthalein pattering was similar for both 2 and 18 hour carbonation curing treatments. For immediately carbonated samples there was a large colourless outer layer surrounding an inner core of purple. The border between the two zones was ill-defined and the core region was very faint. Samples preset prior to carbonation had a thinner colourless outer layer and the core region was much darker and more distinguishable.

Although it was not feasible to collect separate samples from the surface and core of concrete specimens for carbon dioxide analysis, it is probable that the core and surface had comparable carbon dioxide contents. As discussed in Section 4.1.1 similar carbon dioxide contents were found for cement paste and concrete samples, and minimal difference in CO_2 content was observed between surface and core samples from cement paste specimens. These findings are suggestive that the surface and core material in concrete samples was carbonated to a similar degree. Therefore, using phenolphthalein to predict the depth of carbonation does not seem to fit the data obtained during this study.

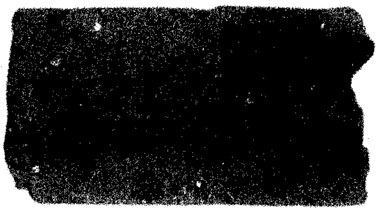

B5 - 2 hour carbonation curing

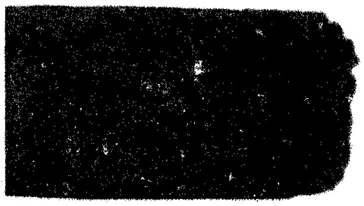

B6 - 17 hour preset and 2 hour carbonation curing

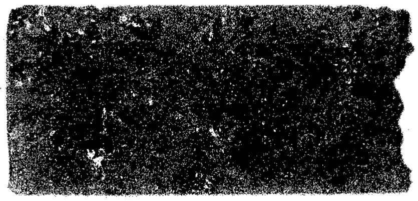

B7 - 18 hour carbonation curing

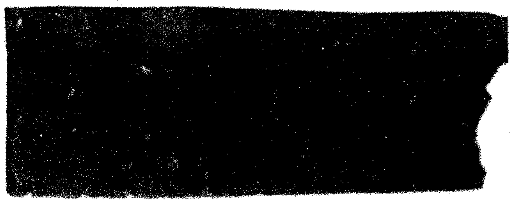

B8 - 17 hour preset and 18 hour carbonation curing

Typical hydration cured sample

Figure 4.10: Qualitative depth of carbonation after carbonation curing for concrete samples

4.1.5 X-ray Diffraction of Selected Cement Paste Samples

X-ray diffraction analysis was performed on selected cemented paste samples to assess the products formed during carbonation curing. The results are shown in Figures 4.11 to 4.14 for fresh and preset samples carbonation cured for 18 hours. The analysis indicated that calcium carbonate in the form of calcite and aragonite were the primary products after 18 hour carbonation curing for both immediately carbonated and preset samples. High intensity peaks were observed for C_3S and C_2S and suggest that a considerable amount of unreacted cement still existed in the samples following carbonation. Moreover, there was no significant evidence of the formation of hydration products, primarily calcium hydroxide, in both the immediately carbonated and preset samples. This suggests that calcium hydroxide formed during presetting was converted to calcium carbonate. XRD patterns from the surface and core of the cement paste samples were comparable and no major differences were noted. These results corroborate the findings from carbon dioxide content analysis which found marginal differences in the degree of carbonation between the surface and core. Furthermore, the patterns of immediately carbonated and preset samples were similar and coincide with the comparable carbon dioxide absorption values observed in Section 4.1.1.1 for batches B3 and B4.

Figure 4.15 shows the XRD pattern for a hydrated sample after 18 hours. The scan shows strong intensity peaks for calcium hydroxide, C_3S and C_2S, indicating that hydration had occurred to a certain degree. In comparing the hydrated sample pattern with those from carbonation curing it can be seen that calcium hydroxide was produced from hydration, while calcium carbonate was produced from carbonation. In the hydrated sample scan there was little evidence of calcium carbonate being produced during curing. However, in the carbonated sample scans there was significant evidence indicating calcite and aragonite had formed, while no high intensity peaks were identified for calcium hydroxide.

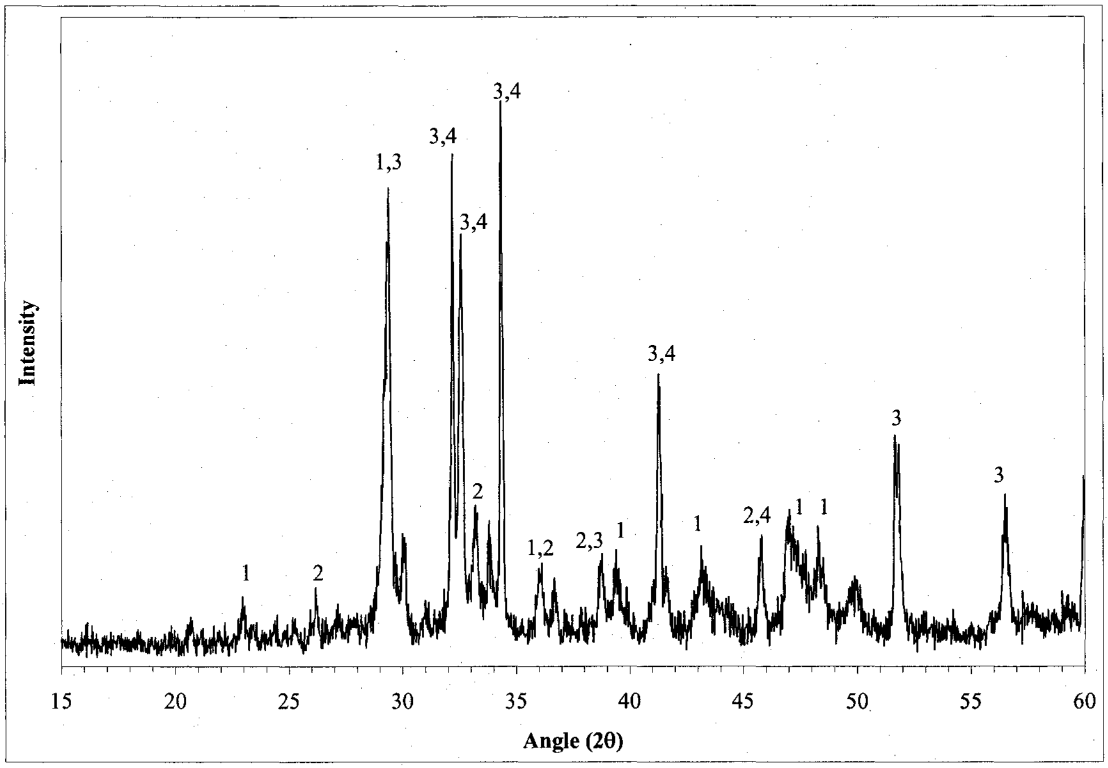

Figure 4.11: XRD Analysis of cement paste sample surface after 18 hour carbonation: (1) calcite, (2) aragonite, (3) C_3S, (4) C_2S

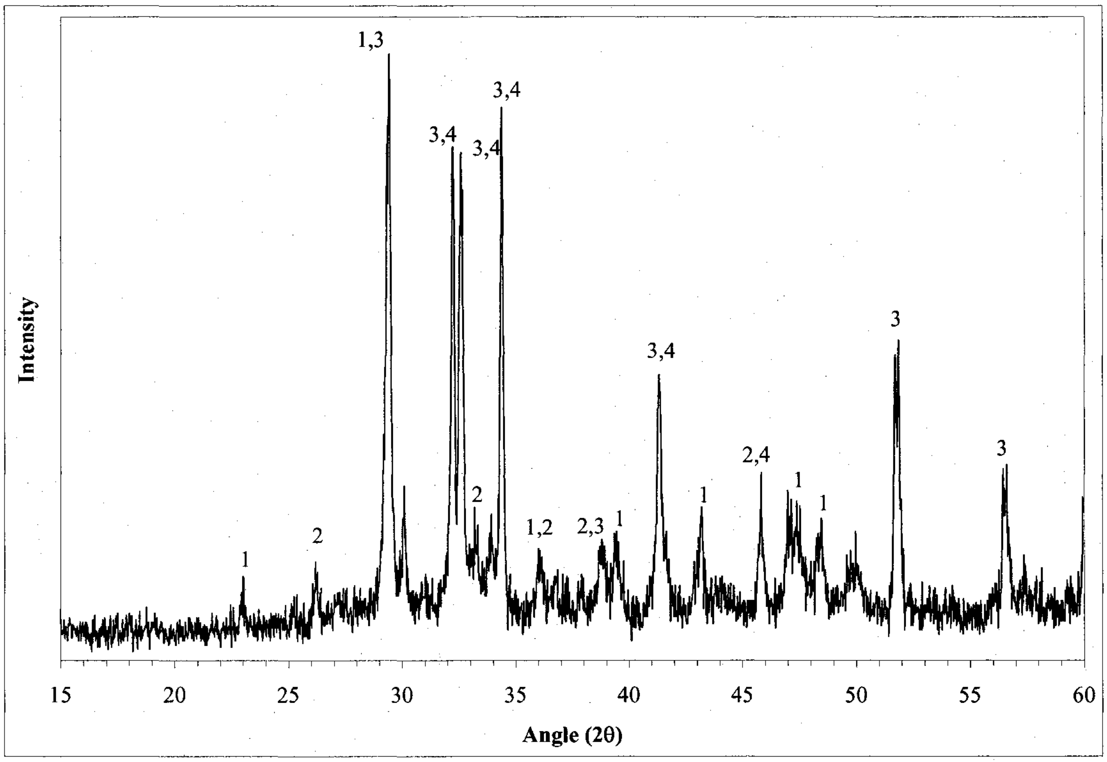

Figure 4.12: XRD Analysis of cement paste sample core after 18 hour carbonation: (1) calcite, (2) aragonite, (3) C_3S, (4) C_2S

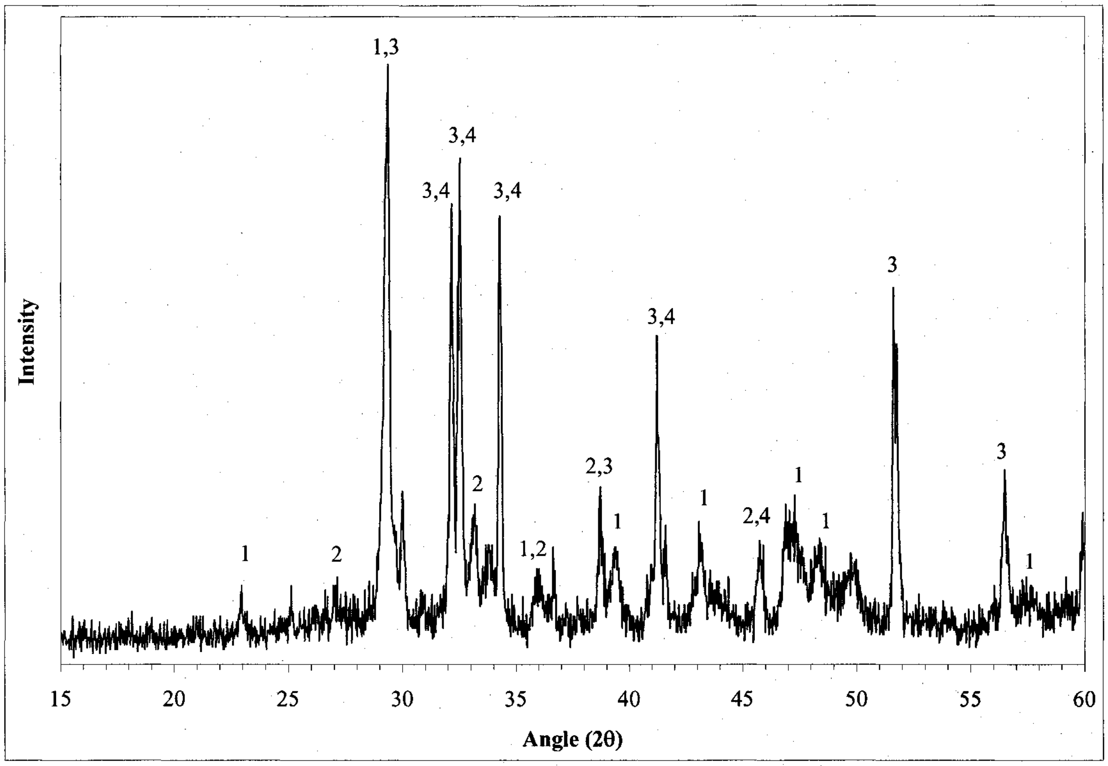

Figure 4.13: XRD Analysis of cement paste sample surface after preset and 18 hour carbonation: (1) calcite, (2) aragonite, (3) C_3S, (4) C_2S

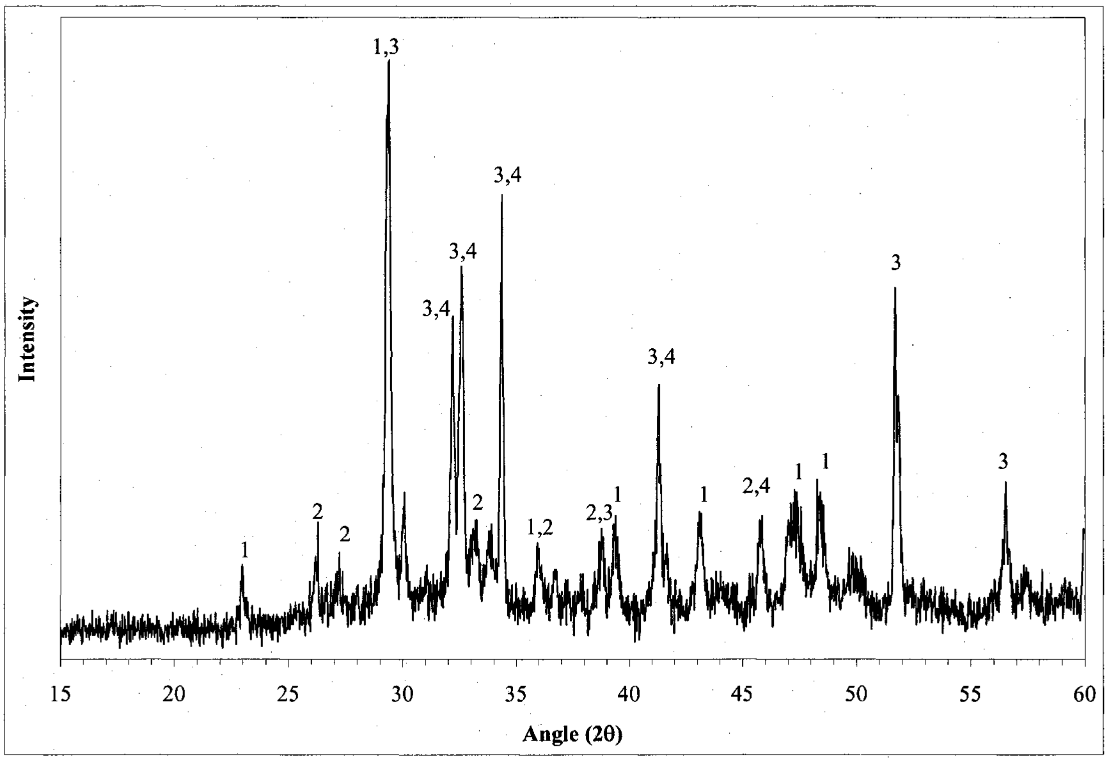

Figure 4.14: XRD Analysis of cement paste sample core after preset and 18 hour carbonation: (1) calcite, (2) aragonite, (3) C_3S, (4) C_2S

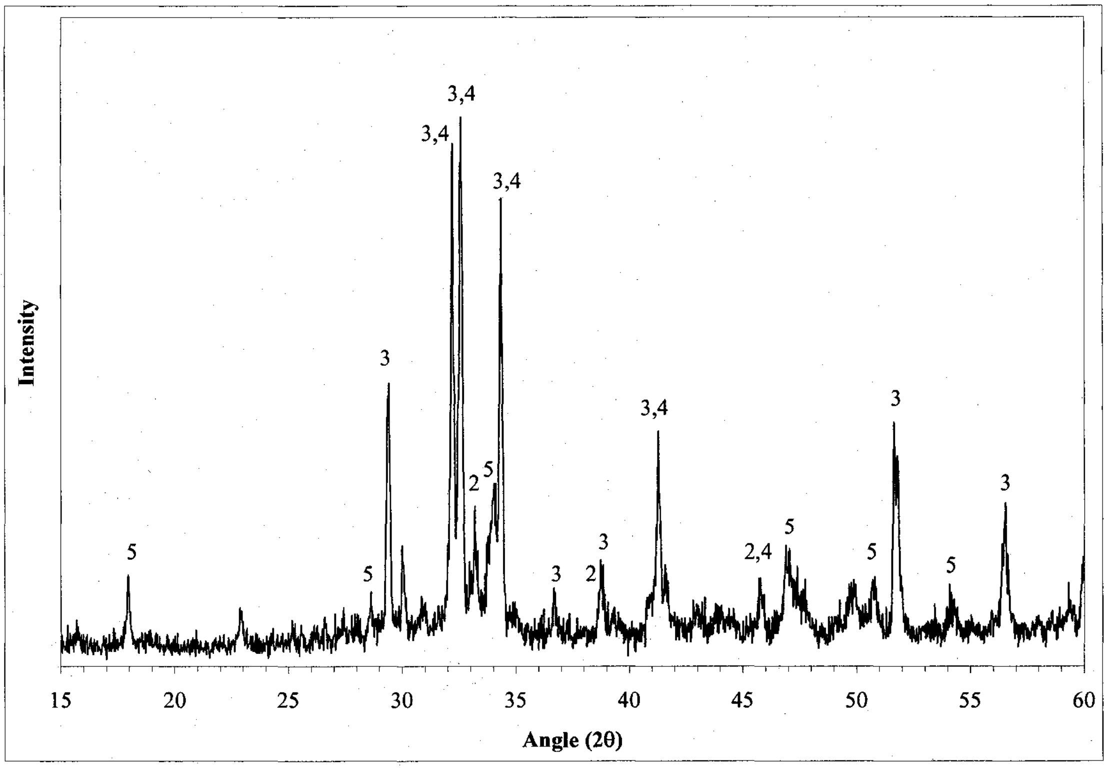

Figure 4.15: XRD Analysis of hydrated cement paste sample core: (1) calcite, (2) aragonite, (3) C_3S, (4) C_2S, (5) calcium hydroxide

4.1.6 Scanning Electron Microscopy of Selected Samples

4.1.6.1 Cement Paste

Scanning electron microscopy was performed on a cement paste sample carbonation cured for 18 hours. Figure 4.16 was taken at a magnification of x300 to show the general microstructure of the surface and core. It can be seen that the core appears slightly more porous than the surface, correlating with carbon dioxide absorption values. It was previously shown in Section 4.1.1.1 that the surface of carbonation cured samples had marginally higher carbon dioxide contents than the core. This translates to more carbonation products being produced in the pore space of the samples, creating a denser structure.

Figure 4.17a shows the microstructure on the sample surface at a magnification of x4000. It is clear that large crystals had formed in the pore space of the sample during carbonation, while no calcium hydroxide crystals were found present. The EDS scan of a crystal in Figure 4.17b indicates that it contained significant amounts of calcium, carbon and oxygen, suggesting calcium carbonate was produced. These results are in agreement with the XRD analysis which found calcium carbonate and cement anhydrite, but no clear evidence of calcium hydroxide. An SEM micrograph of the cement paste core is shown in Figure 4.18a. The microstructure was similar to that of the surface, however slightly smaller crystal growth was observed in the pore space. The EDS scan in Figure 4.18b indicates these crystals are calcium carbonate and the pattern is comparable with that of the surface. Smaller crystal growth in the core reaffirms carbon dioxide content results in Section 4.1.1.1 where marginally lower absorptions were found in the core.

An SEM photomicrograph of hydrated cement paste can be seen in Figure 5.19. In contrast to the carbonation cured samples, hexagonally shaped crystal growth was observed. This morphology is distinct evidence of calcium hydroxide being produced. Results from SEM correlate with XRD analysis finding the presence calcium hydroxide and negligible evidence of carbonation products.

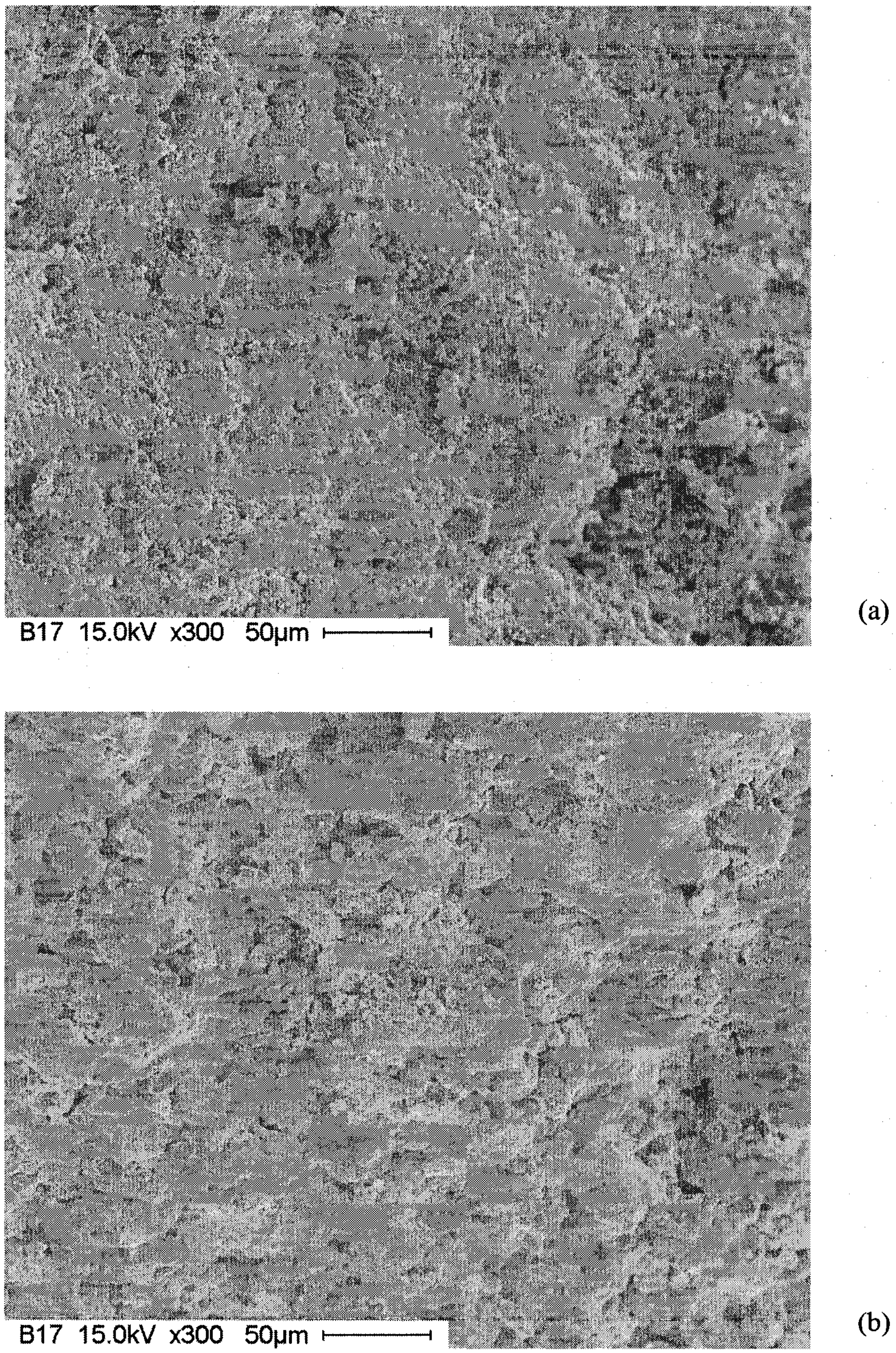

Figure 4.16: SEM photomicrograph of cement paste sample after 18 hours carbonation curing (a) surface, (b) core

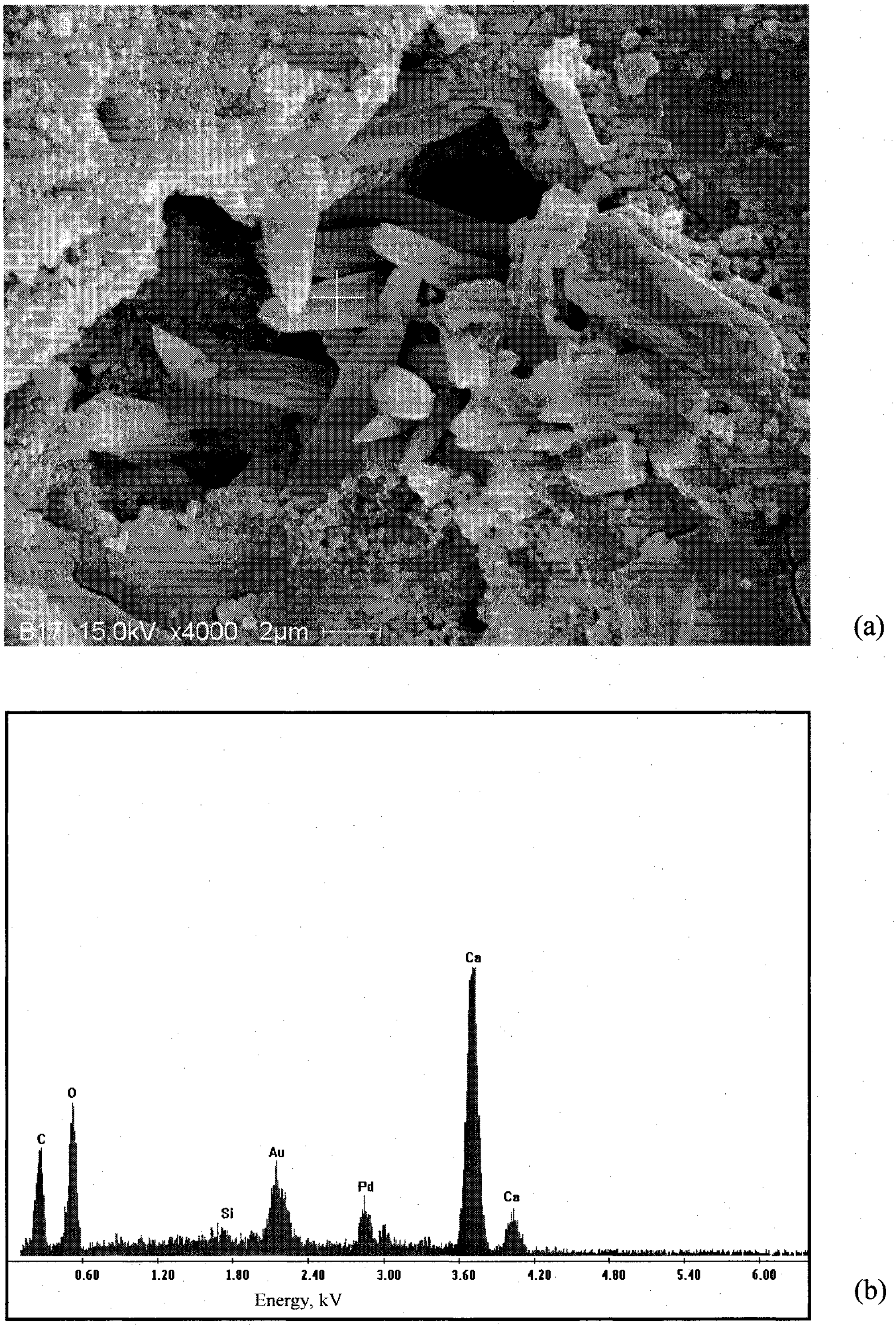

Figure 4.17: Cement paste sample surface after 18 hours carbonation curing (a) SEM photomicrograph, (b) EDS of carbonation product

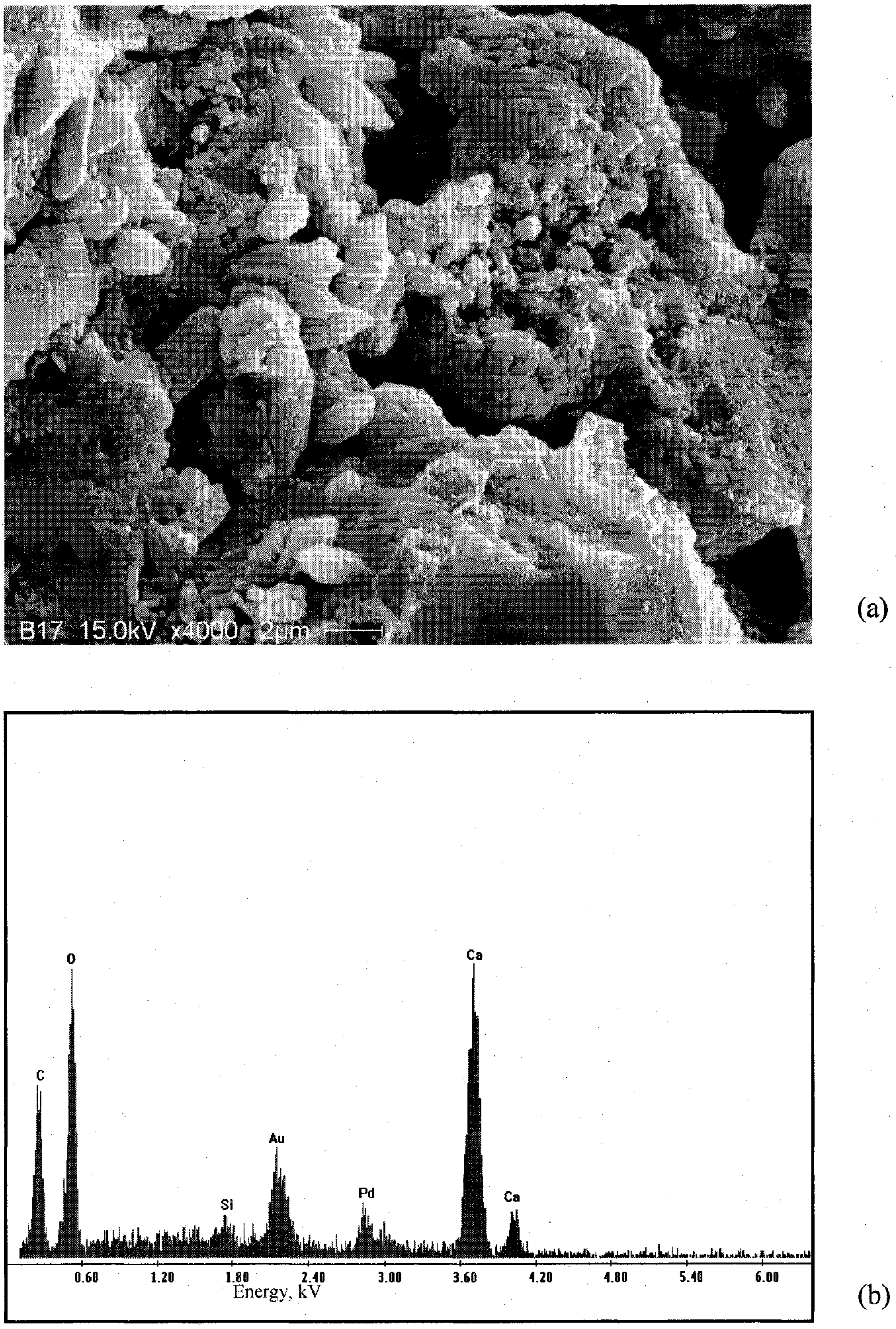

Figure 4.18: Cement paste sample core after 18 hours carbonation curing (a) SEM photomicrograph, (b) EDS of carbonation product

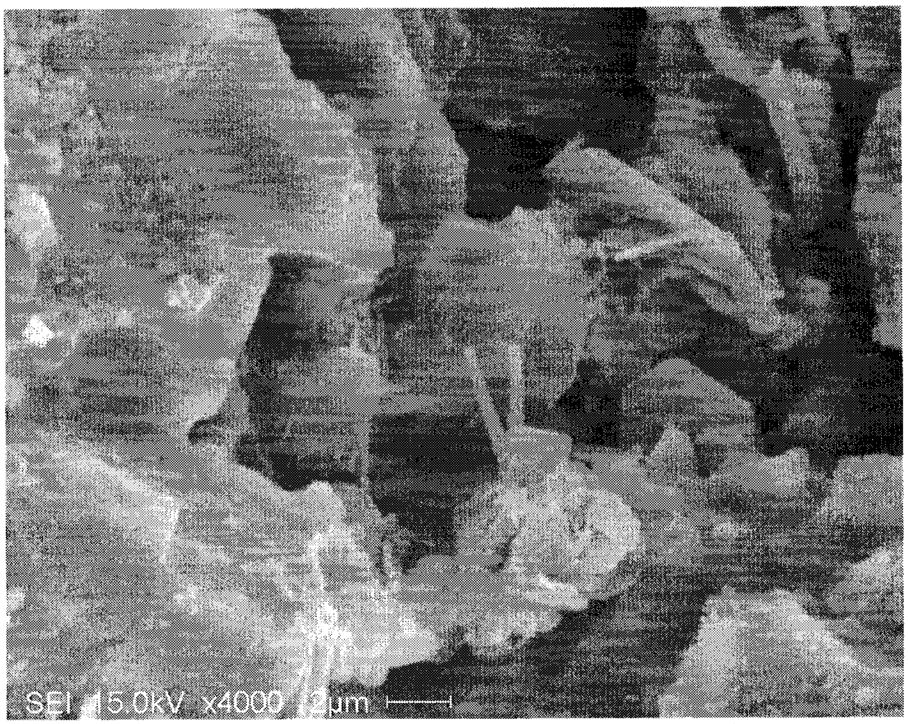

Figure 4.19: SEM photomicrograph of a hydrated cement paste sample

4.1.6.2 Concrete

SEM was conducted on a concrete sample after 18 hours of carbonation curing. Figure 4.20 shows the sample at a magnification of x300 and it can be seen that carbonation products have formed on surfaces of the concrete constituents, giving them a rough speckled appearance. Increasing the magnification to x4000, Figure 4.21a, clearly showed the texture was due to a large quantity of small crystals that had formed in the pore spaces of the sample. The EDS scan in Figure 4.21b of a crystal suggests that they are calcium carbonate due to the strong presence of calcium, oxygen and carbon.

In contrast to the carbonation cured sample, Figure 4.22 shows the microstructure of a hydrated concrete sample at a magnification of x300. The particles appear to be covered in flakey plate like products. At closer inspection in Figure 4.23a the true hexagonal shape of the crystals is apparent; distinct morphological evidence of calcium hydroxide. Further investigation through EDS, Figure 4.23b, supported this conclusion with high intensity peaks for calcium and oxygen.

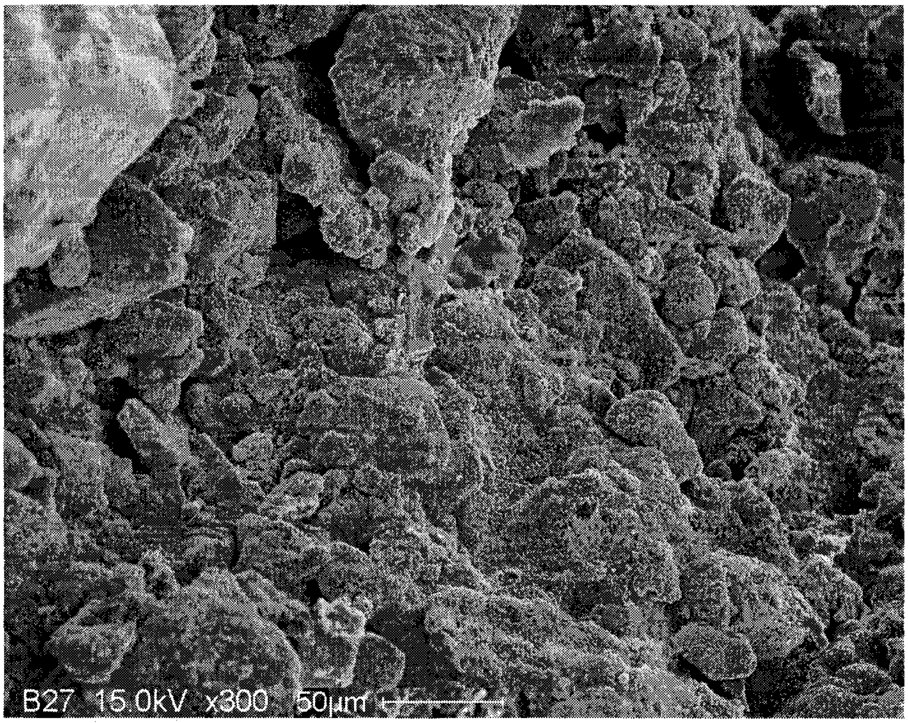

Figure 4.20: SEM photomicrograph of concrete sample after 18 hours carbonation curing

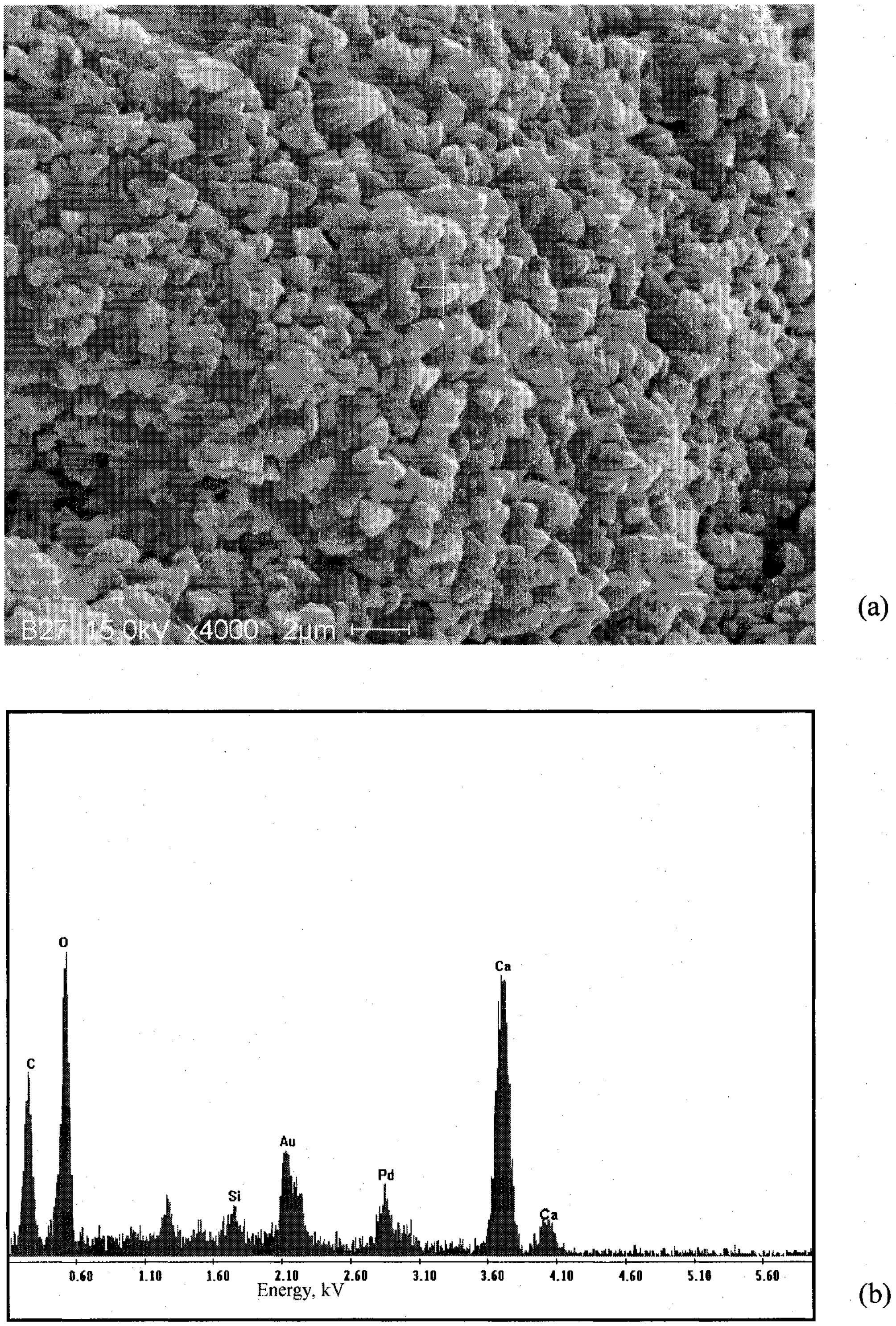

Figure 4.21: Concrete sample after 18 hours carbonation curing (a) SEM photomicrograph, (b) EDS of carbonation product

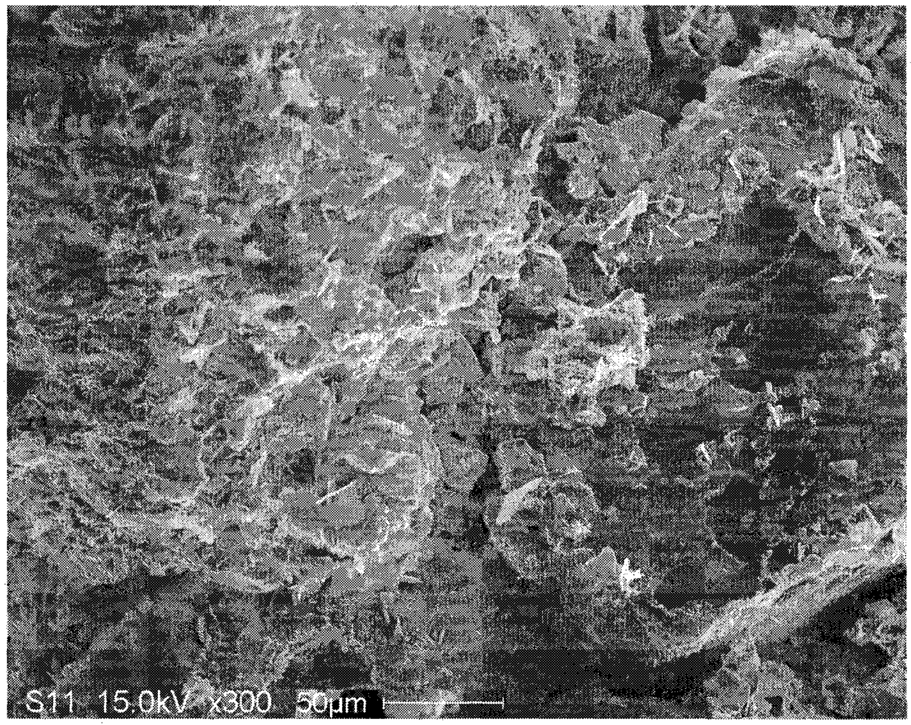

Figure 4.22: SEM photomicrograph of concrete sample after 18 hours hydration

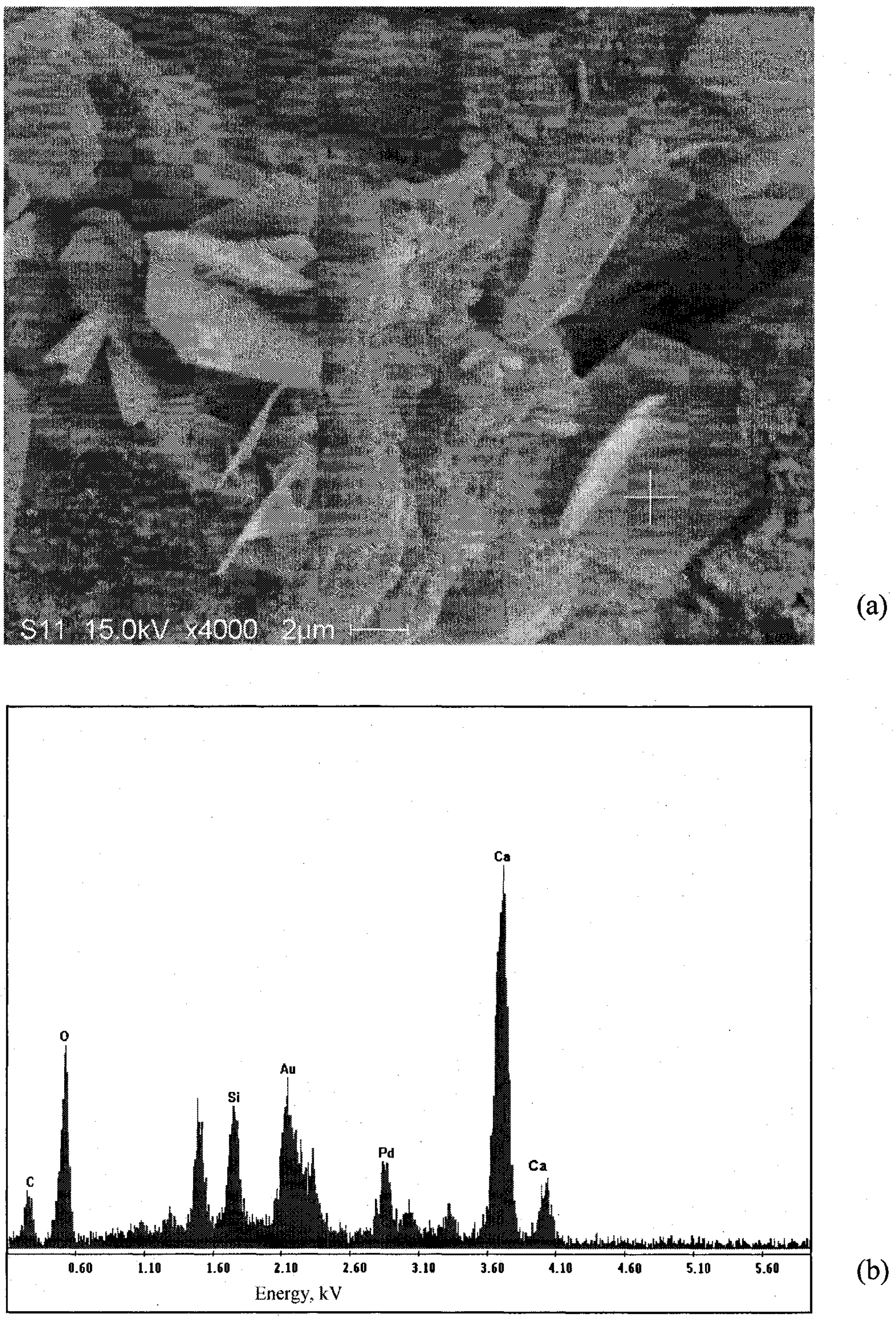

Figure 4.23: Concrete sample after 18 hours hydration (a) SEM photomicrograph, (b) EDS of hydration product

4.2 WEATHERING CARBONATION

Following carbonation curing/conventional hydration and a 7 day post-curing period samples were exposed to accelerated weathering carbonation testing (AWCT). AWCT was conducted to investigate if cement and concrete compacts cured by carbonation could have more resistance to weathering carbonation. As outlined in Section 3.5.9 weathering carbonation was simulated at an accelerated rate using 50% carbon dioxide and 65% relative humidity (rh). Strain and mass measurements were regularly taken during the 61 day exposure period, while destructive compressive strength testing and carbon dioxide content analysis were completed upon termination. Carbonation cured (pre-carbonated) and reference hydrated samples of each batch were tested simultaneously for weathering carbonation so that any variation in exposure conditions would equally influence both sets of samples.

4.2.1 Carbon Dioxide Absorption

4.2.1.1 Cement Paste

Adjusted carbon dioxide content results measured after 61 days of accelerated weathering carbonation testing are displayed in Table 4.17. As discussed in Section 4.1.1.1, adjusted values were determined from the raw data to eliminate detected CO_2 that was present in the as received cement. Despite variation in the carbon dioxide absorption values for pre-carbonated samples prior to service exposure, relatively similar quantities of CO_2 were absorbed during AWCT. This likely occurred because the carbonation cured samples had already been exposed to a high degree of carbonation during curing and under the AWCT carbonation conditions the potential for CO_2 uptake was similar between batches. The average service absorption for carbonation cured samples was 1.54%.

In contrast to carbonation cured samples, conventionally hydrated samples had an average carbon dioxide absorption during AWCT of 9.56%. Hydrated samples absorbed significantly more carbon dioxide than pre-carbonated samples because minimal amounts of CO_2 had previously reacted with the cement anhydrite and hydration products.

Nevertheless, it is interesting to note that absolute quantity of carbon dioxide absorbed after AWCT was comparable between carbonation cured and hydrated samples. On average, pre-carbonated samples had a CO_2 content of 11.62%, in comparison to hydrated samples with 9.81% CO_2. Regardless of the various carbonation curing treatments and CO_2 exposure during curing versus service, there appeared to exist a maximum level of absorption in the order of 10%. This likely occurred because as the carbonation products formed around the source of calcium, be it hydration products or calcium silicates, carbon dioxide was blocked from reacting further with that source. It is thereby suggestive that the degree of hydration occurring prior to carbonation has little effect on the degree of the carbonation reaction.

Table 4.17: Comparison of adjusted average carbon dioxide content before and after 61-day weathering carbonation for cement paste samples

Batch	Carbonation Treatment	Adjusted Average CO_2 Content, %					
		Carbonation Samples			Hydrated Samples		
		Before	After	Increase	Before	After	Increase
B1	2 hr	9.00	10.73	1.73	0.25	9.88	9.63
B2	17 hr Preset + 2 hr	8.71	10.42	1.71	0.23	9.48	9.25
B3	18 hr	10.37	11.63	1.26	0.19	9.99	9.80
B4	17 hr Preset + 18 hr	12.23	13.68	1.45	0.30	9.87	9.57

Unadjusted carbon dioxide content values following AWCT for the surface and core of carbonation cured and hydrated samples are shown in Table 4.18. Similar to the results after carbonation curing, it was noted that the core material had carbonated to a significant degree and was only marginally less than that on the surface after service exposure. Both pre-carbonated and hydrated samples observed comparable differences in CO_2 content between the surface and core. The porosity of the samples was therefore sufficient for carbon dioxide to permeate through the surface to the core and allow carbonation to occur. Carbonation cured samples had an average difference between surface and core of 1.99%, while hydrated samples had a difference of 1.03%.

During AWCT sample mass was affected by two variables, namely moisture and carbon dioxide content. Mass was lost from the samples when they were introduced into the service exposure chamber due to a drop in moisture content. Prior to AWCT the samples were stored at approximately 92% rh and during weathering testing they were exposed to 65% rh. Carbon dioxide content had the influence of increasing the mass of samples during service exposure as they absorbed CO_2 from the chamber. The overall mass behaviour during AWCT is illustrated in Figure 4.24 and is based on the average of two bar and two plate samples for each batch. Because the mass gain measured was influenced by both the above mentioned factors it was not possible to quantify the percentage mass gain in terms of the carbon dioxide absorbed divided by mass of cement for each period. However, it is noteworthy that after one day of service exposure significant mass gain was observed for hydrated samples. The change in mass behaviour of carbonation cured samples was considerably smaller in magnitude. Because pre-carbonated samples had previously absorbed significant amounts of CO_2 during curing, their absorption capacity was notably reduced from that of hydrated samples.

Table 4.18: Carbon dioxide absorption after 61-day weathering carbonation for cement paste samples, as measured by infrared-based CO_2 analyzer

		CO_2 Content, %					
	Carbonation Treatment	Carbonation Samples			Hydrated Samples		
Batch		Surface	Core	Average	Surface	Core	Average
B1	2 hr	12.08	10.92	11.50	10.53	10.28	10.40
B2	17 hr Preset + 2 hr	11.61	10.27	10.94	10.03	9.97	10.00
B3	18 hr	13.65	10.66	12.15	11.14	9.88	10.51
B4	17 hr Preset + 18 hr	15.43	12.98	14.20	11.67	9.11	10.39

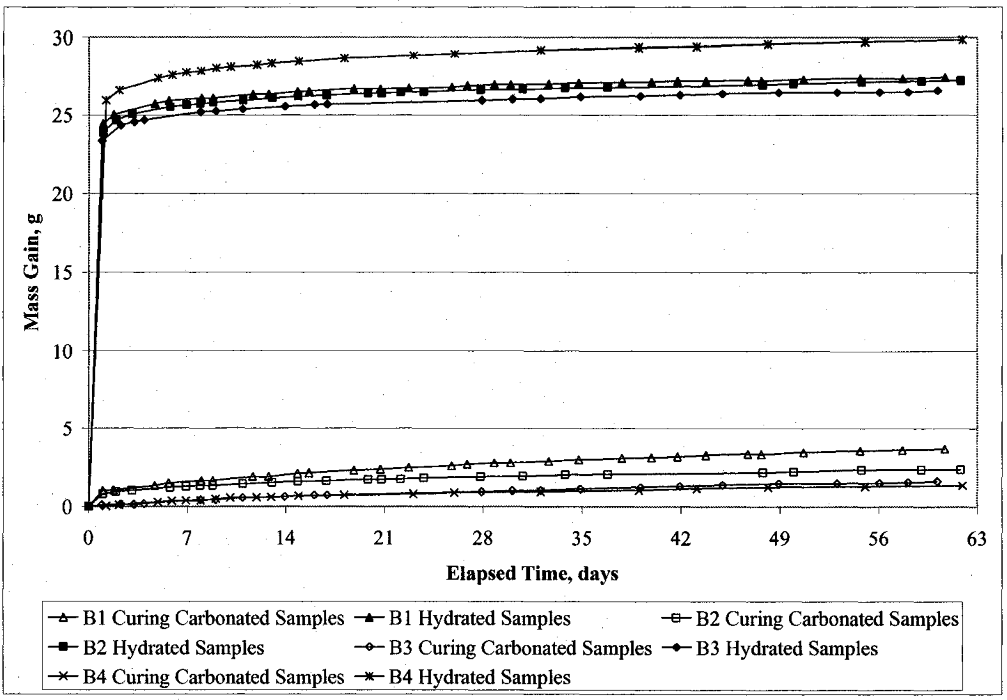

Figure 4.24: Accelerated weathering carbonation mass gain for cement paste samples

4.2.1.2 Concrete

Adjusted carbon dioxide content results from accelerated weathering carbonation testing are displayed in Table 4.19. Raw carbon dioxide content values were adjusted to eliminate CO_2 detected from limestone and as-received cement by quantifying and subtracting the amount of CO_2 in non-carbonated samples. The raw CO_2 content values as measured by infrared-based analysis are shown in Table 4.20. Carbon dioxide absorption during AWCT appeared to vary between carbonation treatments, with samples carbonated for 2 hours absorbing more CO_2 than those carbonated for 18 hours. This was not observed for cement paste samples and likely occurred because concrete samples pre-carbonated for 2 hours absorbed a noticeably smaller amount of CO_2 than did the 18 hour pre-carbonation samples. The 2 hour absorption value was around 8% and they therefore had a higher potential to uptake CO_2.

Table 4.19: Comparison of adjusted average carbon dioxide content before and after 61-day weathering carbonation for concrete samples

		Adjusted Average CO_2 Content, %					
	Carbonation	Carbonation Samples			Hydrated Samples		
Batch	Treatment	Before	After	Diff.	Curing	Weather	Diff.
B5	2 hr	8.01	12.89	4.88	0.00	11.24	11.24
B6	17 hr Preset + 2 hr	7.74	11.20	3.46	0.00	12.46	12.46
B7	18 hr	12.87	15.18	2.31	0.00	12.88	12.88
B8	17 hr Preset + 18 hr	10.86	11.84	0.98	0.00	8.70	8.70

Similar to cement paste samples, hydrated concrete samples exhibited significantly more carbon dioxide absorption during service exposure than pre-carbonated samples. Carbonation cured samples had uptake values in the range of 0.98 to 4.88%, while hydrated samples had an average absorption of 11.32%. Despite carbonation curing treatment and curing versus weathering carbonation it appears that carbon dioxide uptake potential of concrete samples was limited and was in order of 11 to 12%. This result is similar that of cement paste and it is notable that despite two different mix designs, the carbon dioxide uptake potential was of similar magnitude.

Table 4.20: Carbon dioxide absorption after 61-day weathering carbonation for concrete samples, as measured by infrared-based CO_2 analyzer

	Carbonation	CO_2 Content, %	
Batch	Treatment	Carbonation Samples	Hydrated Samples
B1	2 hr	20.10	18.45
B2	17 hr Preset + 2 hr	19.56	20.82
B3	18 hr	22.70	20.40
B4	17 hr Preset + 18 hr	21.09	17.95

Illustrated in Figure 4.25 is a plot of the change in mass for pre-carbonated and hydrated samples during AWCT. It can be seen that significant mass gain was observed for the hydrated samples within the first day of service exposure. As previously discussed for cement paste samples this mass gain represents the net effect of mass gain from CO_2 absorption and mass loss from the evaporation of moisture. Carbon dioxide absorption exceeded water loss and the overall result was mass gain. In contrast, pre-carbonated samples experienced a net mass loss, with the samples losing a larger mass of water than the mass of CO_2 gained. In general, the behaviour of pre-carbonated samples was remarkably different from hydrated samples due to the initial curing process. As observed by the mass change behaviour and final carbon dioxide content results, the capacity of carbonation cured samples to absorb CO_2 during weathering carbonation was substantially reduced because of the pre-treatment.

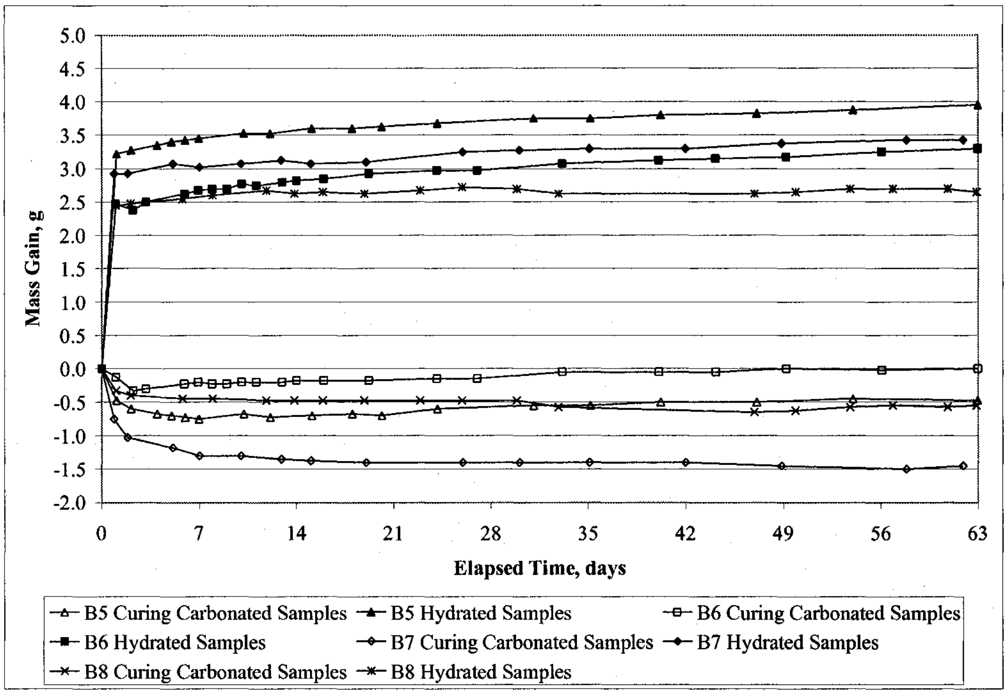

Figure 4.25: Accelerated weathering carbonation mass gain for concrete samples

4.2.2 Dimensional Stability under Service Exposure

4.2.2.1 Cement Paste

Dimensional stability results from AWCT are displayed in Table 4.21. It can be seen that little variation in the strains existed between samples of different carbonation curing treatments. The order of magnitude for strain exhibited in pre-carbonated samples was approximately -400 µε. This seems reasonable since negligible differences in the strains between curing treatments were also recorded during Series One carbonation curing, as described in Section 4.1.2. Moreover, the carbon dioxide absorption values measured during AWCT were similar between batches for pre-carbonated samples, thereby generating comparable amounts of carbonation shrinkage. As previously shown in Table

4.17, the additional CO_2 uptake for carbonation cured cement compacts under accelerated service exposure ranged in value between 1.26 and 1.73%.

Table 4.21: Summary of 61-day weathering carbonation strain for cement paste samples

Batch	Carbonation Treatment	Curing Carbonated Samples		Hydrated Samples	
		Strain, με	Deviation	Strain, με	Deviation
B1	2 hr	-446	±13	-1270	-
B2	17 hr Preset + 2 hr	-377	±27	-1198	±15
B3	18 hr	-386	±40	-1244	±44
B4	17 hr Preset + 18 hr	-467	±9	-1321	±96

In addition to the carbonation reaction, strain may have been generated during AWCT from the change in relative humidity between the post-curing period and service exposure. During post-curing (the period between carbonation curing/conventional hydration and AWCT) the samples were stored for 7 days in a sealed container above a layer of water where the relative humidity was greater than 90%. The internal moisture content of the samples was then reduced when they underwent AWCT, performed at 65% rh. As a result of the change in relative humidity samples were susceptible to drying shrinkage. Drying shrinkage was not individually characterised in this comparative study as the overall difference in shrinkage between pre-carbonated and hydrated samples was of primary concern.

Illustrated in Figure 4.26 is a time-dependant plot of the AWCT strain. It can be seen that the behaviour was similar for each pre-carbonated batch regardless of the carbonation curing treatment. Within the first day of service exposure pre-carbonated samples had already experienced approximately one third of the overall shrinkage observed during AWCT. This coincides with the mass gain plot in Figure 4.24 where a significant portion of the overall mass gain was recorded by the first day. The shrinkage then continued to stabilize with time reaching a steady state strain in the order of -400 με after approximately one month, beyond which only very subtle changes in strain were recorded. Similar behaviour of stabilizing with time was also observed for the mass gain measurements.

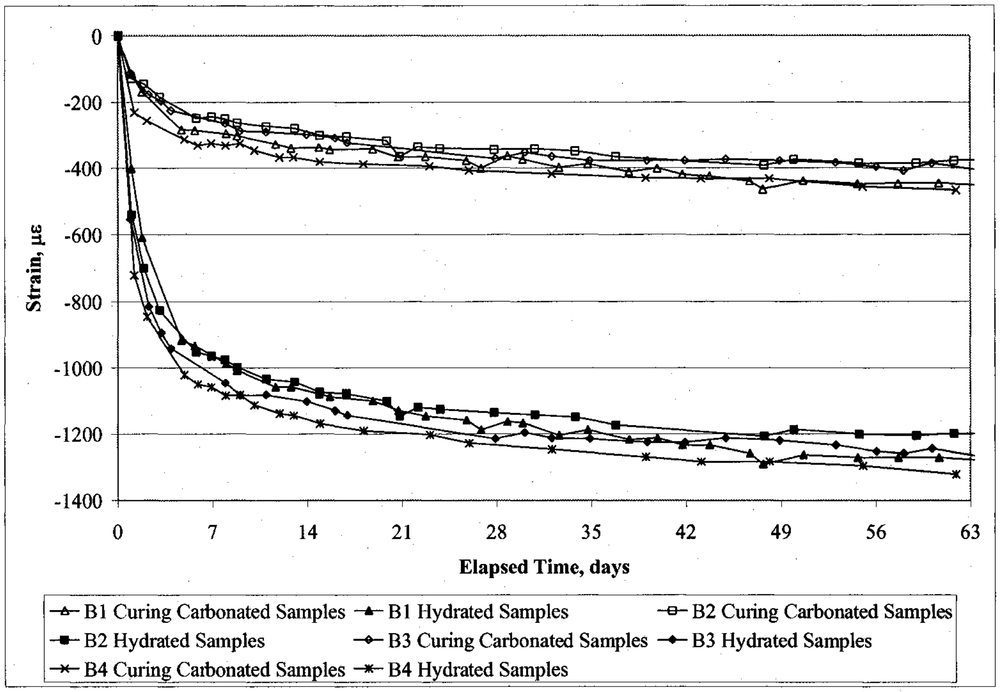

Figure 4.26: Accelerated weathering carbonation strain for cement paste samples

In contrast to pre-carbonated samples, hydrated samples experienced approximately three times greater shrinkage during weathering exposure. As shown in Table 4.21, the strains for hydrated samples were in the order of -1200 με. Larger strains occurred in hydrated samples because the hydration products, mainly $Ca(OH)_2$ and CSH, were readily available for the carbonation reaction to occur. It can been seen from the carbon dioxide absorption values in Table 4.17 that hydrated samples absorbed significantly greater quantities of CO_2 than pre-carbonated samples. Carbon dioxide uptake values for hydrated samples ranged between 9.25 and 9.80%, approximately 7 to 8% higher than carbonation cured samples. Larger carbon dioxide absorptions are indicative of greater carbonation shrinkage and these results support the observed trend. As would be expected, the strain measurements for hydrated samples were similar between batches since each batch underwent the same curing process. Multiple sets of hydrated samples were prepared to coincide with each pre-carbonated set and provide a control to ensure consistency during AWCT.

The total shrinkage observed in hydrated samples was due both to carbonation and drying shrinkage mechanisms, as was the case with pre-carbonated samples. Although both pre-carbonated and hydrated samples were exposed to similar relative humidity conditions, during post-curing and AWCT, the degree of drying shrinkage may have differed based on the quantity of unbound evaporable water. This would have been caused by differences in the chemical and physical structure of hydrated and pre-carbonated samples producing variations in the quantity of water held at >90% and 65% rh. Only the overall shrinkage was determined during this study and the individual contributions of carbonation and drying shrinkage mechanisms were not investigated.

Hydrated samples strain measurements are also plotted above in Figure 4.26. Similar to pre-carbonated samples, hydrated samples reached approximately one third of their overall strain within the first day. The rate of shrinkage then stabilized with time to an equilibrium strain of approximately -1200 με. In comparing the pre-carbonated and hydrated samples strain curves it appears that for each given time the hydrated samples shrank approximately three times more than that of the pre-carbonated samples. It is also noteworthy in Figure 4.26 that the deviation between hydrated sample batches is comparable with that of the carbonation cured batches. Both sets had a maximum deviation of about 100 με, which was likely due variation in the service exposure conditions since hydrated batches were all treated under similar conditions. This reiterates the fact that the small variances in strain noted for carbonation cured samples were negligible and not conclusive of any difference in AWCT behaviour.

4.2.2.2 Concrete

Shown in Table 4.22 are the dimensional stability results for concrete samples. In all cases overall shrinkage was observed and the magnitude was comparable between carbonation treatments. Carbonation cured concrete samples exhibited shrinkage strain in the order of -330 με. As previously discussed for cement paste samples, similar results between carbonation treatments seem reasonable since the difference in carbonation curing process had little effect on shrinkage behaviour. Although slight differences in carbon dioxide absorption values were measured during AWCT, these differences were relatively small and comparable with the variations observed during carbonation curing which caused no major changes in strain.

Table 4.22: Summary of weathering carbonation strain for concrete samples

Batch	Carbonation Treatment	Curing Carbonated Samples		Hydrated Samples	
		Strain, με	Deviation	Strain, με	Deviation
B5	2 hr	-367	±17	-475	±4
B6	17 hr Preset + 2 hr	-338	±13	-500	±0
B7	18 hr	-325	±0	-475	±25
B8	17 hr Preset + 18 hr	-317	±1	-477	±2

The variation in strain with time during AWCT is plotted in Figure 4.27. Similar to cement paste samples it can be seen that the behaviour of pre-carbonated concrete samples during service exposure was comparable for each carbonation treatment. The maximum deviation in strain for both carbonation cured and hydrated concrete samples was about 100 με. Significant shrinkage accounting for approximately half of the overall strain was recorder by the first day of AWCT. Likewise, it was found in Figure 4.25 that a large quantity of the overall change in mass was measured by the first day. The shrinkage then continued to stabilize with time reaching an equilibrium strain in the order of -330 με after approximately one month. This behaviour is again comparable with that of the change in mass which flattened out appreciably after the first day of exposure.

As shown in Table 4.22 and Figure 4.27 hydrated samples experienced approximately one and a half times greater shrinkage during AWCT than pre-carbonated samples. Strains for hydrated samples were relatively consistent and in the order of 500 με. Hydrated concrete samples experienced more shrinkage than carbonation cured samples because of the existence of CO_2 reactive phases, such as $Ca(OH)_2$ and CSH. This coincides with carbon dioxide absorption results that showed hydrated samples absorbing significantly more carbon dioxide than pre-carbonated samples. The average absorption value for hydrated samples during AWCT was 11.32%, while pre-carbonated samples had an average value of 2.91%.

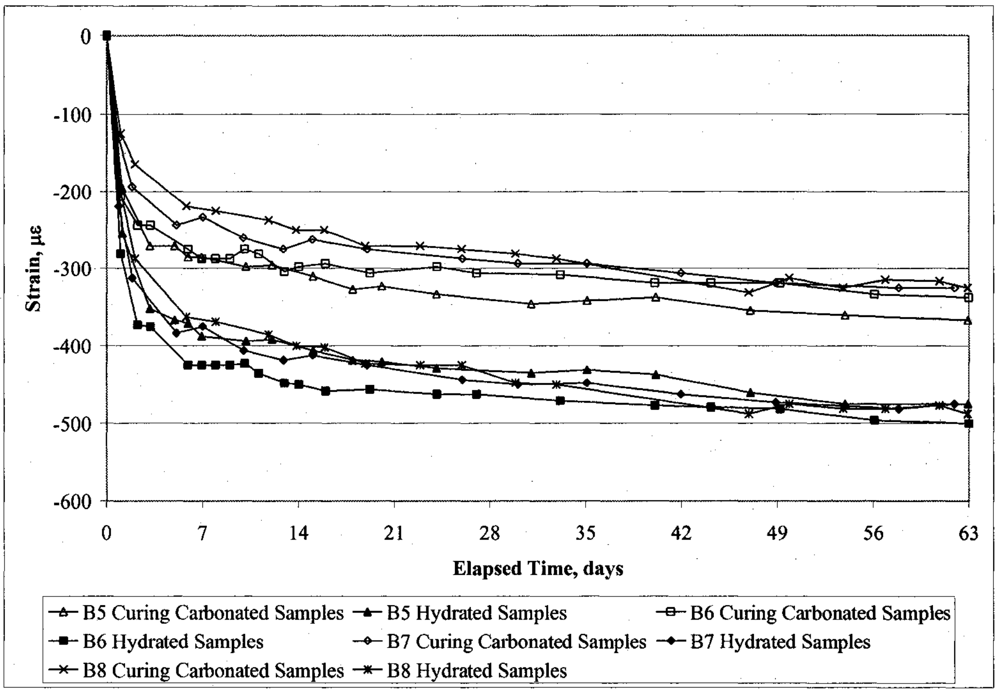

Figure 4.27: Accelerated weathering carbonation strain for concrete samples

Also plotted in Figure 4.27 are the shrinkage strains of hydrated samples measured at various intervals during AWCT. Similar to carbonation cured samples significant strain was observed after the first day of service exposure. The rate of shrinkage then stabilized with time reaching a steady-state strain in the order of -500 $\mu\varepsilon$. In comparing the pre-carbonated and hydrated samples curves it appears that for each given time the hydrated strains were approximately 1.5 times greater than the pre-carbonated strains. The variation in strain between hydrated samples was comparable to that of pre-carbonated samples and reaffirms that the variations in strain measurements between carbonation treatments were not conclusive of any difference in AWCT behaviour.

4.2.3 Compressive Strength Testing

4.2.3.1 Cement Paste

Compressive strength testing results for cement paste samples after 61 days of AWCT are shown in Table 4.23. The strengths are based on the average strength of two plate samples and the deviation of each from the mean is indicated. It can be seen from the results that there was negligible difference between the strengths of various carbonation curing treatments. Compressive strengths ranged from 84.6 to 92.5 MPa and when taking into consideration the deviation, the carbonation curing effect on cement compact strength after accelerated weathering carbonation tests was deemed insignificant. When compared with the average hydrated sample strength of all the batches, calculated as 89.1 MPa, it is evident that both the carbonation cured and purely hydrated samples achieved similar overall strengths in the order of 90 MPa.

Table 4.23: Compressive strength results for cement paste samples after 61-day AWCT

Batch	Carbonation Treatment	Compressive Strength, MPa			
		Carbonated	Deviation	Hydration	Deviation
B1	2 hr	84.6	±0.5	85.4	±3.1
B2	17 hr Preset + 2 hr	91.6	±6.2	74.5	±0.5
B3	18 hr	86.7	±1.3	102.3	±1.2
B4	17 hr Preset + 18 hr	92.5	±6.5	94.1	±4.5

Evaluating the compressive strengths of hydrated samples in Table 4.23 indicates that significant variation existed between each batch after AWCT. While the results obtained within each batch were fairly consistent with deviations no greater than 3.1 MPa, the compressive strengths between hydration batches varied as much as 27.8 MPa. It was previously shown in Table 4.14 that the hydrated strengths after post-curing were consistent between batches with an average of 44.4 MPa. Therefore, the large variation in strength between hydration batches after AWCT was likely due to deviation in the service exposure conditions. Such variables may have included the chamber carbon dioxide concentration and the initial sample moisture content. Following each strain and mass measurement the AWCT chamber was refilled with CO_2 to a concentration of 50%. In between measurements the CO_2 concentration decreased slightly as samples absorbed the gas, thereby causing variations in the level of CO_2 based on the number of samples in the chamber and the measurement frequency. As well, the initial moisture content of the samples may have varied between batches due to variation in the preparation time, room temperature and the sample storage container humidity. Such factors would have an effect on the development of hydration products and weathering carbonation. It is clear from the strength data obtained that the hydration samples were significantly more sensitive to experimental variation than pre-carbonated samples. Because pre-carbonated samples had a more stable structure, factors influencing weathering carbonation had much less impact on these samples. Despite shrinkage and carbon dioxide absorption values being similar between hydrated batches, it appears that variations in the exposure conditions during AWCT had a significant effect on hydrated samples strength development.

A summary of pre-carbonated sample compressive strengths for carbonation curing and AWCT is displayed in Figure 4.28. As previously discussed in Section 4.1.3.1 and shown graphically in Figure 4.28, the strengths of samples preset prior to carbonation curing were greater than those of samples carbonated immediately. It was also noted that the difference in strength between 2 and 18 hour carbonation curing was marginal for immediately carbonated samples, yet distinguishably larger for preset samples. After 7-day post-curing it was found that the difference in strengths between immediately carbonated samples and those preset was still significant. In terms of the 2 and 18 hour carbonation treatments the difference in strengths after post-curing was negligible for both immediately carbonated samples and preset samples. Nonetheless, after 61-day accelerated weathering carbonation testing the strengths for all carbonation curing treatments were found to be comparable and within the measured deviation. Samples preset prior to carbonation curing experienced a slight increase in strength during AWCT of 7 MPa on average for 2 and 18 hour carbonation. However, immediately carbonated samples had a significantly larger increase in strength of 22.5 MPa on average. While immediately carbonated samples lacked strength after 7-day post-curing, in comparison to preset samples, it appears that they made up for the difference during AWCT. It was shown in Table 4.17 that the increases in carbon dioxide content between treatments were comparable and relatively minor in comparison to the uptake during curing. Therefore, the differences in strength development during AWCT between immediately carbonation cured samples and those preset first were likely due primarily to hydration. Although both carbonation and hydration contributed to the strength gain during AWCT, the gain from hydration was significantly greater for immediately carbonation cured samples.

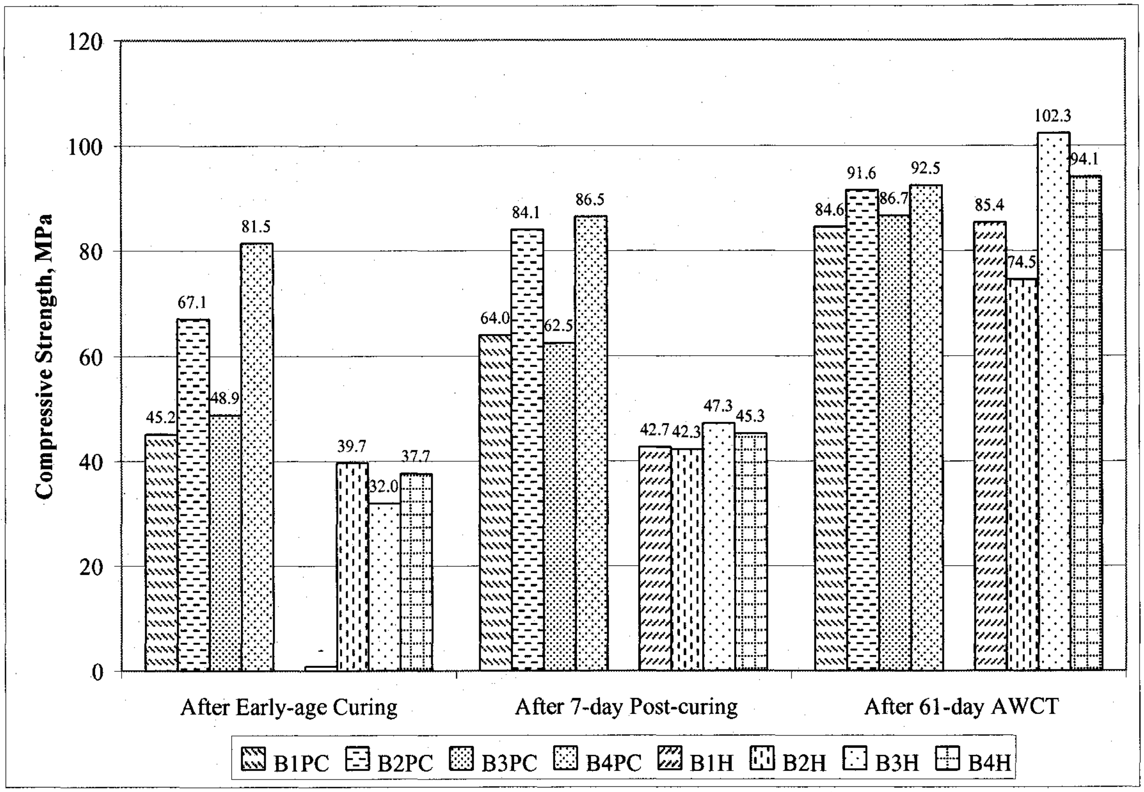

Figure 4.28: Compressive strength summary for carbonation cured and hydrated cement paste samples (PC – Pre-carbonated samples, H – Hydrated samples)

4.2.3.2 Concrete

Results for compressive strength testing of concrete samples are displayed in Table 4.24. Similar to cement paste samples, little variation in compressive strengths existed between carbonation curing treatments after AWCT. The strengths ranged from 16.0 to 21.1 MPa and when considering the deviation for each batch the strengths appear very similar. The average AWCT strength of pre-carbonated samples was calculated to be 18.4 MPa. In comparison to the hydrated sample strengths, with an average value calculated as 14.5 MPa, it is evident that both pre-carbonated and hydrated samples showed AWCT strengths in the same order of magnitude.

Table 4.24: Compressive strength results for concrete samples after 61-day AWCT

Batch	Carbonation Treatment	Compressive Strength, MPa			
		Carbonated	Deviation	Hydration	Deviation
B5	2 hr	16.0	±2.8	13.6	±2.9
B6	17 Preset + 2 hr	20.4	±1.5	16.6	±0.1
B7	18 hr	16.1	±1.5	14.2	±0.7
B8	17 hr Preset + 18 hr	21.1	±1.6	13.6	±0.8

Compressive strengths for hydrated samples following AWCT were fairly consistent and ranged between 13.6 and 16.6 MPa. In contrast to cement paste samples, hydrated concrete samples exhibited only slight variation in strength between batches. The deviation for each batch individually was no greater than 2.6 MPa and between batches it was found to be at most 3.0 MPa. It is possible that due the substantially smaller quantity of cement in concrete samples that variation in the service exposure and fabricating conditions had a less significant impact on the compressive strength than in cement paste samples.

Displayed in Figure 4.29 is a summary of the compressive strengths after carbonation curing, post-curing and AWCT. It is apparent from Figure 4.29 and the discussion in Section 4.1.3.2 that increasing the carbonation curing duration from 2 to 18 hours had negligible effect on the strength of immediately carbonated samples and only minor effect on preset samples. Also of interest was the observation that presetting samples prior to carbonation curing had negligible effect on the compressive strength when carbonated for 2 hours and slight effect after 18 hours. After the 7-day post-curing period the strengths were relatively similar to that after carbonation, with the exception of the preset/2 hour carbonation curing treatment which saw a more significant gain in strength. Following AWCT it was apparent that the strengths of all carbonation curing treatments were comparable and within the measured deviation of one another.

The measured compressive strength of carbonation cured concrete compacts was comparable with that of a commercially produced concrete masonry unit. A commercial masonry unit was found to have a compressive strength of approximately 19 MPa. This strength was obtained by cutting four sections approximately 90 by 40 by 95 mm from the two ends of a masonry unit. The specimens were then tested in compression along the longitudinal (95 mm) axis. Carbonation cured concrete samples had strengths similar to the masonry unit with an average of about 18 MPa, the values shown in Table 4.24.

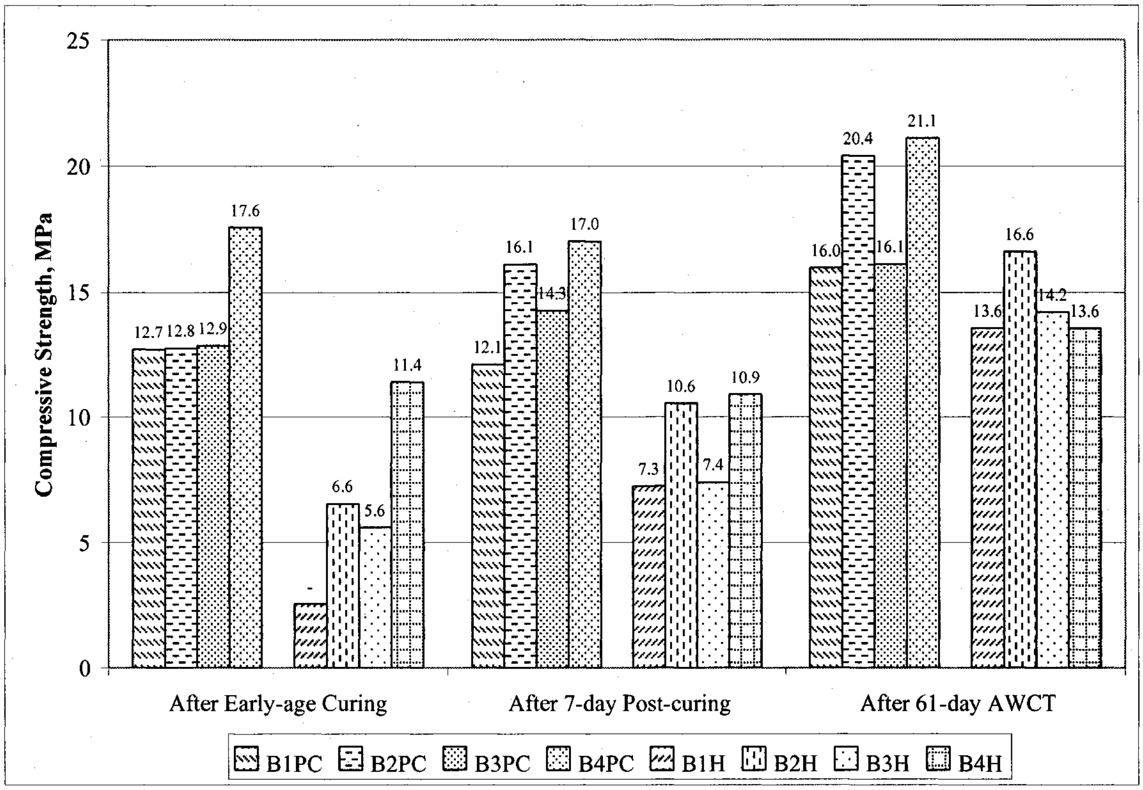

Figure 4.29: Compressive strength summary for carbonation cured and hydrated concrete samples (PC – Pre-carbonated samples, H – Hydrated samples)

4.3 FREEZE/THAW DURABILITY TESTING

Freeze/thaw durability testing was conducted on simulated concrete pavers. The mix design was the same as that previously used for concrete samples in Sections 4.1 and 4.2, however the sample thickness was doubled to approximately 36 mm. The compression moulded samples were preset for 22 hours, either carbonation cured or hydration cured for 22 hours and then left to hydrate in a sealed container for 28 days. Due to the capacity of the carbonation curing chamber two identical batches of concrete samples were made. Each batched contained ten samples, with half of the samples being carbonation cured and the other half hydration cured. The average characteristics of carbonation curing for the two batches, B17 and B18, are shown in Table 4.25. The carbon dioxide uptake values were comparable with those achieved during dimensional stability testing and in the order of 10%, as discussed in Section 4.1.1.2.

Table 4.25 Average characteristics of carbonation curing for Series Three

Batch	Carbonation Treatment	Average Mass Gain, %	Average Water Loss, %	Average Peak Temperature, °C
B17 & B18	22 hr Preset + 22 hr	10.70	4.73	38.1

Compressive strength testing was conducted with the uniaxial load applied to the broad side of the samples and the test set-up is shown in Figure 3.8. The strengths of concrete pavers immediately after curing and after 28 days are shown in Table 4.26. The results cannot be compared with compressive strength results from Section 4.1 due to the increased thickness and different loading orientation. It can be seen that carbonated samples had an average strength of 49.8 MPa immediately after carbonation. In comparison, hydrated samples had a slightly lower average strength of 42.4 MPa. After the 28 day curing period the strengths of carbonated and hydrated samples had increased to 62.3 and 49.7 MPa respectively.

Table 4.26: Compressive strength results for Series Three

	Compressive Strength, MPa			
	Carbonation	Standard Deviation	Hydration	Standard Deviation
Cured Strength	49.8	1.1	42.4	2.8
28 Day Strength	62.3	8.1	49.7	0.4

Results from freeze/thaw durability testing are shown in Table 4.27. It can be seen that carbonation cured samples had considerably smaller mass loss than hydrated samples. The average mass loss after 10 cycles for pre-carbonated samples was 218 g/m^2, approximately 90% less than hydrated samples which lost 1762 g/m^2. After 25 cycles the mass loss values for pre-carbonated and hydrated samples were 1425 and 10601 g/m^2 respectively; marking a similar difference of approximately 90% between carbonation cured and hydrated samples. Freeze/thaw testing was terminated after 25 cycles because the samples had all lost more than 500 g/m^2, as specified in the standard test procedure.

Typical carbonation cured and hydrated samples following 25 freeze/thaw cycles are shown in Figure 4.30. The enhanced resistance of pre-carbonated samples can be seen in Figure 4.30a by the reduced sample deterioration in comparison to the hydrated sample in Figure 4.30b.

Due to the large proportion of coarse aggregate in the concrete mix design causing a high porosity, significant spalling occurred during freeze/thaw testing of both pre-carbonated and hydrated samples. After both 10 and 25 cycles carbonation cured samples had lost considerably less mass than hydrated samples. This likely occurred because pre-carbonated samples had a denser structure and higher compressive strength. The volume of water present in the pore structure was reduced in the more dense pre-carbonated samples and therefore the expansive forces exerted within the sample were lower. As well, higher compressive strengths in the carbonated samples translated to a higher tensile strength that resisted the expansive forces as the water froze.

Table 4.27: Freeze/thaw resistance of simulated concrete pavers

Sample	Carbonation Treatment	Cumulative Mass Loss, g/m^2	
		10 Cycles	25 Cycles
S1C	22 Preset + 22 hr	178	1309
S2C	22 Preset + 22 hr	192	1397
S3C	22 Preset + 22 hr	284	1568
	Average	218	1425
S4H	Hydration	1255	9976
S5H	Hydration	1626	9350
S6H	Hydration	2406	12478
	Average	1762	10601

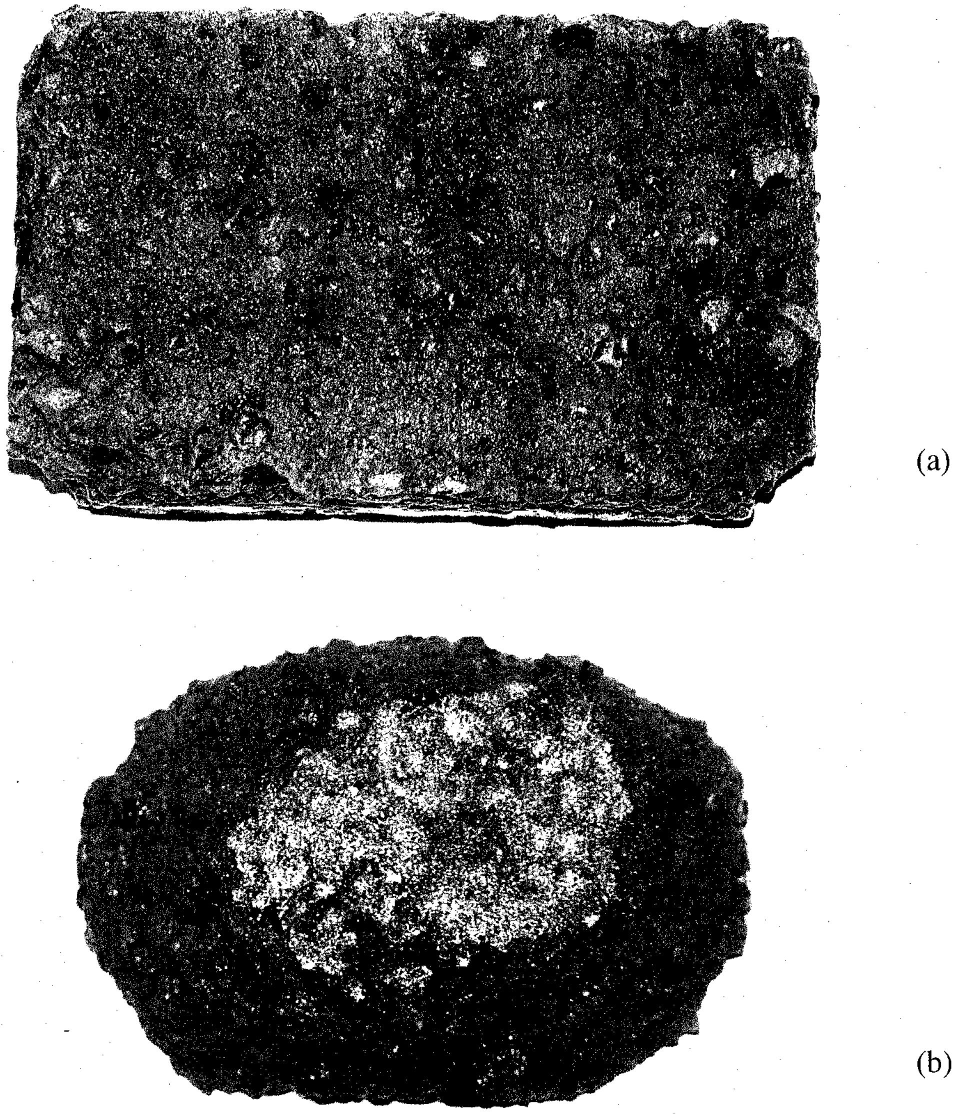

Figure 4.30: Typical concrete samples following 25 freeze/thaw cycles (a) carbonation cured sample, (b) hydrated sample

Commercially moulded concrete pavers were received in a fresh state and carbonation cured at McGill University during a previous investigation. These samples were subsequently used in this study to determine the difference in freeze/thaw resistance between carbonation cured and hydrated samples. The results are shown in Table 4.28 and it can be seen that carbonation cured samples were more durable than the hydrated sample. While the 24 hour preset and 5 hour carbonation curing treatment proved slightly more resistant than 2 hour preset and 4 hour carbonation curing, both treatments preformed considerably better than the hydrated reference sample. Carbonation cured samples P1C and P2C had mass loss values of 37.6 and 5.4 g/m^2 after 25 freeze/thaw cycles, compared with the hydrated sample which had a value of 328 g/m^2. Figure 4.31 shows carbonation cured sample P1C and hydrated sample P3H. It can be seen that little spalling appears to have occurred on the carbonated sample surface, while spalling is clearly evident on the bottom of the hydrated sample. No significant differences in the surface texture of samples P1C and P2C were observed.

Mass loss for commercially produced pavers was considerably less than that determined for the simulated concrete pavers. This occurred because the simulated pavers were significantly more porous due to the large quantity of coarse aggregate. It was also probable that the compaction moulding load for commercial pavers was higher than that used for simulated pavers. The more dense structure of commercial pavers provided less pore space for water to freeze and exert destructive expansive forces on the concrete matrix.

Table 4.28: Freeze/thaw resistance of commercial concrete pavers

Sample	Carbonation Treatment	Cumulative Mass Loss, g/m^2	
		10 Cycles	25 Cycles
P1C	2 hr Preset + 4 hr	2.7	37.6
P2C	24 hr Preset + 5 hr	2.2	5.4
P3H	Hydration	26.9	328.0

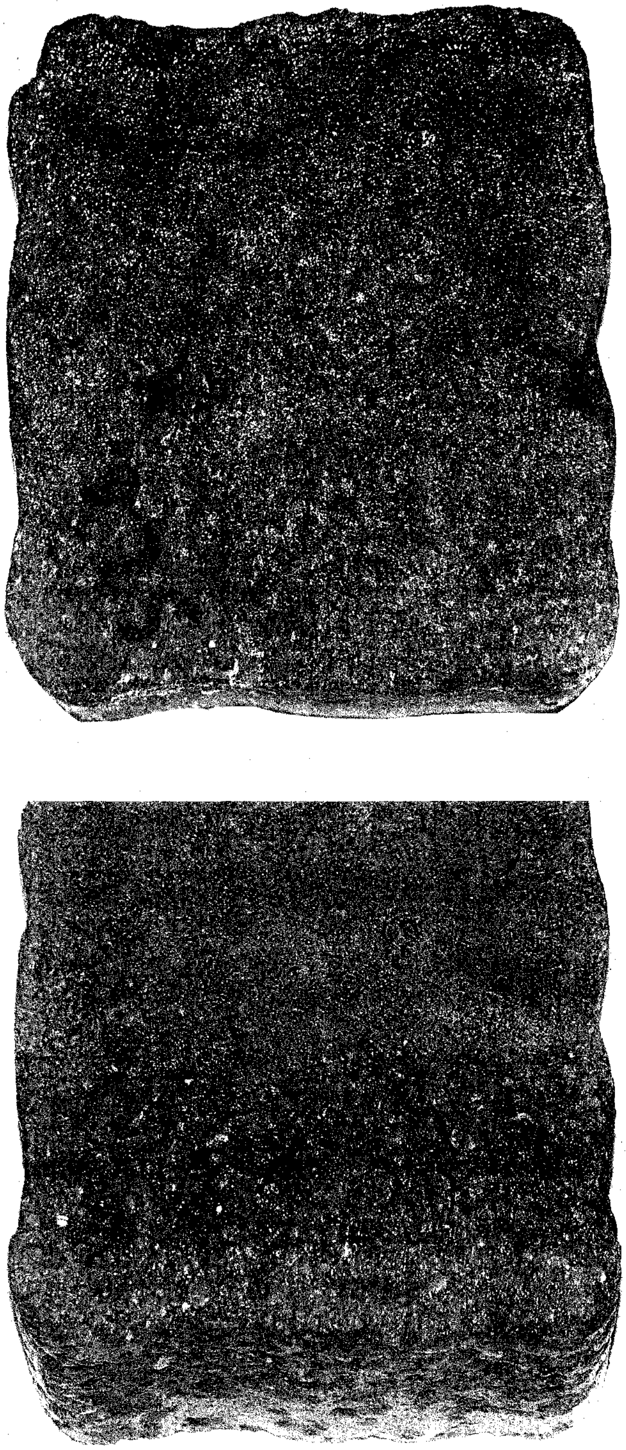

Figure 4.31: Typical commercial concrete pavers following 25 freeze/thaw cycles (a) carbonation cured paver, (b) hydrated paver

CHAPTER 5 CONCLUSIONS AND RECOMMENDATIONS

5.1 CONCLUSIONS

Carbon dioxide absorption and the durability of carbonated concrete were studied to investigate the feasibility of carbon dioxide sequestration through carbonation curing of cementitious products. Both cement paste and concrete samples were examined to quantify the dimensional stability behaviour, carbon dioxide absorption potential and compressive strength as the result of carbonation curing. Qualitative depth of carbonation testing was also performed on these specimens. Similar samples were subsequently exposed to accelerated weathering carbonation testing to quantify their service behaviour in terms of dimensional stability, carbon dioxide absorption and compressive strength. Cement paste samples were used to obtain the most drastic results where as concrete samples were used to simulate concrete masonry units. Durability testing was also conducted on samples simulating concrete pavers to investigate the freeze/thaw resistance of carbonation cured products versus those conventionally hydration cured.

From the Series One test program investigating carbon dioxide absorption and the dimensional stability during early age carbonation curing and in subsequent service exposure, the following conclusions were drawn:

From early age carbonation curing testing:

1) The effect of presetting cement paste samples on carbon dioxide absorption was insignificant. Increasing the duration of carbonation from 2 to 18 hours increased the uptake of carbon dioxide by approximately 2%, however the gain was not remarkable in comparison to the uptake during the initial 2 hours.
2) Higher peak temperatures were observed for immediately carbonated samples than those preset first. Presetting the samples and allowing partial hydration to occur likely dampened the initially rapid carbonation reaction. The peak temperature was also found to be reached within the first 30 minutes, explaining

why comparable peaks were observed for both 2 and 18 hour carbonation durations.

3) Water loss was significantly reduced when samples were preset prior to carbonation curing. This can be attributed to water being bound in hydration products and a lower peak temperature. Water loss was only slightly higher during prolonged carbonation because the exothermic carbonation reaction which evaporated water was short lived and predominately occurred within the initial 2 hours.
4) Carbon dioxide content as analyzed by infrared technology revealed that both the surface and core of specimens were carbonated. The degree of carbonation was in the same order of magnitude between the surface and core with differences of 1-2% after 2 hour carbonation and less than 1% after 18 hours.
5) Contrary to cement paste samples, presetting concrete samples reduced the carbon dioxide uptake by 1-2%. Increasing the duration of carbonation for concrete samples increased the quantity of carbon dioxide absorbed to a greater extend than that observe for cement paste.
6) Peak temperature and water loss trends were similar between concrete and cement paste samples for various carbonation curing treatments. For concrete samples however, the peak temperature and water loss values were lower than for cement paste. This occurred because of the smaller cement content present in concrete samples.
7) Despite the difference in cement content in cement paste and concrete samples, carbon dioxide absorption values were comparable and in the order of 10%.
8) Carbonation curing of cement paste samples resulted in overall shrinkage. In contrast to cement paste samples, concrete samples exhibited overall expansion during carbonation curing. After equilibrating the samples of each batch to room temperature no significant difference in dimensional stability behaviour was observed between the various carbonation curing treatments.
9) The effect of increasing the duration of carbonation curing from 2 to 18 hours on the compressive strength was minimal when samples were carbonated immediately. For preset samples the effect of increasing the duration of

carbonation was a 21% increase in strength for cement paste samples and a 36% increase for concrete samples.

10) Variation in strength development during carbonation from presetting samples depended on the carbonation duration and sample composition. Cement paste samples preset prior to carbonation curing produced strengths approximately 50-70% higher than immediately carbonated samples. Concrete samples carbonation cured for 2 hours had no added strength from presetting while those carbonated for 18 hours had a 36% increase.
11) After a 7-day post-curing hydration period, the strength of samples preset prior to carbonation curing was still greater than that of samples carbonated immediately with no preset by approximately 25-25%.
12) In all instances the compressive strength of carbonation cured samples exceeded that of their parallel hydration samples. After the 7-day hydration period the strength of hydrated samples was still only equal to that of the weakest samples following carbonation curing.
13) Despite a purple core existing in carbonated cement paste samples, carbon dioxide analysis of the core material indicated that carbonation had occurred inside the core. Carbon dioxide content levels in the core material were found to be of the same magnitude as those on the surface of the sample. No correlation was observed in the degree of carbonation determined by phenolphthalein spray method and by infrared analyzer method.
14) Calcium carbonate produced during carbonation curing was formed as calcite and aragonite. Uncarbonated calcium silicates were detected in the samples, while no evidence of calcium hydroxide was found in either immediately carbonated or preset sample.

From accelerated weathering carbonation testing:

15) Carbon dioxide absorption by cement paste and concrete was observed in accelerated weathering carbonation testing. The absorption was reduced by approximately 75-85% when samples were carbonation cured as oppose to cured through conventional hydration. The cumulative quantity of carbon dioxide

absorbed during curing and subsequent exposure was comparable between carbonation cured and hydrated samples and in the same order of 10-12%.

16) The core material of hydration cured samples exposed to service conditions had carbon dioxide contents comparable with those on the surface, indicating carbonation had occurred through the entire thickness of samples.
17) Overall shrinkage was observed for both cement paste and concrete samples once exposed to carbon dioxide environment. Service shrinkage was reduced by approximately 66% when samples were carbonation cured instead of purely hydration cured. For concrete samples the reduction in shrinkage from carbonation curing was 33%.
18) At least 33% of the overall shrinkage observed and a significant portion of the mass gain occurred within the first day of service exposure.
19) The strengths of carbonation cured samples following AWCT were comparable between the various carbonation curing treatments. As well, the strengths of carbonation cured and hydration cured samples were comparable after service exposure.
20) During service exposure carbonation cured samples saw an approximate 20% increase in strength from their 7 day strength, while hydration samples saw a 60-100% increase for the same period. This greater increase in strength by hydration samples made up for their weaker strength than carbonated samples prior to AWCT. As the result, both carbonation cured and hydration cured samples had comparable strengths after service exposure.

The following conclusions were drawn from Series Two testing of the in-situ dimensional stability during carbonation curing:

1) While carbon dioxide absorption results tended to agree between parallel batches of Series One and Series Two experiments, the water loss and peak temperature values were considerably different. This was attributed to the variation in the number of samples in the carbonation chamber. Series One used eight samples per batch, while Series Two employed only one prism for in-situ strain measurement.

2) Shrinkage measurements for Series Two cement paste experiments were approximately 50% less than Series One. This was due to the difference in sample size and the resulting variation in peak temperature and water loss.
3) In series Two testing, cement paste samples carbonated for 18 hours showed approximately 30-40% less shrinkage than that of 2 hour carbonation. It was also found that shrinkage was reduced by about 20-30% when the samples were preset first.
4) In-situ strain measurements during carbonation curing revealed that cement paste samples experienced expansion in first 4 minutes immediately after the CO_2 gas was injected into the chamber. Samples subsequently shrank for about 2 hours, to a greater extent than the initial expansion. For 18 hour carbonation the samples then expanded slightly before eventually reaching equilibrium after 15 hours. Overall, the quantity of shrinkage exceeded that of expansion.
5) Concrete samples experienced overall expansion during carbonation curing. The degree of expansion was comparable between 2 and 18 hour carbonation. Expansion was reduced by approximately 87% when samples were preset prior to carbonation curing.
6) In general, the strain behaviour of cement paste and concrete samples followed a similar trend. The expansive behaviour of concrete as appose to the shrinkage observed for cement paste can be primarily attributed to the magnitude of the shrinkage phase. This shrinkage phase was significantly less for concrete than cement paste and overall the expansive phases in concrete were dominant.

Series Three experiments investing the freeze/thaw resistance of concrete pavers found the following conclusions:

1) The 28-day strength of carbonation cured concrete pavers was 25% greater than conventionally hydration cured pavers.
2) Mass loss for simulated concrete pavers after 10 and 25 cycles of freeze/thaw testing was approximately 90% less for carbonation cured samples than hydration

cured samples. For commercially produced pavers the reduction in mass loss associated with carbonation curing was of similar magnitude.

5.2 RECOMMENDATIONS FOR FUTURE WORK

Many aspects of carbonation require further study and the following list identifies some of the major items:

1) Investigation into the phenolphthalein behaviour of carbonation cured cement paste compacts. While the compact core turned purple when sprayed with phenolphthalein and this behaviour was interpreted as being indicative of negligible carbonation by previous studies, it was found that the core was carbonated to a significant degree. Furthermore, an understanding of the purple bands observed from phenolphthalein testing of cement paste compacts carbonation cured immediately after moulding should be developed.
2) Measurement of the weathering carbonation shrinkage solely attributed to carbonation. Further research should focus on eliminating drying shrinkage during service exposure by equilibrating the samples moisture content prior to testing with that of service conditions.
3) Investigation of the batch size effect during carbonation curing. While batch size had negligible effect on the quantity of carbon dioxide absorbed, it significantly influenced the water loss, peak temperature and shrinkage.
4) Determination of the 68-day compressive strength of samples purely hydrated and not exposed to carbon dioxide. This strength could then be compared with that of carbonation cured and hydrated samples exposed to accelerated weathering carbonation.
5) Quantification of the carbon dioxide absorbed in terms of percent mass gain at each period of measurement during accelerated weathering carbonation. These values could then be directly compared with the percent mass gain during carbonation curing. During this study the service exposure mass change was expressed in grams since the water lose value required to determine the percent mass change was not quantified.

6) Additional testing into the effect of carbon dioxide pressure and concentration during carbonation curing. Significant mass gain was observed for hydrated samples within the first day of service exposure at atmospheric pressure and a carbon dioxide concentration of 50%. Further study should focus on the physical and economical advantages/disadvantages of using a high carbon dioxide pressure and concentration for carbonation curing versus that under lower exposure conditions.

REFERENCES

Bukowski, J.M. and Berger, R.L. (1979). "Reactivity and Strength Development of CO_2 Activated Non-hydraulic Calcium Silicates". *Cement and Concrete Research*, V.9, pp. 57-68.

Dow, C. and Glasser, F.P. (2002). "Calcium Carbonate Efflorescence on Portland Cement and Building Materials" *Cement and Concrete Research*, V.33, pp. 147-154

Field, C.B. and Raupach, M.R. (2004). "The Global Carbon Cycle", Washington: Island Press, pp. 1-2, 431-436.

"GHG Glossary of Terms", (n.d.). Retrieved August 30, 2005, from http://www.evomarkets.com/ghg_glossary.html

Goodbrake, C.J., Young, J.F. and Berger, R.L. (1979). "Reaction of Beta-Dicalcium Silicate and Tricalcium Silicate with Carbon Dioxide and Water Vapour", *Journal of the American Ceramic Society*, V. 62, pp. 168-171.

"Greenhouse Gases, Climate Change, and Energy", (2004). *Energy Information Administration*. Retrieved August 30, 2005, from http://www.eia.doe.gov/oiaf/1605/ggccebro/chapter1.html

Halmann, M.M. and Steinberg, M. (1999). "Greenhouse Gas Carbon Dioxide Mitigation", New York: Lewis Publishers, CRC Press, pp. 1-13, 139-142.

"Impact of the Kyoto Protocol on U.S. Energy Markets & Economic Activity", (2002). *Energy Information Administration*. Retrieved August 30, 2005, from http://www.eia.doe.gov/oiaf/kyoto/kyotorpt.html

IPCC (2005). "Carbon Dioxide Capture and Storage". *Intergovernmental Panel on Climate Change*. Retrieved August 29, 2005, from http://www.ipcc.ch/

IPCC (2001). "Climate Change 2001: The Scientific Basic". *Intergovernmental Panel on Climate Change*. Retrieved September 1, 2005, from http://www.grida.no/climate/ipcc_tar/vol4/english/086.htm

IPCC (2001). "Climate Change 2001: Mitigation". *Intergovernmental Panel on Climate Change*. Retrieved September 2, 2005, from http://www.grida.no/climate/ipcc_tar/wg3/005.htm

IPCC (1995). "IPCC Second Assessment: Climate Change 1995". *Intergovernmental Panel on Climate Change*. Retrieved September 2, 2005, from http://www.ipcc.ch/pub/sa(E).pdf

Jaques, A., Neitzert, F. and Boileau, P. (1997). "Trends in Canada's Greenhouse Gas Emissions 1990-1995", Environment Canada: Canadian Cataloguing in Publication Data, pp. 1-3, 37-38.

Klemm, W.A. and Berger, R.L. (1972). "Accelerated Curing of Cementitious Systems by Carbon Dioxide", *Cement and Concrete Research*, V.2, pp. 567-576.

"Kyoto Protocol", (2005). *Wikipedia, The Free Encyclopedia.* Retrieved September 6, 2005, from http://en.wikipedia.org/wiki/Kyoto_Protocol

Lackner, K.S., Wendt, C.H., Butt, D.P., Joyce Jr., E.L. and Sharp, D.H. (1995). "Carbon Dioxide Disposal in Carbonate Minerals", *Energy*, V.20 (11), pp. 1153-1170.

Lo, Y. and Lee, H.M. (2001). "Curing Effects on Carbonation of Concrete using a Phenolphthalein Indicator and Fourier-transform Infrared Spectroscopy", *Building and Environment*, V.37, pp. 507-514

Metha, P.K. and Monteiro, P.J.M. (1993). "Concrete: Structure, Materials, and Properties", Prentice Hall

Miller, G.T. (1998). "Living in the Environment: Principles, Connections, and Solutions", New York, NY: Brooks Cole, pp. 113-115, 161-162, 370-371, 365-367.

Mourtis, F. (2003). "Capture and Sequestration of Greenhouse Gases in Canada", Natural Resources Canada, Ottawa.

NETL (2004). "Carbon Sequestration: Technology Roadmap and Program Plan", National Energy Technology Laboratory, US Department of Energy.

Neville, A.M. (1981). "Properties of Concrete" 3rd Edition, London, England: Pitman Publishing Limited, pp. 391-395.

Orchard, D.F. (1979). "Concrete Technology" Volume 1, Barking, England: Applied Science Publishers Ltd, pp. 343-345.

Penner, L., O'Connor, W.K., Dahlin, D.C., Gerdemann, S. and Rush, G.E. (2004). "Mineral Carbonation: Energy Costs of Pretreatment Options and Insights Gained from Flow Loop Reaction Studies", *3rd Annual Conference on Carbon Capture and Sequestration*, CDROM, Washington, D.C.

Powers, T.C. (1962). "A Hypothesis on Carbonation Shrinkage", *Journal of the PCA Research and Development Laborartories*, V.4(2), pp. 40-50.

Ramachandran, V.S. and Beaudoin, J.J. (2001). "Handbook of Analytical Techniques in Concrete Science and Technology", Park Ridge, NJ: William Andrew Publishing/Noyes, pp. 395-400.

Ramachandran, V.S., Feldman, R.F. and Beaudoin, J.J. (1981). "Concrete science: treatise on current research", London, England: Heyden & Son Ltd, pp. 381-397.

Reardon, E.J., James, B.R. and Abouchar, J. (1989). "High Pressure Carbonation of Cementitious Grout", *Cement and Concrete Research*, V.19, pp. 385-399

Sanders, R. (2005). "Faster Carbon Dioxide Emissions will overwhelm Capacity of Land and Ocean to absorb Carbon". Retrieved September 3, 2005, from http://www.berkeley.edu/news/media/releases/2005/08/02_carbon.shtml

Shideler, J.J. (1963). "Carbonation Shrinkage of Concrete Masonry Units", *Journal of the PCA Research and Development Laboratories*, V.5(3), pp. 36-51

Short, A. and Kinniburg, W. (1968). "Lightweight Concrete", London, England: CR Books Ltd, pp. 242-252.

Simatupang, M.H., Habighorst, C., Lange, H. and Neubauer, A. (1995). "Investigations on the Influence of the Addition of Carbon Dioxide on the Production and Properties of Rapidly Set Wood-Cement Composities", *Cement &Concrete Composites*, V.17, pp. 187-197.

St. John, D.A., Poole, A.B. and Sims, I. (1998). "Concrete Petrography - A Handbook of Investigative Techniques", London, England: Arnold, Hodder Headline Group, pp. 205-214.

Toennies, H.T. (1960). "Artificial Carbonation of Concrete Masonry Units", *Journal of the American Concrete Institute*, Title No. 56-42, pp.738-755.

Wigley, T.M.L. and Schimel, D.D. (2000). "The Carbon Cycle", New York, NY: Cambridge University Press, pp. 8-13.

Worrell, E., Price, L., Martin, N. (2001). "Carbon Dioxide Emissions from the Global Cement Industry", *Annual Review of Energy and Environment*, 26, pp. 303-329.

Ye, G. (2003). "Carbon Dioxide Uptake by Concrete through Early-age Curing", Montreal, QC: McGill University, Department of Civil Engineering and Applied Mechanics.

Young, J.F., Berger, R.L. and Breese, J. (1974). "Accelerated Curing of Compacted Calcium Silicate Mortars on Exposure to CO_2", *Journal of the American Ceramic Society*, V.57 (9), pp. 394-397.

Zhou, X.D. (2006). "Carbon Dioxide Uptake through Carbonation of Concrete using Simulated and Captured Flue Gas", Montreal, QC: McGill University, Department of Civil Engineering and Applied Mechanics.

APPENDIX A: SERIES ONE EXPERIMENTAL DATA

Definition of Samples

Carbonation Cured Samples

S1C S2C	Carbonation cured bar samples used for strain measurements during carbonation curing and accelerated weathering carbonation.
S5C S6C	Carbonation cured plate samples used for destructive testing following carbonation curing.
S7C S8C	Carbonation cured plate samples used for destructive testing after 7 day post-setting hydration period.
S9C S10C	Carbonation cured plate samples used for destructive testing following accelerated weathering carbonation.

**All samples were used to obtain the characteristics of carbonation curing.*

Hydration Cured Samples

S3H S4H	Hydration cured bar samples used for reference strain measurements during curing and accelerated weathering carbonation.
S11H S12H	Hydration cured plate samples used for destructive testing following carbonation curing.
S13H S14H	Hydration cured plate samples used for destructive testing after 7 day post-setting hydration period.
S15H S16H	Hydration cured plate samples used for destructive testing following accelerated weathering carbonation.

Table A.1: Batch B1 experimental data

i) Mix Design

Cement, g	5000
Water, g	750
Fine (River Sand), g	-
Coarse (Limestone, -4.75 to +2.36), g	-
Water Absorption (fine and coarse), %	-
w/c ratio	0.15

ii) Carbonation Curing Characteristics

Preset, hr	0
Carbonation Curing Duration, hr	2
Mass of Collected Water, g	79.4
Water Loss, %	20.76
Mass Gain, %	10.83
Peak Temperature, °C	89.4

iii) Dimensional Stability

Sample	S1C	S2C	S3H	S4H
Carbonation/Hydration Curing				
Strain Gauge Length, in.	8.0048	8.0042	8.0054	
Initial Strain Gauge Reading, in.	0.0816	0.0810	0.0822	
After Curing Strain Gauge Reading, in.	0.0771	0.0764	0.0857	
After Curing Change in Length, in.	-0.0045	-0.0046	0.0034	
After Curing Strain, $\mu\varepsilon$	-558.0	-570.5	428.9	
After Cooling Strain Gauge Reading, in.	0.0755	0.0745	-	
After Cooling Change in Length, in.	-0.0061	-0.0065	-	
After Cooling Strain, $\mu\varepsilon$	-757.9	-807.9	-	
Accelerated Weathering Carbonation				
Initial Strain Gauge Reading, in.	0.0764	0.0756	0.0878	
After Exposure Strain Gauge Reading, in.	0.0729	0.0719	0.0776	
Change in Length, in.	-0.0035	-0.0037	-0.0102	
Strain, $\mu\varepsilon$	-433.1	-458.1	-1270.0	

iv) Curing Mass Change

	Carbonation Cured Samples								Hydration Samples							
Sample	S1C	S2C	S5C	S6C	S7C	S8C	S9C	S10C	S3H	S4H	S11H	S12H	S13H	S14H	S15H	S16H
Carbonation/Hydration Curing																
Initial Sample Mass, g	364.7	365.3	368.2	368.6	368.6	368.8	368.2	368.7	361.8				367.8	367.1	368.0	367.9
After Curing Sample Mass, g	391.4	390.5	391.9	392.0	392.3	393.1	392.4	395.1	361.8				367.8	367.1	368.0	367.9
Accelerated Weathering Carbonation																
Initial Sample Mass, g	392.4	391.3	-	-	-	-	392.6	393.5	368.3				-	-	369.3	371.5
After Exposure Sample Mass, g	395.8	394.7	-	-	-	-	396.5	397.6	395.9				-	-	396.2	399.3

v) Destructive Testing

	Carbonation Cured Samples						Hydration Samples					
Sample	S5C	S6C	S7C	S8C	S9C	S10C	S11H	S12H	S13H	S14H	S15H	S16H
Test Period*	CC	CC	7D	7D	WC	WC			7D	7D	WC	WC
CO_2 Content Analysis												
Surface CO_2 Content, %	10.42	10.00	10.62	10.90	12.43	11.73			1.09	0.88	10.94	10.12
Core CO_2 Content, %	8.35	9.30	8.36	8.13	10.62	11.21			0.57	0.55	10.24	10.31
Average CO_2 Content, %	9.39	9.65	9.49	9.52	11.53	11.47			0.83	0.72	10.59	10.22
Compressive Strength Testing												
Compressive Strength, MPa	46.0	44.3	66.4	61.5	85.1	84.0			42.5	42.9	82.2	88.5

*CC - carbonation cured; HC - hydration cured; 7D - 7 day post-setting; WC - weathering carbonation

Table A.2: Batch B2 experimental data

i) Mix Design

Cement, g	5000
Water, g	750
Fine (River Sand), g	-
Coarse (Limestone, -4.75 to +2.36), g	-
Water Absorption (fine and coarse), %	-
w/c ratio	0.15

ii) Carbonation Curing Characteristics

Preset, hr	17
Carbonation Curing Duration, hr	2
Mass of Collected Water, g	42.7
Water Loss, %	11.87
Mass Gain, %	10.85
Peak Temperature, °C	77.0

iii) Dimensional Stability

Sample	S1C	S2C	S3H	S4H
Carbonation/Hydration Curing				
Strain Gauge Length, in.	8.0045	8.0028	8.0001	8.0014
Initial Strain Gauge Reading, in.	0.0811	0.0794	0.0767	0.0780
After Curing Strain Gauge Reading, in.	0.0768	0.0756	0.0770	0.0783
After Curing Change in Length, in.	-0.0043	-0.0037	0.0004	0.0003
After Curing Strain, με	-533.0	-466.5	45.8	37.5
After Cooling Strain Gauge Reading, in.	0.0747	0.0737	0.0770	0.0783
After Cooling Change in Length, in.	-0.0064	-0.0056	0.0004	0.0003
After Cooling Strain, με	-795.4	-703.9	45.8	37.5
Accelerated Weathering Carbonation				
Initial Strain Gauge Reading, in.	0.0749	0.0737	0.0796	0.0813
After Exposure Strain Gauge Reading, in.	0.0716	0.0709	0.0701	0.0716
Change in Length, in.	-0.0033	-0.0028	-0.0095	-0.0097
Strain, με	-403.9	-349.9	-1183.3	-1212.3

iv) Curing Mass Change

	Carbonation Cured Samples								Hydration Samples							
Sample	S1C	S2C	S5C	S6C	S7C	S8C	S9C	S10C	S3H	S4H	S11H	S12H	S13H	S14H	S15H	S16H
Carbonation/Hydration Curing																
Initial Sample Mass, g	364.7	364.1	364.4	364.6	365.4	364.8	364.9	365.3	364.0	364.4	365.7		365.7	365.1	366.0	365.4
After Curing Sample Mass, g	394.9	394.1	394.7	393.2	393.7	393.4	393.8	395.3	364.2	364.5	365.9		365.9	365.4	366.1	365.6
Accelerated Weathering Carbonation																
Initial Sample Mass, g	394.7	393.2	-	-	-	-	393.6	395.4	368.0	368.1	-		-	-	370.4	369.2
After Exposure Sample Mass, g	396.3	395.6	-	-	-	-	396.6	397.9	394.3	394.4	-		-	-	398.7	397.2

v) Destructive Testing

	Carbonation Cured Samples						Hydration Samples					
Sample	S5C	S6C	S7C	S8C	S9C	S10C	S11H	S12H	S13H	S14H	S15H	S16H
Test Period*	CC	CC	7D	7D	WC	WC	HC		7D	7D	WC	WC
CO_2 Content Analysis												
Surface CO_2 Content, %	9.33	9.70	9.39	8.07	11.52	11.69	0.82		0.91	0.99	9.59	10.46
Core CO_2 Content, %	8.95	8.95	8.62	8.55	9.87	10.67	0.58		0.58	0.50	9.85	10.08
Average CO_2 Content, %	9.14	9.33	9.01	8.31	10.70	11.18	0.70		0.75	0.75	9.72	10.27
Compressive Strength Testing												
Compressive Strength, MPa	60.3	73.8	89.0	79.1	85.4	97.7	39.7		37.8	46.7	75.0	74.0

*CC - carbonation cured; HC - hydration cured; 7D - 7 day post-setting; WC - weathering carbonation

Table A.3: Batch B3 experimental data

i) Mix Design

Cement, g	5500
Water, g	825
Fine (River Sand), g	-
Coarse (Limestone, -4.75 to +2.36), g	-
Water Absorption (fine and coarse), %	-
w/c ratio	0.15

ii) Carbonation Curing Characteristics

Preset, hr	0
Carbonation Curing Duration, hr	18
Mass of Collected Water, g	87.1
Water Loss, %	22.41
Mass Gain, %	12.68
Peak Temperature, °C	97.3

iii) Dimensional Stability

Sample	S1C	S2C	S3H	S4H
Carbonation/Hydration Curing				
Strain Gauge Length, in.	8.0066	8.0052	8.0051	8.0035
Initial Strain Gauge Reading, in.	0.0832	0.0818	0.0817	0.0801
After Curing Strain Gauge Reading, in.	0.0771	0.0752	0.0836	0.0803
After Curing Change in Length, in.	-0.0061	-0.0066	0.0033	0.0015
After Curing Strain, $\mu\varepsilon$	-761.9	-828.6	416.4	191.6
After Cooling Strain Gauge Reading, in.	0.0772	0.0753	0.0836	0.0803
After Cooling Change in Length, in.	-0.0060	-0.0065	0.0019	0.0002
After Cooling Strain, $\mu\varepsilon$	-753.5	-816.1	241.5	25.0
Accelerated Weathering Carbonation				
Initial Strain Gauge Reading, in.	0.0758	0.0739	0.0860	0.0830
After Exposure Strain Gauge Reading, in.	0.0724	0.0711	0.0757	0.0734
Change in Length, in.	-0.0034	-0.0028	-0.0103	-0.0096
Strain, $\mu\varepsilon$	-424.7	-345.6	-1286.7	-1199.5

iv) Curing Mass Change

	Carbonation Cured Samples								Hydration Samples							
Sample	S1C	S2C	S5C	S6C	S7C	S8C	S9C	S10C	S3H	S4H	S11H	S12H	S13H	S14H	S15H	S16H
Carbonation/Hydration Curing																
Initial Sample Mass, g	369.1	367.5	368.3	368.5	368.5	368.4	368.4	368.6	366.7	366.0	368.4	369.0	368.8	368.6	368.9	368.7
After Curing Sample Mass, g	398.9	399.5	397.6	398.2	397.6	397.1	397.3	398.5	366.3	363.9	365.1	365.7	365.1	365.2	365.6	365.9
Accelerated Weathering Carbonation																
Initial Sample Mass, g	397.8	397.5	-	-	-	-	397.6	398.2	368.9	366.8	-	-	-	-	369.4	370.5
After Exposure Sample Mass, g	399.1	399.0	-	-	-	-	399.5	400.0	394.7	392.5	-	-	-	-	396.6	398.1

v) Destructive Testing

	Carbonation Cured Samples						Hydration Samples					
Sample	S5C	S6C	S7C	S8C	S9C	S10C	S11H	S12H	S13H	S14H	S15H	S16H
Test Period*	CC	CC	7D	7D	WC	WC	HC	HC	7D	7D	WC	WC
CO_2 Content Analysis												
Surface CO_2 Content, %	11.84	11.56	11.69	11.70	13.64	13.65	0.78	0.94	0.94	0.86	11.37	10.90
Core CO_2 Content, %	9.08	11.07	10.43	10.15	10.44	10.88	0.47	0.54	0.54	0.48	9.58	10.18
Average CO_2 Content, %	10.46	11.32	11.06	10.93	12.04	12.27	0.63	0.74	0.74	0.67	10.48	10.54
Compressive Strength Testing												
Compressive Strength, MPa	45.0	52.7	65.9	59.0	85.4	88.0	30.8	33.2	39.8	54.7	101.1	103.5

*CC - carbonation cured; HC - hydration cured; 7D - 7 day post-setting; WC - weathering carbonation

Table A.4: Batch B4 experimental data

i) Mix Design

Cement, g	5500
Water, g	825
Fine (River Sand), g	-
Coarse (Limestone, -4.75 to +2.36), g	-
Water Absorption (fine and coarse), %	-
w/c ratio	0.15

ii) Carbonation Curing Characteristics

Preset, hr	17
Carbonation Curing Duration, hr	18
Mass of Collected Water, g	48.8
Water Loss, %	13.73
Mass Gain, %	13.22
Peak Temperature, °C	86.2

iii) Dimensional Stability

Sample	S1C	S2C	S3H	S4H
Carbonation/Hydration Curing				
Strain Gauge Length, in.	8.0022	8.0018	8.0011	8.0014
Initial Strain Gauge Reading, in.	0.0788	0.0784	0.0777	0.0780
After Curing Strain Gauge Reading, in.	0.0731	0.0718	0.0795	0.0784
After Curing Change in Length, in.	-0.0057	-0.0066	0.0018	0.0004
After Curing Strain, με	-712.3	-829.0	229.1	50.0
After Cooling Strain Gauge Reading, in.	0.0724	0.0711	0.0793	0.0781
After Cooling Change in Length, in.	-0.0064	-0.0073	0.0016	0.0001
After Cooling Strain, με	-799.8	-916.5	204.1	12.5
Accelerated Weathering Carbonation				
Initial Strain Gauge Reading, in.	0.0730	0.0718	0.0819	0.0802
After Exposure Strain Gauge Reading, in.	0.0692	0.0681	0.0706	0.0704
Change in Length, in.	-0.0038	-0.0037	-0.0113	-0.0098
Strain, με	-474.9	-458.2	-1416.5	-1224.8

iv) Curing Mass Change

	Carbonation Cured Samples								Hydration Samples							
Sample	S1C	S2C	S5C	S6C	S7C	S8C	S9C	S10C	S3H	S4H	S11H	S12H	S13H	S14H	S15H	S16H
Carbonation/Hydration Curing																
Initial Sample Mass, g	363.5	363.9	363.8	365.3	363.3	364.6	364.1	365.5	363.2	364.6	364.9	364.6	363.6	363.2	363.4	364.5
After Curing Sample Mass, g	400.4	401.2	399.7	401.4	398.6	400.4	399.4	402.3	364.6	365.5	366.0	365.7	365.5	364.7	364.8	366.2
Accelerated Weathering Carbonation																
Initial Sample Mass, g	401.7	402.4	-	-	-	-	400.9	403.5	369.4	369.8	-	-	-	-	369.0	371.7
After Exposure Sample Mass, g	403.0	403.7	-	-	-	-	402.4	404.8	399.3	399.0	-	-	-	-	398.7	402.2

v) Destructive Testing

	Carbonation Cured Samples						Hydration Samples					
Sample	S5C	S6C	S7C	S8C	S9C	S10C	S11H	S12H	S13H	S14H	S15H	S16H
Test Period*	CC	CC	7D	7D	WC	WC	HC	HC	7D	7D	WC	WC
CO_2 Content Analysis												
Surface CO_2 Content, %	13.29	13.63	13.06	13.29	15.20	15.65	-	-	2.67	2.54	13.79	13.10
Core CO_2 Content, %	11.92	12.15	11.87	12.11	13.02	12.93	-	-	1.93	1.91	11.53	11.94
Average CO_2 Content, %	12.61	12.89	12.47	12.70	14.11	14.29	-	-	2.30	2.23	12.66	12.52
Compressive Strength Testing												
Compressive Strength, MPa	81.9	81.0	83.7	89.3	98.9	86.0	35.4	39.9	48.2	42.3	89.6	98.6

*CC - carbonation cured; HC - hydration cured; 7D - 7 day post-setting; WC - weathering carbonation

Table A.5: Batch B5 experimental data

i) Mix Design

Cement, g	2019
Water, g	525
Fine (River Sand), g	2692
Coarse (Limestone, -4.75 to +2.36), g	5383
Water Absorption (fine and coarse), %	1.0
w/c ratio	0.22

ii) Carbonation Curing Characteristics

Preset, hr	0
Carbonation Curing Duration, hr	2
Mass of Collected Water, g	24.9
Water Loss, %	16.49
Mass Gain, %	10.15
Peak Temperature, °C	59.9

iii) Dimensional Stability

Sample	S1C	S2C	S3H	S4H
Carbonation/Hydration Curing				
Strain Gauge Length, in.	8.0023	8.0027	8.0051	8.0026
Initial Strain Gauge Reading, in.	-	-	-	-
After Curing Strain Gauge Reading, in.	-	-	-	-
After Curing Change in Length, in.	-	-	-	-
After Curing Strain, με	-	-	-	-
After Cooling Strain Gauge Reading, in.	-	-	-	-
After Cooling Change in Length, in.	-	-	-	-
After Cooling Strain, με	-	-	-	-
Accelerated Weathering Carbonation				
Initial Strain Gauge Reading, in.	0.0789	0.0793	0.0817	0.0792
After Exposure Strain Gauge Reading, in.	0.0761	0.0762	0.0779	0.0754
Change in Length, in.	-0.0028	-0.0031	-0.0038	-0.0038
Strain, με	-349.0	-383.2	-470.5	-479.0

iv) Curing Mass Change

	Carbonation Cured Samples								Hydration Samples							
Sample	S1C	S2C	S5C	S6C	S7C	S8C	S9C	S10C	S3H	S4H	S11H	S12H	S13H	S14H	S15H	S16H
Carbonation/Hydration Curing																
Initial Sample Mass, g	383.3	383.4	382.9	382.5	383.8	383.9	383.6	384.0	385.4	381.0	383.5	383.5	383.8	383.7	382.8	383.8
After Curing Sample Mass, g	387.9	388.0	387.4	386.7	387.8	388.2	388.0	387.7	384.7	380.4	383.1	383.1	383.1	383.0	382.1	383.1
Accelerated Weathering Carbonation																
Initial Sample Mass, g	388.1	388.0	-	-	-	-	387.3	386.8	383.8	383.8	-	-	-	-	380.9	382.8
After Exposure Sample Mass, g	387.7	387.7	-	-	-	-	386.5	386.4	387.6	387.7	-	-	-	-	384.7	387.1

v) Destructive Testing

	Carbonation Cured Samples						Hydration Samples					
Sample	S5C	S6C	S7C	S8C	S9C	S10C	S11H	S12H	S13H	S14H	S15H	S16H
Test Period*	CC	CC	7D	7D	WC	WC	HC	HC	7D	7D	WC	WC
CO_2 Content Analysis												
Surface CO_2 Content, %												
Core CO_2 Content, %												
Average CO_2 Content, %	15.44	15.00	17.31	16.45	20.60	19.60	-	-	7.84	6.59	18.44	18.46
Compressive Strength Testing												
Compressive Strength, MPa	12.1	13.3	11.7	12.5	18.7	13.2	2.5	2.6	7.9	6.6	10.7	16.4

*CC - carbonation cured; HC - hydration cured; 7D - 7 day post-setting; WC - weathering carbonation

Table A.6: Batch B6 experimental data

i) Mix Design

Cement, g	2019
Water, g	525
Fine (River Sand), g	2692
Coarse (Limestone, -4.75 to +2.36), g	5383
Water Absorption (fine and coarse), %	1.0
w/c ratio	0.22

ii) Carbonation Curing Characteristics

Preset, hr	17
Carbonation Curing Duration, hr	2
Mass of Collected Water, g	8.2
Water Loss, %	6.67
Mass Gain, %	8.37
Peak Temperature, °C	43.1

iii) Dimensional Stability

Sample	S1C	S2C	S3H	S4H
Carbonation/Hydration Curing				
Strain Gauge Length, in.	8.0010	8.0011	8.0001	8.0013
Initial Strain Gauge Reading, in.	0.0777	0.0778	0.0768	0.0780
After Curing Strain Gauge Reading, in.	0.0795	0.0793	0.0771	0.0782
After Curing Change in Length, in.	0.0018	0.0015	0.0003	0.0002
After Curing Strain, με	225.0	187.5	37.5	25.0
After Cooling Strain Gauge Reading, in.	0.0789	0.0787	0.0763	0.0777
After Cooling Change in Length, in.	0.0012	0.0009	-0.0005	-0.0003
After Cooling Strain, με	150.0	112.5	-62.5	-37.5
Accelerated Weathering Carbonation				
Initial Strain Gauge Reading, in.	0.0784	0.0787	0.0775	0.0786
After Exposure Strain Gauge Reading, in.	0.0758	0.0759	0.0735	0.0746
Change in Length, in.	-0.0026	-0.0028	-0.0040	-0.0040
Strain, με	-325.0	-350.0	-500.0	-499.9

iv) Curing Mass Change

	Carbonation Cured Samples								Hydration Samples							
Sample	S1C	S2C	S5C	S6C	S7C	S8C	S9C	S10C	S3H	S4H	S11H	S12H	S13H	S14H	S15H	S16H
Carbonation/Hydration Curing																
Initial Sample Mass, g	380.7	380.6	380.0	378.9	379.4	379.6	379.8	380.3	381.8	380.9	378.6	379.0	380.6	379.4	379.9	379.9
After Curing Sample Mass, g	385.8	385.7	385.2	383.8	384.5	384.7	384.8	385.4	381.9	381.0	378.5	379.0	380.5	379.5	379.8	379.8
Accelerated Weathering Carbonation																
Initial Sample Mass, g	385.5	385.2	-	-	-	-	384.3	384.9	384.2	383.0	-	-	-	-	381.9	382.3
After Exposure Sample Mass, g	385.5	385.2	-	-	-	-	384.2	385.0	387.2	386.1	-	-	-	-	385.5	385.8

v) Destructive Testing

	Carbonation Cured Samples						Hydration Samples					
Sample	S5C	S6C	S7C	S8C	S9C	S10C	S11H	S12H	S13H	S14H	S15H	S16H
Test Period*	CC	CC	7D	7D	WC	WC	HC	HC	7D	7D	WC	WC
CO_2 Content Analysis												
Surface CO_2 Content, %												
Core CO_2 Content, %												
Average CO_2 Content, %	15.53	16.66	17.54	16.81	19.36	19.75	-	-	9.13	7.59	20.23	21.40
Compressive Strength Testing												
Compressive Strength, MPa	13.7	11.8	17.8	14.4	18.9	21.9	5.0	8.1	16.7	16.5	12.0	9.1

*CC - carbonation cured; HC - hydration cured; 7D - 7 day post-setting; WC - weathering carbonation

Table A.7: Batch B7 experimental data

i) Mix Design

Cement, g	2019
Water, g	525
Fine (River Sand), g	2692
Coarse (Limestone, -4.75 to +2.36), g	5383
Water Absorption (fine and coarse), %	1.0
w/c ratio	0.22

ii) Carbonation Curing Characteristics

Preset, hr	0
Carbonation Curing Duration, hr	18
Mass of Collected Water, g	27.4
Water Loss, %	17.99
Mass Gain, %	15.02
Peak Temperature, °C	56.9

iii) Dimensional Stability

Sample	S1C	S2C	S3H	S4H
Carbonation/Hydration Curing				
Strain Gauge Length, in.	8.0012	8.0027	8.0007	8.0006
Initial Strain Gauge Reading, in.	-	-	-	-
After Curing Strain Gauge Reading, in.	-	-	-	-
After Curing Change in Length, in.	-	-	-	-
After Curing Strain, $\mu\varepsilon$	-	-	-	-
After Cooling Strain Gauge Reading, in.	-	-	-	-
After Cooling Change in Length, in.	-	-	-	-
After Cooling Strain, $\mu\varepsilon$	-	-	-	-
Accelerated Weathering Carbonation				
Initial Strain Gauge Reading, in.	0.0778	0.0793	0.0773	0.0772
After Exposure Strain Gauge Reading, in.	0.0752	0.0767	0.0733	0.0736
Change in Length, in.	-0.0026	-0.0026	-0.0040	-0.0036
Strain, $\mu\varepsilon$	-325.0	-324.9	-500.0	-450.0

iv) Curing Mass Change

	Carbonation Cured Samples								Hydration Samples							
Sample	S1C	S2C	S5C	S6C	S7C	S8C	S9C	S10C	S3H	S4H	S11H	S12H	S13H	S14H	S15H	S16H
Carbonation/Hydration Curing																
Initial Sample Mass, g	383.5	383.5	383.6	383.9	382.8	383.7	383.7	384.0	383.3	383.1	383.5	383.7	383.8	384.0	383.7	383.0
After Curing Sample Mass, g	390.7	390.6	391.7	391.8	390.7	391.6	390.9	390.9	382.6	382.5	382.7	383.0	383.2	383.4	382.9	382.3
Accelerated Weathering Carbonation																
Initial Sample Mass, g	391.0	390.7	-	-	-	-	390.8	390.7	384.9	384.7	-	-	-	-	384.2	383.8
After Exposure Sample Mass, g	389.7	389.4	-	-	-	-	389.2	389.1	387.9	388.0	-	-	-	-	387.7	387.7

v) Destructive Testing

	Carbonation Cured Samples						Hydration Samples					
Sample	S5C	S6C	S7C	S8C	S9C	S10C	S11H	S12H	S13H	S14H	S15H	S16H
Test Period*	CC	CC	7D	7D	WC	WC	HC	HC	7D	7D	WC	WC
CO_2 Content Analysis												
Surface CO_2 Content, %												
Core CO_2 Content, %												
Average CO_2 Content, %	20.50	20.27	19.79	20.15	22.03	23.36	-	-	6.31	8.73	21.43	19.36
Compressive Strength Testing												
Compressive Strength, MPa	13.6	12.1	16.5	12.0	14.6	17.6	5.3	5.9	6.4	8.4	14.9	13.5

*CC - carbonation cured; HC - hydration cured; 7D - 7 day post-setting; WC - weathering carbonation

Table A.8: Batch B8 experimental data

i) Mix Design

Cement, g	2019
Water, g	525
Fine (River Sand), g	2692
Coarse (Limestone, -4.75 to +2.36), g	5383
Water Absorption (fine and coarse), %	1.0
w/c ratio	0.22

ii) Carbonation Curing Characteristics

Preset, hr	17
Carbonation Curing Duration, hr	18
Mass of Collected Water, g	7.9
Water Loss, %	5.93
Mass Gain, %	10.46
Peak Temperature, °C	41.7

iii) Dimensional Stability

Sample	S1C	S2C	S3H	S4H
Carbonation/Hydration Curing				
Strain Gauge Length, in.	8.0014	8.0060	8.0008	8.0008
Initial Strain Gauge Reading, in.	0.0780	0.0826	0.0774	0.0774
After Curing Strain Gauge Reading, in.	0.0790	0.0838	0.0773	0.0771
After Curing Change in Length, in.	0.0010	0.0012	-0.0001	-0.0003
After Curing Strain, με	125.0	150.0	-16.7	-33.3
After Cooling Strain Gauge Reading, in.	0.0784	0.0831	0.0764	0.0765
After Cooling Change in Length, in.	0.0004	0.0005	-0.0010	-0.0009
After Cooling Strain, με	50.0	62.5	-129.2	-108.3
Accelerated Weathering Carbonation				
Initial Strain Gauge Reading, in.	0.0777	0.0824	0.0775	0.0774
After Exposure Strain Gauge Reading, in.	0.0752	0.0799	0.0737	0.0736
Change in Length, in.	-0.0025	-0.0025	-0.0038	-0.0038
Strain, με	-316.6	-316.4	-475.0	-479.1

iv) Curing Mass Change

	Carbonation Cured Samples								Hydration Samples							
Sample	S1C	S2C	S5C	S6C	S7C	S8C	S9C	S10C	S3H	S4H	S11H	S12H	S13H	S14H	S15H	S16H
Carbonation/Hydration Curing																
Initial Sample Mass, g	382.4	381.9	381.2	381.5	380.9	380.4	380.9	380.3	381.9	381.0	380.8	379.5	379.8	379.0	378.5	378.6
After Curing Sample Mass, g	389.1	388.3	387.5	388.3	387.3	386.9	388.0	387.2	382.1	381.2	380.9	379.7	380.0	379.1	378.6	378.7
Accelerated Weathering Carbonation																
Initial Sample Mass, g	388.2	387.5	-	-	-	-	387.4	386.6	383.0	382.0	-	-	-	-	379.7	379.6
After Exposure Sample Mass, g	387.7	387.0	-	-	-	-	386.7	386.0	385.6	384.6	-	-	-	-	382.8	382.1

v) Destructive Testing

	Carbonation Cured Samples						Hydration Samples					
Sample	S5C	S6C	S7C	S8C	S9C	S10C	S11H	S12H	S13H	S14H	S15H	S16H
Test Period*	CC	CC	7D	7D	WC	WC	HC	HC	7D	7D	WC	WC
CO_2 Content Analysis												
Surface CO_2 Content, %												
Core CO_2 Content, %												
Average CO_2 Content, %	20.67	19.54	19.81	20.42	21.33	20.85	-	-	8.32	10.18	17.02	18.88
Compressive Strength Testing												
Compressive Strength, MPa	16.2	18.9	17.1	16.9	22.7	19.5	12.9	9.9	11.6	10.2	14.3	12.8

*CC - carbonation cured; HC - hydration cured; 7D - 7 day post-setting; WC - weathering carbonation

APPENDIX B: SERIES TWO EXPERIMENTAL DATA

Table B.1: Batch B9 to B16 experimental data

	Cement Paste				Concrete			
Batch	B9	B10	B11	B12	B13	B14	B15	B16
i) Mix Design								
Cement, g	340.0	340.0	340.0	340.0	75.0	75.0	75.0	75.0
Water, g	51.0	51.0	51.0	51.0	19.5	19.5	19.5	19.5
Fine (River Sand), g	-	-	-	-	100.0	100.0	100.0	100.0
Coarse (Limestone, -4.75 to +2.36), g	-	-	-	-	200.0	200.0	200.0	200.0
Water Absorption (fine and coarse), %	-	-	-	-	1.0	1.0	1.0	1.0
w/c ratio	0.15	0.15	0.15	0.15	0.22	0.22	0.22	0.22
ii) Carbonation Curing Characteristics								
Preset, hr	0	17	0	17	0	17	0	17
Carbonation Duration, hr	2	2	18	18	2	2	18	18
Mass of Collected Water, g	6.7	2.5	6.9	1.4	1.5	0.1	1.2	0.1
Water Loss, %	13.99	5.71	14.41	3.19	7.88	0.65	6.31	0.60
Mass Gain, %	10.65	9.58	13.78	13.29	9.70	7.38	12.98	11.75
Peak Temperature, °C	51.6	46.6	47.9	41.4	40.2	41.0	41.4	37.6
iii) Carbonation Curing Dimensional Stability								
Strain Gauge Length, in.	7.949	8.002	7.947	8.010	7.993	7.992	8.001	8.011
Initial Strain Gauge Reading, in.	-0.00448	-0.00054	0.00028	0.00248	0.00250	-0.00099	-0.00003	-0.00160
After Vacuum Strain Gauge Reading, in.	-0.00429	-0.00100	0.00047	0.00209	0.00250	-0.00093	-0.00002	-0.00167
End of Curing Strain Gauge Reading, in.	-0.00822	-0.00349	-0.00204	0.00085	0.00250	0.00044	0.00008	-0.00021
Out of Chamber Strain Gauge Reading, in.	-0.00801	-0.00349	-0.00202	0.00068	0.00262	0.00027	0.00019	-0.00022
After Cooling Strain Gauge Reading, in.	-0.00813	-0.00348	-0.00222	0.00069	0.00262	0.00027	0.00018	-0.00047
Minimum Strain Gauge Reading, in.	-0.00834	-0.00368	-0.00317	0.00003	0.00209	-0.00120	-0.00073	-0.00205
Maximum Strain Gauge Reading, in.	-0.00303	0.00250	0.00112	0.00496	0.00344	0.00088	0.00074	0.00032
Displacement*, in.	-0.00353	-0.00295	-0.00230	-0.00180	0.00012	0.00126	0.00022	0.00138
Displacement**, in.	-0.00365	-0.00294	-0.00250	-0.00179	0.00012	0.00126	0.00021	0.00113
Displacement***, in.	-0.00393	-0.00249	-0.00251	-0.00124	0.00000	0.00137	0.00010	0.00146
Min. Displacement**, in.	-0.00386	-0.00314	-0.00345	-0.00245	-0.00041	-0.00021	-0.00070	-0.00045
Max. Displacement**, in.	0.00145	0.00304	0.00084	0.00248	0.00094	0.00187	0.00077	0.00192
Strain*, με	-444.1	-368.6	-289.4	-224.7	15.0	157.7	27.5	172.3
Strain**, με	-459.2	-367.4	-314.6	-223.5	15.0	157.7	26.2	141.1
Strain***, με	-494.4	-311.2	-315.8	-154.8	0.0	171.4	12.5	182.3
Min. Strain**, με	-485.6	-392.4	-434.1	-305.9	-51.3	-26.3	-87.5	239.7
Max. Strain**, με	182.4	379.9	105.7	309.6	117.6	234.0	96.2	-56.2
iv) Carbonation Curing Carbon Dioxide Absorption								
Initial Sample Mass, g	367.2	367.2	367.2	366.9	385.0	381.4	385.0	382.7
Initial Sample Mass with LVDT, g	453.6	453.6	454.5	450.7	468.8	469.3	1153.3	470.6
After Curing Sample Mass with LVDT, g	480.9	481.7	491.6	491.7	474.4	474.6	1161.6	479.1

* Displacement as previously measured, incorporating vacuuming, pressurization, depressurization, vacuuming and removal.

** Displacement as previously measured, including the aforementioned conditions plus cooling.

*** Displacement after initial vacuuming and prior to final depressurization.

APPENDIX C: SERIES THREE EXPERIMENTAL DATA

Definition of Samples

B17 Samples

Carbonation Cured Samples

S1C	Carbonation cured plate samples used for compressive strength testing after carbonation curing.
S2C	
S3C	Carbonation cured plate samples used for compressive strength testing after 28 day post-setting hydration period.
S4C	
S5C	Extra Sample

**All samples were used to obtain the characteristics of carbonation curing.*

Hydration Cured Samples

S6H	Hydration cured plate samples used for compressive strength testing after carbonation curing.
S7H	
S8H	Hydration cured plate samples used for compressive strength testing after 28 day post-setting hydration period.
S9H	
S10H	Extra Sample

B18 Samples

Carbonation Cured Samples

S1C	Carbonation cured plate sample used for compressive strength testing after carbonation curing.
S2C	Carbonation cured plate sample used for compressive strength testing after 28 day post-setting hydration period.
S3C	Carbonation cured plate samples used for freeze/thaw durability testing.
S4C	
S5C	

**All samples were used to obtain the characteristics of carbonation curing.*

Hydration Cured Samples

S6H	Hydration cured plate sample used for compressive strength testing after carbonation curing.
S7H	Hydration cured plate sample used for compressive strength testing after 28 day post-setting hydration period.
S8H	Hydration cured plate samples used for freeze/thaw durability testing.C1
S9H	
S10H	

Table C.1: Batch B17 experimental data

i) Mix Design

Cement, g	1594
Water, g	414
Fine (River Sand), g	2125
Coarse (Limestone, -4.75 to +2.36), g	4250
Water Absorption (fine and coarse), %	1.0
w/c ratio	0.22

ii) Carbonation Curing Characteristics

Preset, hr	22
Carbonation Curing Duration, hr	22
Mass of Collected Water, g	8.6
Water Loss, %	4.60
Mass Gain, %	10.70
Peak Temperature, °C	36.4

iii) Carbonation/Hydration Curing Mass Change

	Carbonation Cured Samples					Hydration Samples				
Sample	S1C	S2C	S3C	S4C	S5C	S6H	S7H	S8H	S9H	S10H
Initial Sample Mass, g	758.7	754.9	751.5	758.9	757.7	753.4	758.5	758.2	758.3	760.8
After Curing Sample Mass, g	772.9	768.7	764.9	771.7	771.8	754.1	759.4	758.7	759.1	761.5

iv) Compressive Strength Testing

	Carbonation Cured Samples					Hydration Samples				
Sample	S1C	S2C	S3C	S4C	S5C	S6H	S7H	S8H	S9H	S10H
Test Period*	CC	CC	28D	28D		HC	HC	28D	28D	
Compressive Strength, MPa	51.0	49.5	57.0	71.6	-	39.4	42.9	50.0	49.2	-

*CC - carbonation cured; HC - hydration cured; 28D - 28 day post-setting; WC - weathering carbonation

Table C.2: Batch B18 experimental data

i) Mix Design

Cement, g	1594
Water, g	414
Fine (River Sand), g	2125
Coarse (Limestone, -4.75 to +2.36), g	4250
Water Absorption (fine and coarse), %	1.0
w/c ratio	0.22

ii) Carbonation Curing Characteristics

Preset, hr	22
Carbonation Curing Duration, hr	22
Mass of Collected Water, g	9.1
Water Loss, %	4.86
Mass Gain, %	10.69
Peak Temperature, °C	39.7

iii) Carbonation/Hydration Curing Mass Change

	Carbonation Cured Samples					Hydration Samples				
Sample	S1C	S2C	S3C	S4C	S5C	S6H	S7H	S8H	S9H	S10H
Initial Sample Mass, g	758.4	753.4	758.2	759.3	759.0	760.2	759.1	759.5	759.4	757.1
After Curing Sample Mass, g	772.4	766.7	772.1	773.0	772.0	761.3	760.0	760.6	760.2	758.1

iv) Compressive Strength Testing

	Carbonation Cured Samples					Hydration Samples				
Sample	S1C	S2C	S3C	S4C	S5C	S6H	S7H	S8H	S9H	S10H
Test Period*	CC	28D				WC	28D			
Compressive Strength, MPa	48.9	58.4	-	-	-	44.9	49.9	-	-	-

*CC - carbonation cured; HC - hydration cured; 28D - 28 day post-setting; WC - weathering carbonation